



Measurement of the cross section for isolated-photon plus jet production in pp collisions at $\sqrt{s}=13$ TeV using the ATLAS detector

Aaboud, M.; Aad, G.; Abbott, B.; Abdinov, O.; Abeloos, B.; Abidi, S.H.; Abouzeid, Ossama Sherif Alexander; Abraham, NL; Abramowicz, H.; Abreu, H.; Abreu, R.; Abulaiti, Y.; Acharya, B.S.; Adachi, Shin-ichi; Adamczyk, L.; Adelman, J.; Adersberger, M.; Adye, T.; Affolder, A. A.; Afik, Y. ; Bajic, Milena; Besjes, Geert-Jan; Alonso Diaz, Alejandro; de Almeida Dias, Flavia; Dam, Mogens; Galster, Gorm Aske Gram Krohn; Hansen, Peter Henrik; Thiele, Fabian Alexander Jürgen; Hansen, Jørgen Beck; Petersen, Troels Christian; Hansen, Jørn Dines; Xella, Stefania; Monk, James William; Stark, Simon Holm; Wiglesworth, Graig

Published in:
Physics Letters B

DOI:
[10.1016/j.physletb.2018.03.035](https://doi.org/10.1016/j.physletb.2018.03.035)

Publication date:
2018

Document version
Publisher's PDF, also known as Version of record

Document license:
[CC BY](#)

Citation for published version (APA):
Aaboud, M., Aad, G., Abbott, B., Abdinov, O., Abeloos, B., Abidi, S. H., Abouzeid, O. S. A., Abraham, NL., Abramowicz, H., Abreu, H., Abreu, R., Abulaiti, Y., Acharya, B. S., Adachi, S., Adamczyk, L., Adelman, J., Adersberger, M., Adye, T., Affolder, A. A., ... Wiglesworth, G. (2018). Measurement of the cross section for isolated-photon plus jet production in pp collisions at $\sqrt{s}=13$ TeV using the ATLAS detector. *Physics Letters B*, 780, 578-602. <https://doi.org/10.1016/j.physletb.2018.03.035>



Measurement of the cross section for isolated-photon plus jet production in pp collisions at $\sqrt{s} = 13$ TeV using the ATLAS detector

The ATLAS Collaboration ^{*}



ARTICLE INFO

Article history:

Received 30 December 2017
Received in revised form 27 February 2018
Accepted 13 March 2018
Available online 15 March 2018
Editor: W.-D. Schlatter

ABSTRACT

The dynamics of isolated-photon production in association with a jet in proton–proton collisions at a centre-of-mass energy of 13 TeV are studied with the ATLAS detector at the LHC using a dataset with an integrated luminosity of 3.2 fb^{-1} . Photons are required to have transverse energies above 125 GeV. Jets are identified using the anti- k_t algorithm with radius parameter $R = 0.4$ and required to have transverse momenta above 100 GeV. Measurements of isolated-photon plus jet cross sections are presented as functions of the leading-photon transverse energy, the leading-jet transverse momentum, the azimuthal angular separation between the photon and the jet, the photon–jet invariant mass and the scattering angle in the photon–jet centre-of-mass system. Tree-level plus parton-shower predictions from SHERPA and PYTHIA as well as next-to-leading-order QCD predictions from JETPHOX and SHERPA are compared to the measurements.

© 2018 The Author. Published by Elsevier B.V. This is an open access article under the CC BY license (<http://creativecommons.org/licenses/by/4.0/>). Funded by SCOAP³.

1. Introduction

The production of prompt photons in association with at least one jet in proton–proton (pp) collisions provides a testing ground for perturbative QCD (pQCD). In pp collisions, all photons that are not secondaries from hadron decays are considered to be “prompt”. The measurements of angular correlations between the photon and the jet can be used to probe the dynamics of the hard-scattering process. The dominant source in pp collisions at the LHC is the $qg \rightarrow q\gamma$ process. These measurements are also useful for tuning Monte Carlo (MC) models and testing t -channel quark exchange [1, 2]. Furthermore, precise measurements of these processes validate the generators used for background studies in searches for physics beyond the Standard Model which involve photons, such as the search for new phenomena in final states with a photon and a jet [3,4].

The production of $pp \rightarrow \gamma + \text{jet} + X$ events proceeds via two processes: direct, in which the photon originates from the hard process, and fragmentation, in which the photon arises from the fragmentation of a coloured high transverse momentum¹ (p_T) par-

ton [5,6]. The direct and fragmentation contributions are only well defined at leading order (LO) in QCD; at higher orders this distinction is no longer possible. These two processes exhibit distinct behaviours in the observables considered here. Precise measurements test the interplay of direct and fragmentation processes.

Measurements of prompt-photon production in a final state with accompanying hadrons necessitate an isolation requirement on the photon to avoid the large contribution from neutral-hadron decays into photons. The production of isolated photons in association with jets in pp collisions at $\sqrt{s} = 7$ and 8 TeV was studied by the ATLAS [1,2,7] and CMS [8–10] Collaborations. The increase in the centre-of-mass energy of pp collisions at the LHC to 13 TeV allows the exploration of the dynamics of photon+jet production in a new regime with the goal of testing the pQCD predictions at higher energy transfers than achieved before. It is also possible to investigate whether the data in the new energy regime are well described by the predictions of parton-shower event generators, such as SHERPA [11] and PYTHIA [12].

The dynamics of the underlying processes in $2 \rightarrow 2$ hard collinear scattering can be investigated using the variable θ^* , where $\cos \theta^* \equiv \tanh(\Delta y/2)$ and Δy is the difference between the rapidities of the two final-state particles. The variable θ^* coincides with the scattering polar angle in the centre-of-mass frame for collinear scattering of massless particles, and its distribution is sensitive to the spin of the exchanged particle. For processes dom-

where E is the energy and p_z is the z -component of the momentum, and transverse energy is defined as $E_T = E \sin \theta$.

^{*} E-mail address: atlas.publications@cern.ch.

¹ ATLAS uses a right-handed coordinate system with its origin at the nominal interaction point (IP) in the centre of the detector and the z -axis along the beam pipe. The x -axis points from the IP to the centre of the LHC ring, and the y -axis points upwards. Cylindrical coordinates (r, ϕ) are used in the transverse plane, ϕ being the azimuthal angle around the z -axis. The pseudorapidity is defined in terms of the polar angle θ as $\eta = -\ln \tan(\theta/2)$. The angular distance is measured in units of $\Delta R \equiv \sqrt{(\Delta\eta)^2 + (\Delta\phi)^2}$. The rapidity is defined as $y = 0.5 \ln[(E + p_z)/(E - p_z)]$.

inated by t -channel gluon exchange, such as dijet production in pp collisions, the differential cross section behaves as $(1 - |\cos\theta^*|)^{-2}$ when $|\cos\theta^*| \rightarrow 1$. In contrast, processes dominated by t -channel quark exchange are expected to exhibit a $(1 - |\cos\theta^*|)^{-1}$ behaviour when $|\cos\theta^*| \rightarrow 1$. This fundamental prediction of QCD can be tested in photon plus jet production in pp collisions. The direct-photon contribution, dominated by t -channel quark exchange, is expected to exhibit a $(1 - |\cos\theta^*|)^{-1}$ dependence when $|\cos\theta^*| \rightarrow 1$, whereas that of fragmentation processes is predicted to be the same as in dijet production, namely $(1 - |\cos\theta^*|)^{-2}$. For both processes, there are also s -channel contributions which are, however, non-singular when $|\cos\theta^*| \rightarrow 1$. As a result, a measurement of the cross section for prompt-photon plus jet production as a function of $|\cos\theta^*|$ provides a handle on the relative contributions of the direct and fragmentation components as well as the possibility of testing the dominance of t -channel quark exchange.

The results presented here include a study of the kinematics of the photon plus one-jet system via measurements of the cross sections as functions of the leading-photon transverse energy (E_T^γ) and the leading-jet transverse momentum ($p_T^{\text{jet-lead}}$). The dynamics of the photon plus one-jet system are studied by measuring the azimuthal angular separation between the leading photon and the leading jet ($\Delta\phi^{\gamma\text{-jet}}$), the invariant mass of the leading photon and the leading jet ($m^{\gamma\text{-jet}}$) and $\cos\theta^*$. The distribution in $m^{\gamma\text{-jet}}$ is predicted to be monotonically decreasing in QCD due to the absence of resonances that decay into a photon and a jet. The analysis is performed using 3.2 fb^{-1} of $\sqrt{s} = 13 \text{ TeV}$ pp collision data recorded by ATLAS. Next-to-leading-order (NLO) QCD predictions from JETPHOX [13,14] and SHERPA as well as the tree-level predictions of PYTHIA and SHERPA are compared to the measurements.

2. ATLAS detector

The ATLAS detector [15] is a multi-purpose detector with a forward-backward symmetric cylindrical geometry. It consists of an inner tracking detector surrounded by a thin superconducting solenoid, electromagnetic and hadronic calorimeters, and a muon spectrometer incorporating three large superconducting toroid magnets. The inner-detector system is immersed in a 2 T axial magnetic field and provides charged-particle tracking in the range $|\eta| < 2.5$. The high-granularity silicon pixel detector is closest to the interaction region and provides four measurements per track; the innermost layer, known as the insertable B-layer [16], provides high-resolution hits at small radius to improve the tracking performance. The pixel detector is followed by the silicon microstrip tracker, which typically provides four three-dimensional space point measurements per track. These silicon detectors are complemented by the transition radiation tracker, which enables radially extended track reconstruction up to $|\eta| = 2.0$. The calorimeter system covers the range $|\eta| < 4.9$. Within the region $|\eta| < 3.2$, electromagnetic (EM) calorimetry is provided by barrel and end-cap high-granularity lead/liquid-argon (LAr) EM calorimeters, with an additional thin LAr presampler covering $|\eta| < 1.8$ to correct for energy loss in material upstream of the calorimeters; for $|\eta| < 2.5$ the EM calorimeter is divided into three layers in depth. Hadronic calorimetry is provided by a steel/scintillator-tile calorimeter, segmented into three barrel structures within $|\eta| < 1.7$, and two copper/LAr hadronic endcap calorimeters, which cover the region $1.5 < |\eta| < 3.2$. The solid-angle coverage is completed out to $|\eta| = 4.9$ with forward copper/LAr and tungsten/LAr calorimeter modules, which are optimised for EM and hadronic measurements, respectively. Events are selected using a first-level trigger implemented in custom electronics, which reduces the maximum event rate of 40 MHz to a design value of 100 kHz using a subset of

detector information. Software algorithms with access to the full detector information are then used in the high-level trigger to yield a recorded event rate of about 1 kHz [17].

3. Data sample and Monte Carlo simulations

The data used in this analysis were collected with the ATLAS detector during the pp collision running period of 2015, when the LHC operated with a bunch spacing of 25 ns and at a centre-of-mass energy of 13 TeV. Only events taken during stable beam conditions and satisfying detector and data-quality requirements, which include the calorimeters and inner tracking detectors being in nominal operation, are considered. The average number of pp interactions per bunch crossing in the dataset is 13. The total integrated luminosity of the collected sample is $3.16 \pm 0.07 \text{ fb}^{-1}$. The uncertainty in the integrated luminosity is 2.1% and is derived, following a methodology similar to that detailed in Ref. [18], from a calibration of the luminosity scale using x - y beam-separation scans performed in August 2015.

Samples of MC events were generated to study the characteristics of signal events. The MC programs PYTHIA 8.186 and SHERPA 2.1.1 were used to generate the simulated events. In both generators, the partonic processes were simulated using tree-level matrix elements, with the inclusion of initial- and final-state parton showers. Fragmentation into hadrons was performed using the Lund string model [19] in the case of PYTHIA, and in SHERPA by a modified version of the cluster model [20]. The LO NNPDF2.3 [21] parton distribution functions (PDF) set was used for PYTHIA while the NLO CT10 [22] PDF set was used for SHERPA to parameterise the proton structure. Both samples include a simulation of the underlying event (UE). The event-generator parameters were set according to the ATLAS 2014 tune series (A14 tune) for PYTHIA [23] and to the tune developed in conjunction with the NLO CT10 PDF set for SHERPA. The PYTHIA simulation of the signal includes LO photon-plus-jet events from both direct processes (the hard subprocesses $qg \rightarrow q\gamma$ and $q\bar{q} \rightarrow g\gamma$, called the “hard” component) and photon bremsstrahlung in LO QCD dijet events (called the “bremsstrahlung” component). The bremsstrahlung component is modelled by final-state QED radiation arising from calculations of all $2 \rightarrow 2$ QCD processes. In the particle-level phase space of the presented measurements the fraction of the bremsstrahlung component decreases from 35% at $E_T^\gamma = 125 \text{ GeV}$ to 15% at $E_T^\gamma = 1 \text{ TeV}$. The SHERPA samples were generated with LO matrix elements for photon-plus-jet final states with up to three additional partons ($2 \rightarrow n$ processes with n from 2 to 5); the matrix elements were merged with the SHERPA parton shower using the ME+PS@LO prescription [24]. The bremsstrahlung component is accounted for in SHERPA through the matrix elements of $2 \rightarrow n$ processes with $n \geq 3$. In the generation of the SHERPA samples, a requirement on the photon isolation at the matrix-element level was imposed using the criterion defined in Ref. [25]. This criterion, commonly called Frixiene’s criterion, requires the total transverse energy inside a cone of size \mathcal{V} around the generated final-state photon, excluding the photon itself, to be below a certain threshold, $E_T^{\text{max}}(\mathcal{V}) = \epsilon E_T^\gamma ((1 - \cos \mathcal{V})/(1 - \cos \mathcal{R}))^n$, for all $\mathcal{V} < \mathcal{R}$. The parameters for the threshold were chosen to be $\mathcal{R} = 0.3$, $n = 2$ and $\epsilon = 0.025$. The SHERPA predictions from this computation are referred to as LO SHERPA.

All the samples of generated events were passed through the GEANT4-based [26] ATLAS detector and trigger full simulation programs [27]. They are reconstructed and analysed with the same program chain as the data. Pile-up from additional pp collisions in the same and neighbouring bunch crossings was simulated by overlaying each MC event with a variable number of simulated inelastic pp collisions generated using PYTHIA 8.153 with the ATLAS

set of tuned parameters for minimum bias events (A2 tune) [28]. The MC events are weighted to reproduce the distribution of the average number of interactions per bunch crossing ($\langle\mu\rangle$) observed in the data, referred to as “pile-up reweighting”. In this procedure, the $\langle\mu\rangle$ value from the data is divided by a factor of 1.16 ± 0.07 , a rescaling which makes the number of reconstructed primary vertices agree better between data and simulation and reproduces the visible cross section of inelastic pp collisions as measured in the data [29].

4. Event selection

Events were recorded using a single-photon trigger, with a transverse energy threshold of 120 GeV and “loose” identification requirements based on the shower shapes in the second layer of the EM calorimeter as well as on the energy leaking into the hadronic calorimeter from the EM calorimeter [17]. Events are required to have a reconstructed primary vertex. If multiple primary vertices are reconstructed, the one with the highest sum of the p_T^2 of the associated tracks is selected as the primary vertex.

Photon candidates are reconstructed from clusters of energy deposited in the EM calorimeter and classified [30] as unconverted photons (candidates without a matching track or matching reconstructed conversion vertex in the inner detector) or converted photons (candidates with a matching reconstructed conversion vertex or a matching track consistent with originating from a photon conversion). The measurement of the photon energy is based on the energy collected in calorimeter cells in an area of size $\Delta\eta \times \Delta\phi = 0.075 \times 0.175$ in the barrel and 0.125×0.125 in the endcaps. A dedicated energy calibration [31] is then applied to the candidates to account for upstream energy loss and both lateral and longitudinal leakage. The photon identification is based primarily on shower shapes in the calorimeter [30]. An initial selection is derived using the information from the hadronic calorimeter and the lateral shower shape in the second layer of the EM calorimeter, where most of the photon energy is contained. The final tight selection applies stringent criteria [30] to the same variables used in the initial selection, separately for converted and unconverted photon candidates. It also places requirements on the shower shape in the finely segmented first calorimeter layer to ensure the compatibility of the measured shower profile with that originating from a single photon impacting the calorimeter. When applying the photon identification criteria to simulated events, corrections are made for small differences in the average values of the shower-shape variables between data and simulation. Events with at least one photon candidate with calibrated $E_T^\gamma > 125$ GeV, where the trigger is maximally efficient, and $|\eta^\gamma| < 2.37$ are selected. Candidates in the region $1.37 < |\eta^\gamma| < 1.56$, which includes the transition region between the barrel and endcap calorimeters, are not considered. The photon candidate is required to be isolated based on the amount of transverse energy inside a cone of size $\Delta R = 0.4$ in the η - ϕ plane around the photon candidate, excluding an area of size $\Delta\eta \times \Delta\phi = 0.125 \times 0.175$ centred on the photon. The isolation transverse energy is computed from topological clusters of calorimeter cells [32] and is denoted by E_T^{iso} . Topological clusters are built from neighbouring calorimeter cells containing energy significantly above a noise threshold that is estimated from measurements of calorimeter electronic noise and simulated pile-up noise. The measured value of E_T^{iso} is corrected for the expected leakage of the photon energy into the isolation cone as well as for the estimated contributions from the UE and pile-up [33,34]. The corrections for pile-up and the UE are computed simultaneously on an event-by-event basis using the jet-area method [35,36] as follows: the k_\perp jet algorithm [37,38] with jet radius $R = 0.5$ is used to reconstruct all jets, taking topological clus-

ters of calorimeter cells as input; no explicit transverse momentum threshold is applied. The ambient transverse energy density for the event (ρ), from pile-up and the UE, is computed using the median of the distribution of the ratio of the jet's transverse energy to its area. Finally, ρ is multiplied by the area of the isolation cone to compute the correction to E_T^{iso} . The combined correction is typically 2 GeV and depends weakly on E_T^γ . In addition, for simulated events, data-driven corrections to E_T^{iso} are applied such that the peak position in the E_T^{iso} distribution coincides in data and simulation. After all these corrections, E_T^{iso} is required to be less than $E_{T,\text{cut}}^{\text{iso}} \equiv 4.2 \cdot 10^{-3} \cdot E_T^\gamma + 4.8$ GeV [39]. The isolation requirement significantly reduces the main background, which consists of multi-jet events where one jet typically contains a π^0 or η meson that carries most of the jet energy and is misidentified as a photon because it decays into an almost collinear photon pair. A small fraction of the events contain more than one photon candidate satisfying the selection criteria. In such events, the highest- E_T^γ (leading) photon is considered for further study.

Jets are reconstructed using the anti- k_t algorithm [40,41] with a radius parameter $R = 0.4$, using topological clusters as input. The calorimeter cell energies are measured at the EM scale, corresponding to the energy deposited by electromagnetically interacting particles. The jet four-momenta are computed from the sum of the jet-constituent four-momenta, treating each as a four-vector with zero mass. The jets are then further calibrated using the method described in Ref. [42] and these jets are referred to as detector-level jets. The four-momentum of each jet is recalculated to point to the selected primary vertex of the event rather than the centre of the detector. The contribution from the UE and pile-up is then subtracted on a jet-by-jet basis using the jet-area method. A jet-energy calibration is derived from MC simulations as a correction relating the calorimeter response to the true jet energy. To determine these corrections, the jet reconstruction procedure applied to the topological clusters is also applied to the generated stable particles, which are defined as those with a decay length of $c\tau > 10$ mm, excluding muons and neutrinos; these jets are referred to as particle-level jets. In addition, sequential jet corrections, derived from MC simulated events and using global properties of the jet such as tracking information, calorimeter energy deposits and muon spectrometer information, are applied [43]. Finally, the detector-level jets are further calibrated with additional correction factors derived in situ from a combination of γ + jet, Z + jet and multi-jet p_T balance methods [44,45].²

Jets reconstructed from calorimeter signals not originating from a pp collision are rejected by applying jet-quality criteria [45,46]. These criteria suppress spurious jets from electronic noise in the calorimeter, cosmic rays and beam-related backgrounds. Remaining jets are required to have calibrated transverse momenta greater than 60 GeV and rapidity $|y^{\text{jet}}| < 2.37$. Jets overlapping with the candidate photon are not considered if the jet axis lies within a cone of size $\Delta R = 0.8$ around the photon candidate; this requirement prevents any overlap between the photon isolation cone ($\Delta R = 0.4$) and the jet cone ($\Delta R = 0.4$). Finally, the event is retained if the jet with highest transverse energy (leading jet) has $p_T^{\text{jet}} > 100$ GeV.

The total number of data events selected by using the requirements discussed above is 895 726. This sample of events is used to measure the cross section as a function of E_T^γ , $p_T^{\text{jet-lead}}$ and $\Delta\phi^{\gamma\text{-jet}}$. For the measurements of the cross sections as functions

² The effect of the correlation between the events used in the in situ γ +jet analysis and the events selected here has a negligible effect on the experimental uncertainties associated to the measurements.

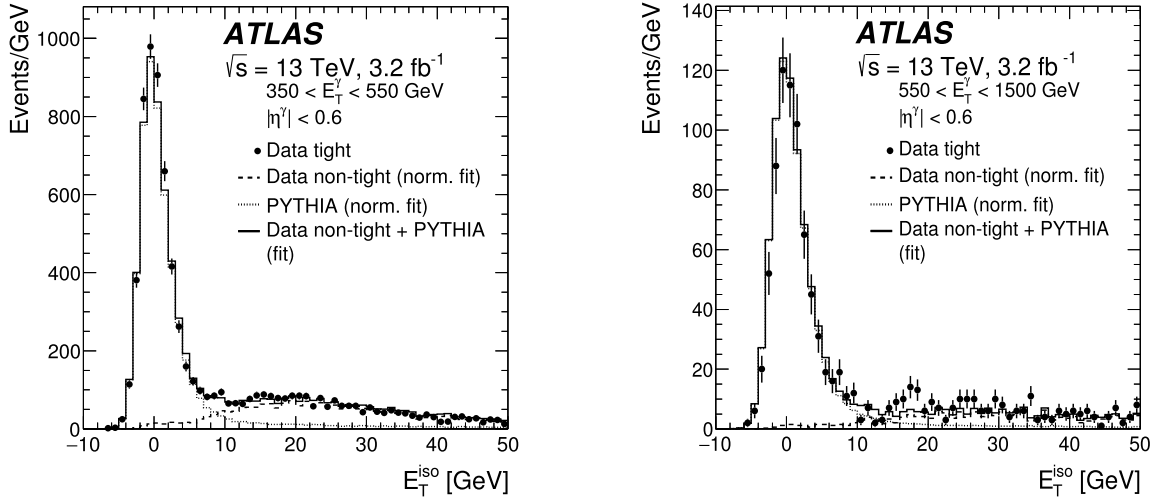


Fig. 1. E_T^{iso} distribution for tight (black dots) and non-tight (dashed histogram, normalised according to the fit, see text) photon candidates in data with $|\eta^\gamma| < 0.6$ in different E_T^γ regions. The MC simulation of the signal using PYTHIA is also shown (dotted histogram). The solid histogram is the sum of the contributions of the MC simulation of the signal using PYTHIA and that of the non-tight photon candidates normalised according to the fit.

of $m^{\gamma\text{-jet}}$ and $|\cos\theta^*|$, the additional constraints $|\eta^\gamma + y^{\text{jet-lead}}| < 2.37$, $|\cos\theta^*| < 0.83$ and $m^{\gamma\text{-jet}} > 450$ GeV are imposed to remove the bias [1,2] due to the rapidity and transverse-momentum requirements on the photon and the jet³; the number of events selected in the data after these additional requirements is 137 738.

5. Background estimation and signal extraction

After the requirements on photon identification and isolation are applied to the sample of events, there is still a residual background contribution, which arises primarily from jets identified as photons in multi-jet events. This background contribution is estimated and subtracted bin-by-bin using a data-driven technique which makes use of the same two-dimensional sideband method employed in a previous analysis [47]. In this approach, the photon is classified as:

- “Isolated”, if $E_T^{\text{iso}} < E_{T,\text{cut}}^{\text{iso}}$.
- “Non-isolated”, if $E_T^{\text{iso}} > E_{T,\text{cut}}^{\text{iso}} + 2$ GeV and $E_T^{\text{iso}} < 50$ GeV. The non-isolated region is separated by 2 GeV from the isolated region to reduce the signal contamination. The upper bound is applied to avoid highly non-isolated photons.⁴
- “Tight”, if it satisfies the tight photon identification criteria.
- “Non-tight”, if it fails at least one of four tight requirements on the shower-shape variables computed from the energy deposits in the first layer of the EM calorimeter, but satisfies the tight requirement on the total lateral shower width in the first layer and all the other tight identification criteria in other layers [30].

The distributions in E_T^{iso} for tight and non-tight photon candidates with $|\eta^\gamma| < 0.6$ in the data are shown separately in Fig. 1 for two regions in E_T^γ . The MC simulation of the prompt-photon signal using PYTHIA is also shown. A fit of the sum of the distributions of the PYTHIA signal photons and the non-tight photon candidates

to the distribution of the tight photon candidates is also included. A clear signal of prompt photons centred at E_T^{iso} about zero is observed.

For the estimation of the background contamination in the signal region a two-dimensional plane is formed by E_T^{iso} and a binary variable (“tight” vs. “non-tight” photon candidate) since these two variables are expected to be largely uncorrelated for background events. In this plane, four regions are defined: the “signal” region (A), containing tight and isolated photon candidates; the “non-isolated” background control region (B), containing tight and non-isolated photon candidates; the “non-tight” background control region (C), containing isolated and non-tight photon candidates; the background control region containing non-isolated and non-tight photon candidates (D).

The signal yield N_A^{sig} in region A is estimated by using the relation

$$N_A^{\text{sig}} = N_A - R^{\text{bg}} \cdot (N_B - f_B N_A^{\text{sig}}) \cdot \frac{(N_C - f_C N_A^{\text{sig}})}{(N_D - f_D N_A^{\text{sig}})}, \quad (1)$$

where N_K , with $K = A, B, C, D$, is the number of events in region K and $R^{\text{bg}} = N_A^{\text{bg}} \cdot N_D^{\text{bg}} / (N_B^{\text{bg}} \cdot N_C^{\text{bg}})$ is the so-called background correlation and is taken as $R^{\text{bg}} = 1$ for the nominal results; N_K^{bg} with $K = A, B, C, D$ is the unknown number of background events in each region. Equation (1) takes into account the expected number of signal events in each of the three background control regions (N_K^{sig}) via the signal leakage fractions, $f_K = N_K^{\text{sig}} / N_A^{\text{sig}}$ with $K = B, C, D$, which are estimated using the MC simulations of the signal.

The only assumption underlying Eq. (1) is that the isolation and identification variables are uncorrelated for background events, thus $R^{\text{bg}} = 1$. This assumption is verified in data typically within $\pm 10\%$ in validation regions,⁵ which are dominated by background. Deviations of R^{bg} from unity in the validation regions, after accounting for signal leakage using either the PYTHIA or LO SHERPA simulations, are propagated through Eq. (1) and taken as systematic uncertainties. The signal purity, defined as N_A^{sig} / N_A , is above 90% in all bins of the measured distributions. The use of PYTHIA

³ The first two constraints avoid the bias induced by requirements on η^γ and $y^{\text{jet-lead}}$, yielding slices of $\cos\theta^*$ with the same length along the $\eta^\gamma + y^{\text{jet-lead}}$ axis. The third constraint avoids the bias due to the $E_T^\gamma > 125$ GeV requirement.

⁴ In this way, the determination of the signal yield does not depend on the description by the MC generators of the distribution of E_T^{iso} for prompt photons with high values of E_T^{iso} .

⁵ The validation regions are defined within the control regions B and D by splitting each of them into two subregions.

Table 1

Summary of the requirements at particle level that define the fiducial phase-space region of the measurements.

Requirements on photons
$E_T^\gamma > 125 \text{ GeV}$, $ \eta^\gamma < 2.37$ (excluding $1.37 < \eta^\gamma < 1.56$)
$E_T^{\text{iso}} < 4.2 \cdot 10^{-3} \cdot E_T^\gamma + 10 \text{ GeV}$
Requirements on jets
anti- k_t algorithm with $R = 0.4$
the leading jet within $ y^{\text{jet}} < 2.37$ and $\Delta R^{\gamma\text{-jet}} > 0.8$ is selected
$p_T^{\text{jet-lead}} > 100 \text{ GeV}$
UE subtraction using k_\perp algorithm with $R = 0.5$ (cf. Section 4)
Additional requirements for $d\sigma/dm^{\gamma\text{-jet}}$ and $d\sigma/d \cos\theta^* $
$ \eta^\gamma + y^{\text{jet-lead}} < 2.37$, $ \cos\theta^* < 0.83$ and $m^{\gamma\text{-jet}} > 450 \text{ GeV}$

or LO SHERPA to extract the signal leakage fractions lead to similar signal purities; the difference in the signal purity is taken as a systematic uncertainty.

The background from electrons misidentified as photons, mainly produced in Drell-Yan $Z^{(*)}/\gamma^* \rightarrow e^+e^-$ and $W^{(*)} \rightarrow e\nu$ processes, is also studied. Such misidentified electrons are largely suppressed by the photon selection. This background is estimated using MC samples of fully simulated events and found to be negligible in the phase-space region of the analysis presented here. These processes were simulated using the SHERPA 2.2.1 generator. Matrix-elements were calculated for up to two additional partons at NLO and up to four partons at LO [48,49].

6. Fiducial phase space and unfolding

6.1. Fiducial phase space

The cross sections are unfolded to a phase-space region close to the applied event selection. The fiducial phase-space region is defined at the particle level. A summary of the requirements at particle level that define the fiducial phase-space region of the measurements is given in Table 1. The cross sections as functions of $|\cos\theta^*|$ and $m^{\gamma\text{-jet}}$ are measured in a fiducial phase-space region with additional requirements, as detailed in the last row of Table 1. The particle-level isolation requirement on the photon is built by summing the transverse energy of all stable particles (see Section 4), except for muons and neutrinos, in a cone of size $\Delta R = 0.4$ around the photon direction after the contribution from the UE is subtracted. The same underlying-event subtraction procedure used at the reconstruction level is applied at the particle level. The particle-level requirement on E_T^{iso} is optimised to best match the acceptance at reconstruction level using the PYTHIA and LO SHERPA MC samples by comparing the calorimeter isolation transverse energy with the particle-level isolation transverse energy on an event-by-event basis. The particle-level requirement on E_T^{iso} thus optimised is $E_T^{\text{iso}}(\text{particle}) < 4.2 \cdot 10^{-3} \cdot E_T^\gamma + 10 \text{ GeV}$; the same requirement is obtained whether PYTHIA or LO SHERPA is used. Particle-level jets are reconstructed using the anti- k_t jet algorithm with radius parameter $R = 0.4$ and are built from stable particles, excluding muons and neutrinos. At particle level, the particles associated with the overlaid pp collisions (pile-up) are not considered.

6.2. Unfolding

The distributions of the background-subtracted signal yield as functions of E_T^γ , $p_T^{\text{jet-lead}}$, $\Delta\phi^{\gamma\text{-jet}}$, $m^{\gamma\text{-jet}}$ and $|\cos\theta^*|$ are used to measure the corresponding differential cross sections for isolated-photon plus jet production. The distributions are unfolded to the

particle level using MC samples of events via a bin-by-bin technique which corrects for resolution effects and the efficiency of the photon and jet reconstruction through the formula

$$\frac{d\sigma}{dO}(i) = \frac{N_A^{\text{sig}}(i) C^{\text{MC}}(i)}{\mathcal{L} \Delta O(i)},$$

where $d\sigma/dO(i)$ is the cross section as a function of observable O in bin i , $N_A^{\text{sig}}(i)$ is the number of background-subtracted data events in bin i , $C^{\text{MC}}(i)$ is the correction factor in bin i , \mathcal{L} is the integrated luminosity and $\Delta O(i)$ is the width of bin i . The correction factors are computed from the MC samples as $C^{\text{MC}}(i) = N_{\text{part}}^{\text{MC}}(i)/N_{\text{reco}}^{\text{MC}}(i)$, where $N_{\text{part}}^{\text{MC}}(i)$ is the number of events that satisfy the kinematic constraints of the phase-space region at the particle level, and $N_{\text{reco}}^{\text{MC}}(i)$ is the number of events which meet all the selection criteria at the reconstruction level.

The distributions of the signal yields as functions of E_T^γ , $p_T^{\text{jet-lead}}$, $\Delta\phi^{\gamma\text{-jet}}$, $m^{\gamma\text{-jet}}$ and $|\cos\theta^*|$ in data after background subtraction are well described by the LO SHERPA MC simulations, but some differences are observed when compared to the PYTHIA MC simulations, in particular in the tail of the $p_T^{\text{jet-lead}}$ distribution. A better description of the data distributions as functions of E_T^γ , $p_T^{\text{jet-lead}}$, $\Delta\phi^{\gamma\text{-jet}}$, $m^{\gamma\text{-jet}}$ and $|\cos\theta^*|$ by PYTHIA is obtained by increasing/decreasing the relative contribution from direct processes with respect to bremsstrahlung processes [1,2]; the resulting PYTHIA simulations are referred to as PYTHIA-adjusted simulations.

The unfolded cross sections are measured using the signal leakage fractions from PYTHIA-adjusted simulations since these include an unbiased sample of non-isolated photons,⁶ and the correction factors, C^{MC} , from LO SHERPA since these simulations give somewhat better agreement with the data distributions as functions of E_T^γ , $p_T^{\text{jet-lead}}$, $\Delta\phi^{\gamma\text{-jet}}$, $m^{\gamma\text{-jet}}$ and $|\cos\theta^*|$. The correction factors vary between 1.08 and 1.21 depending on the observable. The results of the bin-by-bin unfolding procedure are checked with an iterative Bayesian unfolding method [50] based on LO SHERPA simulations, giving consistent results.

7. Uncertainties in the cross-section measurements

Photon energy scale and resolution. A detailed assessment of the uncertainties in the photon energy scale and resolution is made using the method reported in Ref. [47]. The photon energy scale uncertainties come mostly from calibration studies using 8 TeV data [31], with additional systematic uncertainties to take into account the differences between the 2012 and 2015 configurations. The uncertainties are split into independent components to account for correlations of the uncertainties between different bins of the measured cross sections. The individual sources of uncertainty are varied by $\pm 1\sigma$ in the MC simulations and propagated through the analysis separately to maintain the full information about the correlations of the uncertainties between different bins of the measured cross sections. The impact of the photon energy resolution uncertainty is much smaller than that of the photon energy scale uncertainty. The resulting uncertainty in the measured cross sections is obtained by adding in quadrature all the individual components and increases from 1% at $E_T^\gamma = 125 \text{ GeV}$ to 4.5% at $E_T^\gamma \sim 1.5 \text{ TeV}$.

⁶ In the LO SHERPA samples, the application of the Frixiore's criterion to the photon isolation at matrix-element level prevents the radiated photon from being close to a parton. In the PYTHIA samples, the bremsstrahlung component is simulated with a parton shower approach and, as a result, the radiated photon can be close to a parton.

Jet energy scale and resolution. A detailed assessment of the uncertainties in the jet energy scale and resolution is made using the method reported in Ref. [42]. The individual sources of uncertainty [42] are varied by $\pm 1\sigma$ in the MC simulations and propagated through the analysis separately, to maintain the full information about the correlations of the uncertainties between different bins of the measured cross sections. The resulting uncertainty in the measured cross sections is obtained by adding in quadrature all the individual components and increases from 1.9% at $p_T^{\text{jet-lead}} = 100$ GeV to 7.5% at $p_T^{\text{jet-lead}} \sim 1$ TeV.

Parton-shower and hadronisation model dependence. The effects due to the parton-shower and hadronisation models on the signal purity and detector-to-particle-level correction factors are studied separately. The effects on the signal purity are estimated as the differences observed between the nominal results and those obtained using either the (non-adjusted) PYTHIA or LO SHERPA MC samples for the determination of the signal leakage fractions. The difference between the nominal results and those obtained using the PYTHIA-adjusted MC samples for the determination of the unfolding correction factors is taken as a systematic uncertainty. The resulting uncertainties in the measured cross sections are typically smaller than 2%.

Photon identification efficiency. The uncertainty in the photon identification efficiency is estimated from the effect of differences between shower-shape variable distributions in data and simulation. From the studies presented in Refs. [30,51], this procedure is found to provide a conservative estimate of the uncertainties. The resulting uncertainty in the measured cross sections is in the range 1–2%. The effects on the measured cross sections due to the uncertainty in the photon reconstruction efficiency, which are evaluated by repeating the full analysis using a different detector simulation with increased material in front of the calorimeter, are found to be negligible.

Photon isolation modelling. The differences between the nominal results and those obtained without applying the data-driven corrections to E_T^{iso} in simulated events are taken as systematic uncertainties in the measurements due to the modelling of E_T^{iso} in the MC simulation. The resulting uncertainty in the measured cross sections is less than 1.1%.

Definition of the background control regions. The estimation of the background contamination in the signal region is affected by the choice of background control regions. The control regions B and D are defined by the lower and upper limits on E_T^{iso} and the choice of inverted photon identification variables used in the selection of non-tight photons. To study the dependence on the specific choices, these definitions are varied over a wide range. The lower limit on E_T^{iso} in regions B and D is varied by ± 1 GeV, which is larger than any difference between data and simulations and still provides a sufficient sample to perform the data-driven subtraction. The upper limit on E_T^{iso} in regions B and D is removed. The resulting uncertainty in the measured cross sections is negligible. Likewise, the choice of inverted photon identification variables is varied. The analysis is repeated using different sets of variables: tighter (looser) identification criteria are defined by applying tight requirements to an extended (restricted) set of shower-shape variables in the first calorimeter layer [30,51]. The resulting uncertainty in the measured cross sections is smaller than 1.3%.

Photon identification and isolation correlation in the background. The photon isolation and identification variables used to define

the plane in the two-dimensional sideband method to subtract the background are assumed to be independent for background events ($R^{\text{bg}} = 1$ in Eq. (1)). Any correlation between these variables affects the estimation of the purity of the signal sample and leads to systematic uncertainties in the background-subtraction procedure. A range in R^{bg} is set to cover the deviations from unity measured in the validation regions after subtracting the signal leakage with either PYTHIA-adjusted or LO SHERPA MC samples. The resulting uncertainty in all measured cross sections is less than 2%.

Pile-up. The uncertainty is estimated by changing the nominal rescaling factor of 1.16 to 1.09 or 1.23 and re-evaluating the reweighting factors. The resulting uncertainty in the measured cross sections is typically less than 0.5%.

Unfolding procedure. The uncertainty is estimated by comparing the nominal results with those obtained by unfolding with LO SHERPA MC samples reweighted to match the data distributions. The resulting uncertainty in the measured cross sections is negligible.

The total systematic uncertainty is computed by adding in quadrature the uncertainties from the sources listed above, the statistical uncertainty of the MC samples, the uncertainty in the trigger efficiency (1%) and the uncertainty in the integrated luminosity, which is fully correlated between all bins of all the measured cross sections. There are large correlations in the systematic uncertainties across bins of one observable, particularly in the uncertainties due to the photon and jet energy scales, which are dominant. The total systematic uncertainty, excluding that in the luminosity, is less than 5% for E_T^γ , 4% for $\Delta\phi^{\gamma\text{-jet}}$, 6% for $m^{\gamma\text{-jet}}$ and 4% for $|\cos\theta^*|$ and increases from 4% at $p_T^{\text{jet-lead}} = 100$ GeV to 10% at $p_T^{\text{jet-lead}} \sim 1.5$ TeV. Fig. 2 shows the total systematic uncertainty for each measured cross section, excluding that in the luminosity; the dominant components are shown separately in this Figure. The systematic uncertainty dominates the total experimental uncertainty for $E_T^\gamma \lesssim 700$ GeV and $m^{\gamma\text{-jet}} \lesssim 1.5$ TeV, whereas for higher E_T^γ and $m^{\gamma\text{-jet}}$ values, the statistical uncertainty of the data limits the precision of the measurements. For $p_T^{\text{jet-lead}}$, $\Delta\phi^{\gamma\text{-jet}}$ and $|\cos\theta^*|$, the systematic uncertainty dominates in the whole measured range.

8. Theoretical predictions

The NLO pQCD predictions presented in this Letter are computed using two programs, namely JETPHOX 1.3.1.2 and SHERPA 2.2.2. The JETPHOX program includes a full NLO pQCD calculation of both the direct and fragmentation contributions to the cross section for the $pp \rightarrow \gamma + \text{jet} + X$ process. The number of massless quark flavours is set to five. The renormalisation scale μ_R , factorisation scale μ_F and fragmentation scale μ_f are chosen to be $\mu_R = \mu_F = \mu_f = E_T^\gamma$ [14]. The calculations are performed using the MMHT2014 [52] PDF set and the BFG set II of parton-to-photon fragmentation functions [53], both at NLO. The strong coupling constant is set to $\alpha_s(m_Z) = 0.120$. The calculations are performed using a parton-level isolation criterion which requires the total transverse energy from the partons inside a cone of size $\Delta R = 0.4$ around the photon direction to be below $4.2 \cdot 10^{-3} \cdot E_T^\gamma + 10$ GeV. The NLO pQCD predictions from JETPHOX are at the parton level while the measurements are at the particle level. Thus, there can be differences between the two levels concerning the photon isolation as well as the photon and jet four-momenta. Since the data are corrected for pile-up and UE effects and the distributions are unfolded to a phase-space definition in which the requirement on

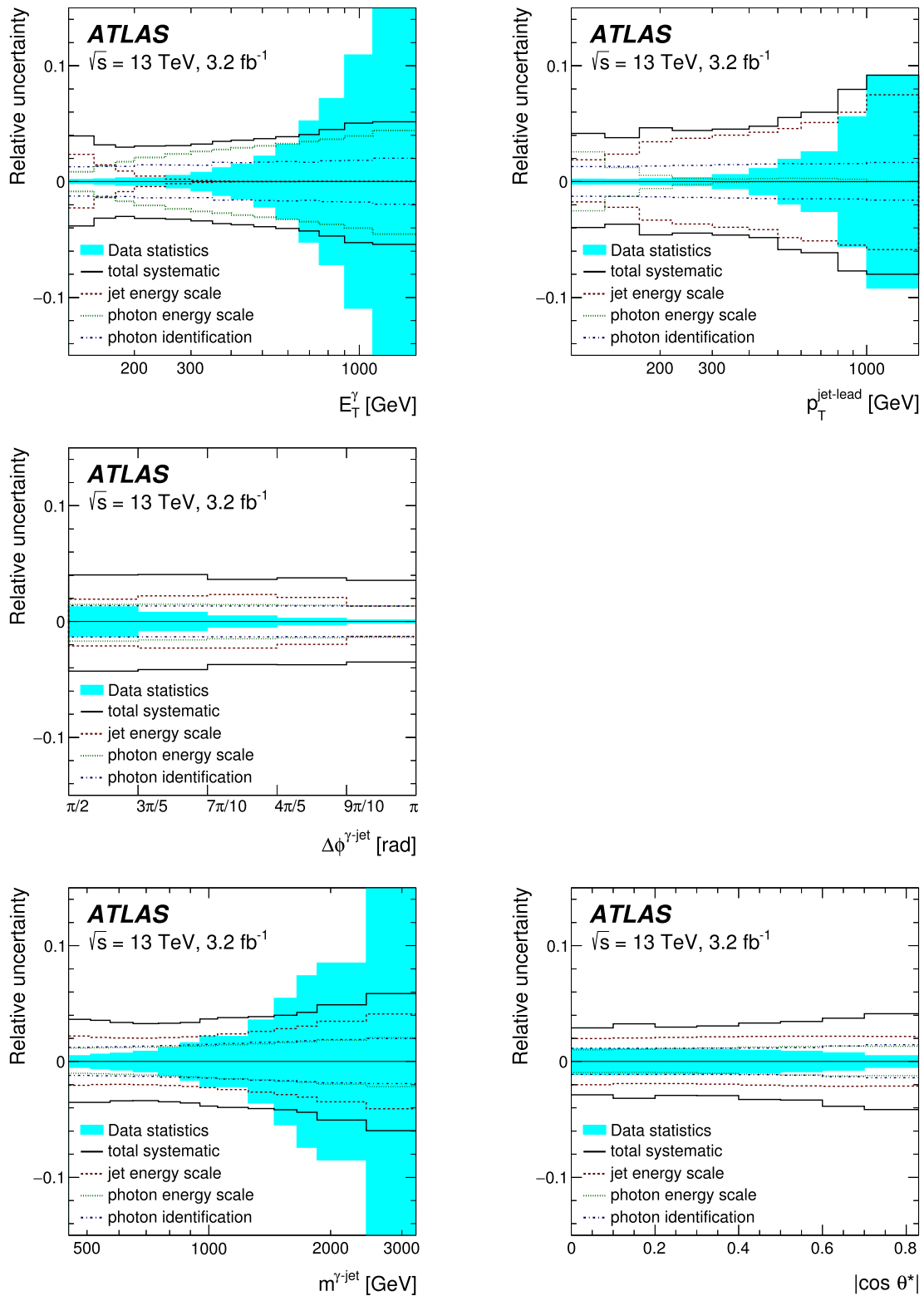


Fig. 2. Total relative systematic uncertainty (solid lines), excluding that in the luminosity measurement, as a function of E_T^γ , $p_T^{\text{jet-lead}}$, $\Delta\phi^{\gamma\text{-jet}}$, $m^{\gamma\text{-jet}}$ and $|\cos\theta^*|$. The three dominant contributions are also included separately: the jet energy scale (dashed lines), the photon energy scale (dotted lines) and the photon identification (dot-dashed lines). The shaded band displays the relative statistical uncertainty; for the last point in E_T^γ ($m^{\gamma\text{-jet}}$) the relative statistical uncertainty is 32% (30%).

E_T^{iso} at particle level is applied after subtraction of the UE, it is expected that parton-to-hadron corrections to the NLO pQCD predictions are small. Correction factors to the JETPHOX predictions are estimated by computing the ratio of the particle-level cross section for a PYTHIA sample with UE effects to the parton-level cross section without UE effects. These factors are close to unity within $\pm 5\%$ for the observables studied, except for $p_T^{\text{jet-lead}} \gtrsim 600$ GeV; in this region, which is dominated by the bremsstrahlung component, the factors can differ by up to 30% from unity since hadronisation of a nearby parton can significantly change the particle-level isolation compared to the parton-level isolation.

The SHERPA 2.2.2 program consistently combines parton-level calculations of $\gamma + (1, 2) - \text{jet}$ events at NLO and $\gamma + (3, 4) - \text{jet}$ events at LO [48,49] supplemented with a parton shower [54] while avoiding double-counting effects [55]. A requirement on the photon isolation at the matrix-element level is imposed using Frixi- one's criterion with $\mathcal{R} = 0.1$, $n = 2$ and $\epsilon = 0.1$. Dynamic factorisation and renormalisation scales are adopted as well as a dynamical merging scale with $\bar{Q}_{\text{cut}} = 20$ GeV [56]. The strong coupling constant is set to $\alpha_s(m_Z) = 0.118$. Fragmentation into hadrons and simulation of the UE are performed using the same models as for the LO SHERPA samples. The next-to-next-to-leading-order (NNLO) NNPDF3.0 PDF set [57] is used in conjunction with the corresponding SHERPA tuning. All the NLO SHERPA predictions are based on the particle-level observables from this computation after applying the requirements listed in Table 1.

8.1. Uncertainties in the predictions

The uncertainty in the NLO pQCD predictions from JETPHOX due to terms beyond NLO is estimated by repeating the calculations using values of μ_R , μ_F and μ_f scaled by the factors 0.5 and 2. The three scales are either varied simultaneously, individually or by fixing one and varying the other two. In all cases, the condition $0.5 \leq \mu_A/\mu_B \leq 2$ is imposed, where $A, B = R, F, f$. The final uncertainty is taken as the largest deviation from the nominal value among the 14 possible variations. In the case of the NLO SHERPA prediction, which does not include the fragmentation contribution, μ_R and μ_F are varied as above and the largest deviation from the nominal value among the 6 possible variations is taken as the uncertainty.

The uncertainty in the NLO pQCD predictions from JETPHOX due to the choice of proton PDFs is estimated by repeating the calculations using the 50 sets from the MMHT2014 error analysis [52] and applying the Hessian method [58] for evaluation of the PDF uncertainties. In the case of NLO SHERPA, it is estimated using 100 replicas from the NNPDF3.0 analysis [57].

The uncertainty in the NLO pQCD predictions from JETPHOX (NLO SHERPA) due to the uncertainty in α_s is estimated by repeating the calculations using two additional sets of proton PDFs from the MMHT2014 (NNPDF3.0) analysis, for which different values of α_s at m_Z were assumed in the fits, namely 0.118 (0.117) and 0.122 (0.119); in this way, the correlation between α_s and the PDFs is preserved.

The uncertainty in the parton-to-hadron correction is estimated by comparing the values obtained using different tunes of PYTHIA: the ATLAS set of tuned parameters for the underlying event (tune AU2) [28] with the CTEQ6L1 PDF set [59], the A14 tune with the LO NNPDF2.3 PDF set as well as the tunes in which the parameter settings of the latter related to the modelling of the UE are varied [23]. Larger differences are obtained from the comparison of the two central tunes than from the variations around the A14 tune. The nominal correction is taken as the average of the corrections using the two central tunes, while the uncertainty is estimated as half of the difference between the two central tunes.

The dominant theoretical uncertainty is that arising from the terms beyond NLO and, in the case of JETPHOX (NLO SHERPA), is $\approx 10\%$ (15–25%) for E_T^γ , $m^{\gamma-\text{jet}}$ and $|\cos\theta^*|$ and increases from 5% (15%) at $p_T^{\text{jet-lead}} = 130$ GeV to 30% (30%) for $p_T^{\text{jet-lead}} = 1.5$ TeV. In the case of the NLO SHERPA prediction for $d\sigma/d\Delta\phi^{\gamma-\text{jet}}$, the uncertainty increases from 10% at $\Delta\phi^{\gamma-\text{jet}} \sim \pi$ to 40% at $\Delta\phi^{\gamma-\text{jet}} \sim \pi/2$. The uncertainty in the predictions of JETPHOX (NLO SHERPA) arising from that in the PDFs is $\lesssim 2\%$ (3%) for all observables. The uncertainty arising from the value of $\alpha_s(m_Z)$ is below 2% (5%). The uncertainty in the parton-to-hadron correction is in the range 1–3% except for $p_T^{\text{jet-lead}} \gtrsim 600$ GeV, where it increases to 20% at $p_T^{\text{jet-lead}} = 1.5$ TeV; this uncertainty is included in the JETPHOX predictions, but not in the case of NLO SHERPA since it is a particle-level Monte Carlo generator.⁷ The total theoretical uncertainty is obtained by adding in quadrature the individual uncertainties listed above and, in the case of JETPHOX (NLO SHERPA), is 10–15% (15–25%) except for $p_T^{\text{jet-lead}}$, where it is in the range 10–40% (15–30%); in the case of the NLO SHERPA prediction for $d\sigma/d\Delta\phi^{\gamma-\text{jet}}$, the total uncertainty is 10–40%.

9. Results

The measurements presented here apply to isolated prompt photons with $E_T^{\text{iso}} < 4.2 \cdot 10^{-3} \cdot E_T^\gamma + 10$ GeV at particle level and jets of hadrons. The measured fiducial cross section for isolated-photon plus one-jet production in the phase-space region given in Table 1 is $\sigma_{\text{meas}} = 300 \pm 10$ (exp.) ± 6 (lumi.) pb, where “exp.” denotes the sum in quadrature of the statistical and systematic uncertainties excluding that due to the luminosity and “lumi.” denotes the uncertainty due to that in the integrated luminosity. The fiducial cross sections predicted by NLO QCD JETPHOX (multi-leg NLO QCD plus parton-shower SHERPA) using the MMHT2014 (NNPDF3.0) PDF set are

$$\sigma_{\text{JETPHOX}} = 291_{-21}^{+25} (\text{scale})_{-3}^{+2} (\text{PDF})_{-5}^{+4} (\alpha_s) \pm 6 (\text{non-perturb.}) \text{ pb}$$

and

$$\sigma_{\text{NLOSHERPA}} = 319_{-45}^{+54} (\text{scale}) \pm 3 (\text{PDF})_{-11}^{+10} (\alpha_s) \text{ pb},$$

which are consistent with the measurement within the theoretical uncertainties.

Fig. 3 shows the isolated-photon plus jet cross sections as functions of E_T^γ , $p_T^{\text{jet-lead}}$, $\Delta\phi^{\gamma-\text{jet}}$, $m^{\gamma-\text{jet}}$ and $|\cos\theta^*|$. The measured $d\sigma/dE_T^\gamma$ decreases by almost six orders of magnitude over the E_T^γ range studied. Values of E_T^γ up to 1.5 TeV are measured. The measured $d\sigma/dp_T^{\text{jet-lead}}$ decreases by more than four orders of magnitude from $p_T^{\text{jet-lead}} = 100$ GeV up to the highest measured value, $p_T^{\text{jet-lead}} \approx 1.5$ TeV. The measurement of $d\sigma/d\Delta\phi^{\gamma-\text{jet}}$ is restricted to $\Delta\phi^{\gamma-\text{jet}} > \pi/2$ to avoid the phase-space region dominated by photon production in association with a multi-jet system. The measured $d\sigma/d\Delta\phi^{\gamma-\text{jet}}$ increases as $\Delta\phi^{\gamma-\text{jet}}$ increases. The measured $d\sigma/dm^{\gamma-\text{jet}}$ decreases by more than four orders of magnitude up to the highest measured value, $m^{\gamma-\text{jet}} = 3.25$ TeV. The measured $d\sigma/d|\cos\theta^*|$ increases as $|\cos\theta^*|$ increases.

The tree-level predictions of the PYTHIA and LO SHERPA MC models are compared to the measurements in Fig. 3. These predictions are normalised to the measured integrated fiducial cross

⁷ An uncertainty related to the modelling of the hadronisation process should also be assigned to the NLO SHERPA predictions, but no tune other than the default one is available. It is expected that the uncertainty should be of similar size as that evaluated using PYTHIA.

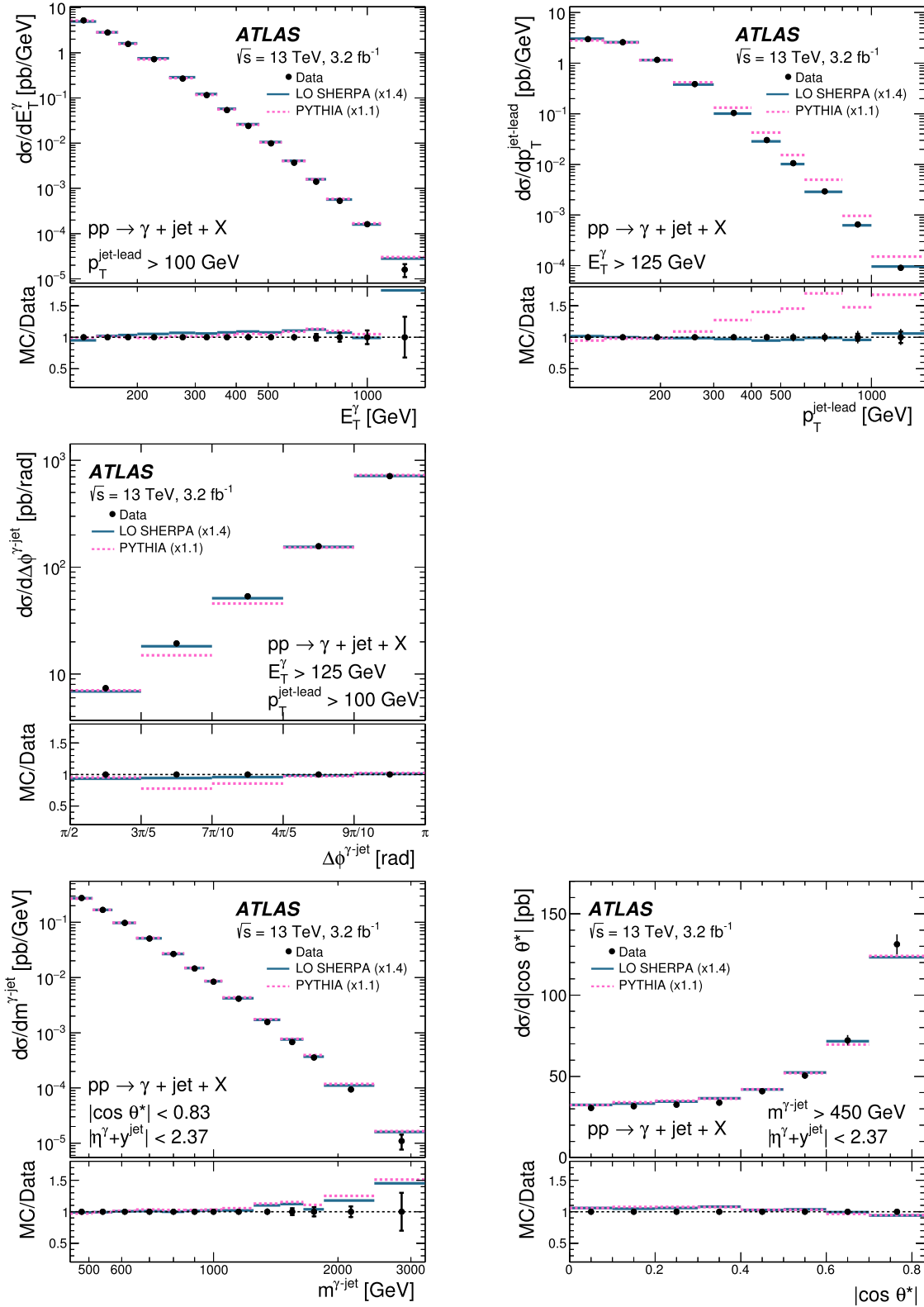


Fig. 3. Measured cross sections for isolated-photon plus jet production (dots) as functions of E_T^γ , $p_T^{\text{jet-lead}}$, $\Delta\phi^{\gamma\text{-jet}}$, $m^{\gamma\text{-jet}}$ and $|\cos\theta^*|$; the observables are constructed using the leading photon and the leading jet. For comparison, the tree-level plus parton-shower predictions from LO SHERPA (solid lines) and PYTHIA (dashed lines) normalised to the integrated measured cross sections (using the factors indicated in parentheses) are also shown. The theoretical uncertainties associated with the tree-level predictions are not included. The bottom part of each figure shows the ratios of the MC predictions to the measured cross section. The inner (outer) error bars represent the statistical uncertainties (the statistical and systematic uncertainties added in quadrature). For most of the points, the inner error bars are smaller than the marker size and, thus, not visible.

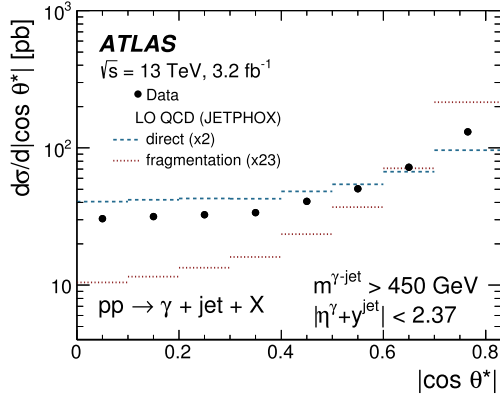


Fig. 4. Measured cross section for isolated-photon plus jet production (dots) as a function of $|\cos \theta^*|$; the observable is constructed using the leading photon and the leading jet. For comparison, the LO QCD predictions from JETPHOX, normalised to the integrated measured cross section by the factors shown in parentheses, of direct (dashed lines) and fragmentation (dotted lines) processes are shown separately. The error bars are smaller than the marker size and, thus, not visible.

section. The difference in normalisation between data and PYTHIA (LO SHERPA) is $\sim +10\%$ ($+40\%$) and attributed to the fact that these generators are based on tree-level matrix elements, which are affected by a large normalisation uncertainty due to missing higher-order terms; for this reason, the theoretical uncertainties are not included in Fig. 3. Both predictions give an adequate description of the shape of the measured $d\sigma/dE_T^\gamma$, although PYTHIA is slightly better than LO SHERPA for $E_T^\gamma \lesssim 600$ GeV. For $d\sigma/dp_T^{\text{jet-lead}}$, the prediction from LO SHERPA gives an adequate description of the data in the whole measured range, whereas that from PYTHIA overestimates the data for $p_T^{\text{jet-lead}} \gtrsim 200$ GeV; the overestimation is attributed to a large contribution from photon bremsstrahlung predicted by the tune used in PYTHIA (see Section 3). The prediction from LO SHERPA gives a good description of the measured $d\sigma/d\Delta\phi^{\gamma\text{-jet}}$, whereas PYTHIA underestimates the data for $3\pi/5 < \Delta\phi^{\gamma\text{-jet}} < 4\pi/5$ rad; this is expected from the inclusion of additional partons in the matrix elements in SHERPA as compared to PYTHIA, for which additional partons must necessarily come from the parton shower. Both predictions give a good description of the data for $m_T^{\gamma\text{-jet}} < 1.25$ TeV and for all of the measured $|\cos \theta^*|$ range.

To illustrate the sensitivity to t -channel quark or gluon exchange, the predicted cross-sections $d\sigma/d|\cos \theta^*|$ from JETPHOX for LO direct and fragmentation processes are compared to the measurement in Fig. 4. Even though the two components are no longer distinguishable at NLO, the LO calculations are useful in illustrating the basic differences in the dynamics of the two processes. The contribution from fragmentation, dominated by gluon exchange, shows a steeper increase as $|\cos \theta^*| \rightarrow 1$ than that from direct processes, dominated by quark exchange. The shape of the measured cross-section $d\sigma/d|\cos \theta^*|$ is closer to that of the direct processes than that of fragmentation. This is consistent with the dominance of processes in which the exchanged particle is a quark.

The predictions of the fixed-order NLO QCD calculations of JETPHOX based on the MMHT2014 proton PDF set and corrected for hadronisation and UE effects as explained in Section 8 are compared to the measurements⁸ in Fig. 5. The predictions of the multi-leg NLO QCD plus parton-shower calculations of SHERPA based on the NNPDF3.0 PDF set are also compared to the measurements in Fig. 5. Both types of predictions describe the data within the ex-

perimental and theoretical uncertainties. For the cross section as a function of $\Delta\phi^{\gamma\text{-jet}}$, the only well-founded prediction is that of NLO SHERPA, which is able to reproduce the data down to $\Delta\phi^{\gamma\text{-jet}} = \pi/2$ due to the inclusion of the matrix elements for $2 \rightarrow n$ processes with $n = 4$ and 5. For most of the points, the theoretical uncertainties are larger than those of experimental origin. Predictions for JETPHOX (SHERPA NLO) are also obtained with other PDF sets, namely NLO CT14 [60] and NLO NNPDF3.0 (CT14 and MMHT2014), and differ by less than 5% with respect to those using MMHT2014 (NNPDF3.0). Thus, the description of the data achieved by the predictions does not depend significantly on the specific PDF set used. It is concluded that the NLO pQCD predictions provide an adequate description of the measurements within the uncertainties.

10. Summary

Measurements of the cross section for the production of an isolated photon in association with jets in pp collisions at $\sqrt{s} = 13$ TeV, $pp \rightarrow \gamma + \text{jet} + X$, are presented. These measurements are based on an integrated luminosity of 3.2 fb^{-1} of ATLAS data recorded at the LHC. The photon is required to have $E_T^\gamma > 125$ GeV and $|\eta^\gamma| < 2.37$, excluding the region $1.37 < |\eta^\gamma| < 1.56$. The jets are reconstructed using the anti- k_t algorithm with radius parameter $R = 0.4$. The cross sections are measured as functions of E_T^γ , $p_T^{\text{jet-lead}}$ and $\Delta\phi^{\gamma\text{-jet}}$ with $p_T^{\text{jet-lead}} > 100$ GeV; the measurements extend up to values of 1.5 TeV in E_T^γ and $p_T^{\text{jet-lead}}$. The dependence on $m_T^{\gamma\text{-jet}}$ and $|\cos \theta^*|$ is measured for $m_T^{\gamma\text{-jet}} > 450$ GeV.

The predictions of the tree-level plus parton-shower MC models by PYTHIA and LO SHERPA give a satisfactory description of the shape of the data distributions, except for $p_T^{\text{jet-lead}}$ in the case of PYTHIA. The fixed-order NLO QCD calculations of JETPHOX, corrected for hadronisation and UE effects, and the multi-leg NLO QCD plus parton-shower calculations of SHERPA describe the measured cross sections within the experimental and theoretical uncertainties. The comparison of predictions based on different parameterisations of the proton PDFs shows that the description of the data achieved does not depend significantly on the specific PDF set used. The only well-founded prediction for $d\sigma/d\Delta\phi^{\gamma\text{-jet}}$ is that of NLO SHERPA, which is able to reproduce the data down to $\Delta\phi^{\gamma\text{-jet}} = \pi/2$ due to the inclusion of the matrix elements for $2 \rightarrow n$ processes with $n = 4$ and 5. The measured dependence on $|\cos \theta^*|$ is consistent with the dominance of processes in which a quark is exchanged. All these studies provide tests of the pQCD description of the dynamics of isolated-photon plus jet production in pp collisions at $\sqrt{s} = 13$ TeV. The experimental uncertainties are, in general, much smaller than the uncertainties in the predictions and, thus, calculations with higher precision will allow stringent tests of the theory.

Acknowledgements

We thank CERN for the very successful operation of the LHC, as well as the support staff from our institutions without whom ATLAS could not be operated efficiently.

We acknowledge the support of ANPCyT, Argentina; YerPhI, Armenia; ARC, Australia; BMWFW and FWF, Austria; ANAS, Azerbaijan; SSTC, Belarus; CNPq and FAPESP, Brazil; NSERC, NRC and CFI, Canada; CERN; CONICYT, Chile; CAS, MOST and NSFC, China; COLCIENCIAS, Colombia; MSMT CR, MPO CR and VSC CR, Czech Republic; DNRF and DNSRC, Denmark; IN2P3-CNRS, CEA-DRF/IRFU, France; SRNSFG, Georgia; BMBF, HGF, and MPG, Germany; GSRT, Greece; RGC, Hong Kong SAR, China; ISF, I-CORE and Benoziyo Center, Israel; INFN, Italy; MEXT and JSPS, Japan; CNRST, Morocco;

⁸ As shown in Ref. [1], the NLO QCD predictions of JETPHOX cannot describe $d\sigma/d\Delta\phi^{\gamma\text{-jet}}$ due to the limited number of final-state partons.

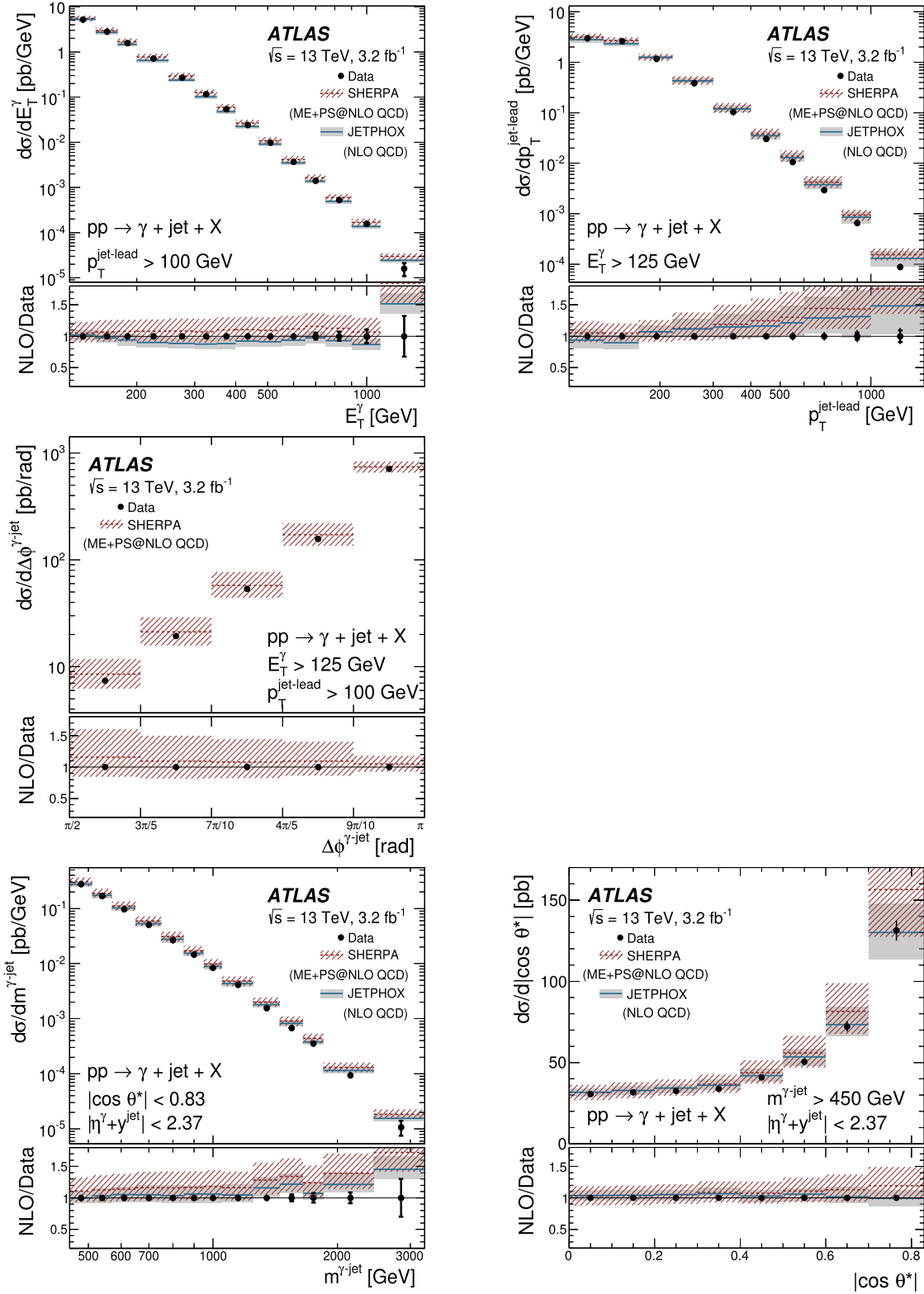


Fig. 5. Measured cross sections for isolated-photon plus jet production (dots) as functions of E_T^γ , $p_T^{\text{jet-lead}}$, $\Delta\phi^{\gamma\text{-jet}}$, $m^{\gamma\text{-jet}}$ and $|\cos\theta^*|$; the observables are constructed using the leading photon and the leading jet. For comparison, the multi-leg NLO QCD plus parton shower predictions from NLO SHERPA (dashed lines) and the NLO QCD predictions from JETPHOX corrected for hadronisation and UE effects (solid lines) are also shown. The bottom part of each figure shows the ratios of the predictions to the measured cross section. The inner (outer) error bars represent the statistical uncertainties (the statistical and systematic uncertainties added in quadrature) and the bands display the theoretical uncertainty. For most of the points, the inner error bars are smaller than the marker size and, thus, not visible.

NWO, Netherlands; RCN, Norway; MNiSW and NCN, Poland; FCT, Portugal; MNE/IFA, Romania; MES of Russia and NRC KI, Russian Federation; JINR; MESTD, Serbia; MSSR, Slovakia; ARRS and MIZŠ, Slovenia; DST/NRF, South Africa; MINECO, Spain; SRC and Wallenberg Foundation, Sweden; SERI, SNSF and Cantons of Bern and Geneva, Switzerland; MOST, Taiwan; TAEK, Turkey; STFC, United Kingdom; DOE and NSF, United States of America. In addition, individual groups and members have received support from BCKDF, the Canada Council, Canarie, CRC, Compute Canada, FQRNT, and the Ontario Innovation Trust, Canada; EPLANET, ERC, ERDF, FP7, Horizon 2020 and Marie Skłodowska-Curie Actions, European Union; Investissements d'Avenir Labex and Idex, ANR, Région Auvergne and Fondation Partager le Savoir, France; DFG and AvH Foundation, Germany; Herakleitos, Thales and Aristeia programmes co-financed by EU-ESF and the Greek NSRF; BSF, GIF and Minerva, Israel; BRF, Norway; CERCA Programme Generalitat de Catalunya, Generalitat Valenciana, Spain; the Royal Society and Leverhulme Trust, United Kingdom.

The crucial computing support from all WLCG partners is acknowledged gratefully, in particular from CERN, the ATLAS Tier-1 facilities at TRIUMF (Canada), NDGF (Denmark, Norway, Sweden), CC-IN2P3 (France), KIT/GridKA (Germany), INFN-CNAF (Italy), NL-T1 (Netherlands), PIC (Spain), ASGC (Taiwan), RAL (UK) and BNL (USA), the Tier-2 facilities worldwide and large non-WLCG resource providers. Major contributors of computing resources are listed in Ref. [61].

References

- [1] ATLAS Collaboration, Dynamics of isolated-photon plus jet production in pp collisions at $\sqrt{s} = 7$ TeV with the ATLAS detector, Nucl. Phys. B 875 (2013) 483, arXiv:1307.6795 [hep-ex].
- [2] ATLAS Collaboration, High- E_T isolated-photon plus jets production in pp collisions at $\sqrt{s} = 8$ TeV with the ATLAS detector, Nucl. Phys. B 918 (2017) 257, arXiv:1611.06586 [hep-ex].
- [3] ATLAS Collaboration, Search for new phenomena with photon+jet events in proton–proton collisions at $\sqrt{s} = 13$ TeV with the ATLAS detector, J. High Energy Phys. 1603 (2016) 041, arXiv:1512.05910 [hep-ex].
- [4] ATLAS Collaboration, Search for new phenomena in high-mass final states with a photon and a jet from pp collisions at $\sqrt{s} = 13$ TeV with the ATLAS detector, arXiv:1709.10440 [hep-ex], 2017.
- [5] T. Pietrycki, A. Szczurek, Photon–jet correlations in pp and $p\bar{p}$ collisions, Phys. Rev. D 76 (2007) 034003, arXiv:0704.2158 [hep-ph].
- [6] Z. Belghobsi, et al., Photon–jet correlations and constraints on fragmentation functions, Phys. Rev. D 79 (2009) 114024, arXiv:0903.4834 [hep-ph].
- [7] ATLAS Collaboration, Measurement of the production cross section of an isolated photon associated with jets in proton–proton collisions at $\sqrt{s} = 7$ TeV with the ATLAS detector, Phys. Rev. D 85 (2012) 092014, arXiv:1203.3161 [hep-ex].
- [8] CMS Collaboration, Rapidity distributions in exclusive Z +jet and γ +jet events in pp collisions at $\sqrt{s} = 7$ TeV, Phys. Rev. D 88 (2013) 112009, arXiv:1310.3082 [hep-ex].
- [9] CMS Collaboration, Measurement of the triple-differential cross section for photon+jets production in proton–proton collisions at $\sqrt{s} = 7$ TeV, J. High Energy Phys. 1406 (2014) 009, arXiv:1311.6141 [hep-ex].
- [10] CMS Collaboration, Comparison of the $Z/\gamma^* + \text{jets}$ to $\gamma + \text{jets}$ cross sections in pp collisions at $\sqrt{s} = 8$ TeV, J. High Energy Phys. 1510 (2015) 128, arXiv:1505.06520 [hep-ex].
- [11] T. Gleisberg, et al., Event generation with SHERPA 1.1, J. High Energy Phys. 0902 (2009) 007, arXiv:0811.4622 [hep-ph].
- [12] T. Sjöstrand, S. Mrenna, P. Skands, A brief introduction to PYTHIA 8.1, Comput. Phys. Commun. 178 (2008) 852, arXiv:0710.3820 [hep-ph].
- [13] S. Catani, M. Fontannaz, J.Ph. Guillet, E. Pilon, Cross section of isolated prompt photons in hadron–hadron collisions, J. High Energy Phys. 0205 (2002) 028, arXiv:hep-ph/0204023.
- [14] P. Aurenche, J.Ph. Guillet, E. Pilon, M. Werlen, M. Fontannaz, Recent critical study of photon production in hadronic collisions, Phys. Rev. D 73 (2006) 094007, and references therein, arXiv:hep-ph/0602133.
- [15] ATLAS Collaboration, The ATLAS experiment at the CERN large hadron collider, J. Instrum. 3 (2008) S08003.
- [16] ATLAS Collaboration, ATLAS Insertable B-Layer Technical Design Report, CERN-LHCC-2010-013, ATLAS-TDR-19, 2010, <https://cds.cern.ch/record/1291633>, 2012, ATLAS Insertable B-Layer Technical Design Report Addendum, ATLAS-TDR-19-ADD-1, CERN-LHCC-2012-009, <https://cds.cern.ch/record/1451888>.
- [17] ATLAS Collaboration, Performance of the ATLAS trigger system in 2015, Eur. Phys. J. C 77 (2017) 317, arXiv:1611.09661 [hep-ex].
- [18] ATLAS Collaboration, Luminosity determination in pp collisions at $\sqrt{s} = 8$ TeV using the ATLAS detector at the LHC, Eur. Phys. J. C 76 (2016) 653, arXiv:1608.03953 [hep-ex].
- [19] B. Andersson, G. Gustafson, G. Ingelman, T. Sjöstrand, Parton fragmentation and string dynamics, Phys. Rep. 97 (1983) 31.
- [20] J.-C. Winter, F. Krauss, G. Soff, A modified cluster-hadronisation model, Eur. Phys. J. C 36 (2004) 381, arXiv:hep-ph/0311085.
- [21] NNPDF Collaboration, R.D. Ball, et al., Parton distributions with LHC data, Nucl. Phys. B 867 (2013) 244, arXiv:1207.1303 [hep-ph].
- [22] H.-L. Lai, et al., New parton distributions for collider physics, Phys. Rev. D 82 (2010) 074024, arXiv:1007.2241 [hep-ph].
- [23] ATLAS Collaboration, ATLAS Run 1 Pythia8 tunes, ATL-PHYS-PUB-2014-021, <https://cds.cern.ch/record/1966419>, 2014.
- [24] S. Höche, F. Krauss, S. Schumann, F. Siegert, QCD matrix elements and truncated showers, J. High Energy Phys. 0905 (2009) 053, arXiv:0903.1219 [hep-ph].
- [25] S. Frixione, Isolated photons in perturbative QCD, Phys. Lett. B 429 (1998) 369, arXiv:hep-ph/9801442.
- [26] S. Agostinelli, et al., Geant4—a simulation toolkit, Nucl. Instrum. Methods A 506 (2003) 250.
- [27] ATLAS Collaboration, The ATLAS simulation infrastructure, Eur. Phys. J. C 70 (2010) 823, arXiv:1005.4568 [physics.ins-det].
- [28] ATLAS Collaboration, Summary of ATLAS Pythia 8 tunes, ATL-PHYS-PUB-2012-003, <https://cds.cern.ch/record/1474107>, 2012.
- [29] ATLAS Collaboration, Measurement of the inelastic proton–proton cross-section at $\sqrt{s} = 7$ TeV with the ATLAS detector, Nat. Commun. 2 (2011) 463, arXiv:1104.0326 [hep-ex].
- [30] ATLAS Collaboration, Measurement of the photon identification efficiencies with the ATLAS detector using LHC Run-1 data, Eur. Phys. J. C 76 (2016) 666, arXiv:1606.01813 [hep-ex].
- [31] ATLAS Collaboration, Electron and photon energy calibration with the ATLAS detector using LHC Run 1 data, Eur. Phys. J. C 74 (2014) 3071, arXiv:1407.5063 [hep-ex].
- [32] ATLAS Collaboration, Topological cell clustering in the ATLAS calorimeters and its performance in LHC Run 1, Eur. Phys. J. C 77 (2017) 490, arXiv:1603.02934 [hep-ex].
- [33] ATLAS Collaboration, Measurement of the inclusive isolated prompt photon cross section in pp collisions at $\sqrt{s} = 7$ TeV with the ATLAS detector, Phys. Rev. D 83 (2011) 052005, arXiv:1012.4389 [hep-ex].
- [34] ATLAS Collaboration, Measurement of the inclusive isolated prompt photon cross-section in pp collisions at $\sqrt{s} = 7$ TeV using 35 pb^{-1} of ATLAS data, Phys. Lett. B 706 (2011) 150, arXiv:1108.0253 [hep-ex].
- [35] M. Cacciari, G.P. Salam, G. Soyez, The catchment area of jets, J. High Energy Phys. 0804 (2008) 005, arXiv:0802.1188 [hep-ph].
- [36] M. Cacciari, G.P. Salam, S. Sapeta, On the characterisation of the underlying event, J. High Energy Phys. 1004 (2010) 065, arXiv:0912.4926 [hep-ph].
- [37] S.D. Ellis, D.E. Soper, Successive combination jet algorithm for hadron collisions, Phys. Rev. D 48 (1993) 3160.
- [38] S. Catani, Yu.L. Dokshitzer, M.H. Seymour, B.R. Webber, Longitudinally-invariant k_T -clustering algorithms for hadron–hadron collisions, Nucl. Phys. B 406 (1993) 187.
- [39] ATLAS Collaboration, Measurement of the inclusive isolated prompt photon cross section in pp collisions at $\sqrt{s} = 8$ TeV with the ATLAS detector, J. High Energy Phys. 1608 (2016) 005, arXiv:1605.03495 [hep-ex].
- [40] M. Cacciari, G.P. Salam, G. Soyez, The anti- k_T jet clustering algorithm, J. High Energy Phys. 0804 (2008) 063, arXiv:0802.1189 [hep-ph].
- [41] M. Cacciari, G.P. Salam, G. Soyez, Fastjet user manual, Eur. Phys. J. C 72 (2012) 1896, arXiv:1111.6097 [hep-ph].
- [42] ATLAS Collaboration, Jet energy scale measurements and their systematic uncertainties in proton–proton collisions at $\sqrt{s} = 13$ TeV with the ATLAS detector, Phys. Rev. D 96 (2017) 072002, arXiv:1703.09665 [hep-ex].
- [43] ATLAS Collaboration, Jet global sequential corrections with the ATLAS detector in proton–proton collisions at $\sqrt{s} = 8$ TeV, ATLAS-CONF-2015-002, 2015, <https://cds.cern.ch/record/2001682>.
- [44] ATLAS Collaboration, Jet energy measurement and its systematic uncertainty in proton–proton collisions at $\sqrt{s} = 7$ TeV with the ATLAS detector, Eur. Phys. J. C 75 (2015) 17, arXiv:1406.0076 [hep-ex].
- [45] ATLAS Collaboration, Monte Carlo calibration and combination of in-situ measurements of jet energy scale, jet energy resolution and jet mass in ATLAS, ATLAS-CONF-2015-037, 2015, <https://cds.cern.ch/record/2044941>.
- [46] ATLAS Collaboration, Jet energy measurement with the ATLAS detector in proton–proton collisions at $\sqrt{s} = 7$ TeV, Eur. Phys. J. C 73 (2013) 2304, arXiv:1112.6426 [hep-ex].
- [47] ATLAS Collaboration, Measurement of the cross section for inclusive isolated-photon production in pp collisions at $\sqrt{s} = 13$ TeV using the ATLAS detector, Phys. Lett. B 770 (2017) 473, arXiv:1701.06882 [hep-ex].
- [48] F. Krauss, R. Kuhn, G. Soff, AMEGIC++ 1.0, A matrix element generator in C++, J. High Energy Phys. 0202 (2002) 044, arXiv:hep-ph/0109036.

- [49] F. Cascioli, P. Maierhöfer, S. Pozzorini, Scattering amplitudes with open loops, *Phys. Rev. Lett.* **108** (2012) 111601, arXiv:1111.5206 [hep-ph].
- [50] G. D'Agostini, A multidimensional unfolding method based on Bayes' theorem, *Nucl. Instrum. Methods A* **362** (1995) 487.
- [51] ATLAS Collaboration, Photon identification in 2015 ATLAS data, ATL-PHYS-PUB-2016-014, <https://cds.cern.ch/record/2203125>, 2016.
- [52] L.A. Harland-Lang, A.D. Martin, P. Motylinski, R.S. Thorne, Parton distributions in the LHC era: MMHT 2014 PDFs, *Eur. Phys. J. C* **75** (2015) 204, arXiv:1412.3989 [hep-ph].
- [53] L. Bourhis, M. Fontannaz, J.Ph. Guillet, Quark and gluon fragmentation functions into photons, *Eur. Phys. J. C* **2** (1998) 529, arXiv:hep-ph/9704447.
- [54] S. Schumann, F. Krauss, A parton shower algorithm based on Catani–Seymour dipole factorisation, *J. High Energy Phys.* **0803** (2008) 038, arXiv:0709.1027 [hep-ph].
- [55] S. Höche, F. Krauss, M. Schönherr, F. Siegert, QCD matrix elements + parton showers: the NLO case, *J. High Energy Phys.* **1304** (2013) 027, arXiv:1207.5030 [hep-ph].
- [56] F. Siegert, A practical guide to event generation for prompt photon production with Sherpa, *J. Phys. G* **44** (2017) 044007, arXiv:1611.07226 [hep-ph].
- [57] NNPDF Collaboration, R.D. Ball, et al., Parton distributions for the LHC run II, *J. High Energy Phys.* **1504** (2015) 040, arXiv:1410.8849 [hep-ph].
- [58] J. Pumplin, et al., Uncertainties of predictions from parton distribution functions. II. The Hessian method, *Phys. Rev. D* **65** (2001) 014013, arXiv:hep-ph/0101032.
- [59] J. Pumplin, et al., New generation of parton distributions with uncertainties from global QCD analysis, *J. High Energy Phys.* **0207** (2002) 012, arXiv:hep-ph/0201195.
- [60] S. Dulat, et al., New parton distribution functions from a global analysis of quantum chromodynamics, *Phys. Rev. D* **93** (2016) 033006, arXiv:1506.07443 [hep-ph].
- [61] ATLAS Collaboration, ATLAS computing acknowledgements 2016–2017, ATL-GEN-PUB-2016-002, <https://cds.cern.ch/record/2202407>, 2016.

The ATLAS Collaboration

M. Aaboud^{137d}, G. Aad⁸⁸, B. Abbott¹¹⁵, O. Abidinov^{12,*}, B. Abeloos¹¹⁹, S.H. Abidi¹⁶¹, O.S. AbouZeid¹³⁹, N.L. Abraham¹⁵¹, H. Abramowicz¹⁵⁵, H. Abreu¹⁵⁴, R. Abreu¹¹⁸, Y. Abulaiti^{148a,148b}, B.S. Acharya^{167a,167b,a}, S. Adachi¹⁵⁷, L. Adamczyk^{41a}, J. Adelman¹¹⁰, M. Adersberger¹⁰², T. Adye¹³³, A.A. Affolder¹³⁹, Y. Afik¹⁵⁴, T. Agatonovic-Jovin¹⁴, C. Agheorghiesei^{28c}, J.A. Aguilar-Saavedra^{128a,128f}, S.P. Ahlen²⁴, F. Ahmadov^{68,b}, G. Aielli^{135a,135b}, S. Akatsuka⁷¹, H. Akerstedt^{148a,148b}, T.P.A. Åkesson⁸⁴, E. Akilli⁵², A.V. Akimov⁹⁸, G.L. Alberghi^{22a,22b}, J. Albert¹⁷², P. Albicocco⁵⁰, M.J. Alconada Verzini⁷⁴, S.C. Alderweireldt¹⁰⁸, M. Aleksa³², I.N. Aleksandrov⁶⁸, C. Alexa^{28b}, G. Alexander¹⁵⁵, T. Alexopoulos¹⁰, M. Alhroob¹¹⁵, B. Ali¹³⁰, M. Aliev^{76a,76b}, G. Alimonti^{94a}, J. Alison³³, S.P. Alkire³⁸, B.M.M. Allbrooke¹⁵¹, B.W. Allen¹¹⁸, P.P. Allport¹⁹, A. Aloisio^{106a,106b}, A. Alonso³⁹, F. Alonso⁷⁴, C. Alpigiani¹⁴⁰, A.A. Alshehri⁵⁶, M.I. Alstady⁸⁸, B. Alvarez Gonzalez³², D. Álvarez Piqueras¹⁷⁰, M.G. Alvigi^{106a,106b}, B.T. Amadio¹⁶, Y. Amaral Coutinho^{26a}, C. Amelung²⁵, D. Amidei⁹², S.P. Amor Dos Santos^{128a,128c}, S. Amoroso³², G. Amundsen²⁵, C. Anastopoulos¹⁴¹, L.S. Ancu⁵², N. Andari¹⁹, T. Andeen¹¹, C.F. Anders^{60b}, J.K. Anders⁷⁷, K.J. Anderson³³, A. Andreazza^{94a,94b}, V. Andrei^{60a}, S. Angelidakis³⁷, I. Angelozzi¹⁰⁹, A. Angerami³⁸, A.V. Anisenkov^{111,c}, N. Anjos¹³, A. Annovi^{126a}, C. Antel^{60a}, M. Antonelli⁵⁰, A. Antonov^{100,*}, D.J. Antrim¹⁶⁶, F. Anulli^{134a}, M. Aoki⁶⁹, L. Aperio Bella³², G. Arabidze⁹³, Y. Arai⁶⁹, J.P. Araque^{128a}, V. Araujo Ferraz^{26a}, A.T.H. Arce⁴⁸, R.E. Ardell⁸⁰, F.A. Arduh⁷⁴, J-F. Arguin⁹⁷, S. Argyropoulos⁶⁶, M. Arik^{20a}, A.J. Armbruster³², L.J. Armitage⁷⁹, O. Arnaz¹⁶¹, H. Arnold⁵¹, M. Arratia³⁰, O. Arslan²³, A. Artamonov^{99,*}, G. Artoni¹²², S. Artz⁸⁶, S. Asai¹⁵⁷, N. Asbah⁴⁵, A. Ashkenazi¹⁵⁵, L. Asquith¹⁵¹, K. Assamagan²⁷, R. Astalos^{146a}, M. Atkinson¹⁶⁹, N.B. Atlay¹⁴³, K. Augsten¹³⁰, G. Avolio³², B. Axen¹⁶, M.K. Ayoub^{35a}, G. Azuelos^{97,d}, A.E. Baas^{60a}, M.J. Baca¹⁹, H. Bachacou¹³⁸, K. Bachas^{76a,76b}, M. Backes¹²², P. Bagnaia^{134a,134b}, M. Bahmani⁴², H. Bahrasemani¹⁴⁴, J.T. Baines¹³³, M. Bajic³⁹, O.K. Baker¹⁷⁹, P.J. Bakker¹⁰⁹, E.M. Baldin^{111,c}, P. Balek¹⁷⁵, F. Balli¹³⁸, W.K. Balunas¹²⁴, E. Banas⁴², A. Bandyopadhyay²³, Sw. Banerjee^{176,e}, A.A.E. Bannoura¹⁷⁸, L. Barak¹⁵⁵, E.L. Barberio⁹¹, D. Barberis^{53a,53b}, M. Barbero⁸⁸, T. Barillari¹⁰³, M-S Barisits³², J.T. Barkeloo¹¹⁸, T. Barklow¹⁴⁵, N. Barlow³⁰, S.L. Barnes^{36c}, B.M. Barnett¹³³, R.M. Barnett¹⁶, Z. Barnovska-Blenessy^{36a}, A. Baroncelli^{136a}, G. Barone²⁵, A.J. Barr¹²², L. Barranco Navarro¹⁷⁰, F. Barreiro⁸⁵, J. Barreiro Guimarães da Costa^{35a}, R. Bartoldus¹⁴⁵, A.E. Barton⁷⁵, P. Bartos^{146a}, A. Basalae¹²⁵, A. Bassalat^{119,f}, R.L. Bates⁵⁶, S.J. Batista¹⁶¹, J.R. Batley³⁰, M. Battaglia¹³⁹, M. Bause^{134a,134b}, F. Bauer¹³⁸, H.S. Bawa^{145,g}, J.B. Beacham¹¹³, M.D. Beattie⁷⁵, T. Beau⁸³, P.H. Beauchemin¹⁶⁵, P. Bechtel²³, H.P. Beck^{18,h}, H.C. Beck⁵⁷, K. Becker¹²², M. Becker⁸⁶, C. Becot¹¹², A.J. Beddall^{20e}, A. Beddall^{20b}, V.A. Bednyakov⁶⁸, M. Bedognetti¹⁰⁹, C.P. Bee¹⁵⁰, T.A. Beermann³², M. Begalli^{26a}, M. Begel²⁷, J.K. Behr⁴⁵, A.S. Bell⁸¹, G. Bella¹⁵⁵, L. Bellagamba^{22a}, A. Bellerive³¹, M. Bellomo¹⁵⁴, K. Belotskiy¹⁰⁰, O. Beltramello³², N.L. Belyaev¹⁰⁰, O. Benary^{155,*}, D. Bencheekroun^{137a}, M. Bender¹⁰², N. Benekos¹⁰, Y. Benhammou¹⁵⁵, E. Benhar Noccioli¹⁷⁹, J. Benitez⁶⁶, D.P. Benjamin⁴⁸, M. Benoit⁵², J.R. Bensinger²⁵, S. Bentvelsen¹⁰⁹, L. Beresford¹²², M. Beretta⁵⁰, D. Berge¹⁰⁹, E. Bergeaas Kuutmann¹⁶⁸, N. Berger⁵, L.J. Bergsten²⁵, J. Beringer¹⁶, S. Berlendis⁵⁸, N.R. Bernard⁸⁹, G. Bernardi⁸³, C. Bernius¹⁴⁵, F.U. Bernlochner²³, T. Berry⁸⁰, P. Berta⁸⁶, C. Bertella^{35a}, G. Bertoli^{148a,148b}, I.A. Bertram⁷⁵, C. Bertsche⁴⁵, G.J. Besjes³⁹, O. Bessidskaia Bylund^{148a,148b}, M. Bessner⁴⁵, N. Besson¹³⁸, A. Bethani⁸⁷,

S. Bethke¹⁰³, A. Betti²³, A.J. Bevan⁷⁹, J. Beyer¹⁰³, R.M. Bianchi¹²⁷, O. Biebel¹⁰², D. Biedermann¹⁷, R. Bielski⁸⁷, K. Bierwagen⁸⁶, N.V. Biesuz^{126a,126b}, M. Biglietti^{136a}, T.R.V. Billoud⁹⁷, H. Bilokon⁵⁰, M. Bindi⁵⁷, A. Bingul^{20b}, C. Bini^{134a,134b}, S. Biondi^{22a,22b}, T. Bisanz⁵⁷, C. Bittrich⁴⁷, D.M. Bjergaard⁴⁸, J.E. Black¹⁴⁵, K.M. Black²⁴, R.E. Blair⁶, T. Blazek^{146a}, I. Bloch⁴⁵, C. Blocker²⁵, A. Blue⁵⁶, U. Blumenschein⁷⁹, Dr. Blunier^{34a}, G.J. Bobbink¹⁰⁹, V.S. Bobrovnikov^{111,c}, S.S. Bocchetta⁸⁴, A. Bocci⁴⁸, C. Bock¹⁰², M. Boehler⁵¹, D. Boerner¹⁷⁸, D. Bogavac¹⁰², A.G. Bogdanchikov¹¹¹, C. Boehm^{148a}, V. Boisvert⁸⁰, P. Bokan^{168,i}, T. Bold^{41a}, A.S. Boldyrev¹⁰¹, A.E. Bolz^{60b}, M. Bomben⁸³, M. Bona⁷⁹, M. Boonekamp¹³⁸, A. Borisov¹³², G. Borissov⁷⁵, J. Bortfeldt³², D. Bortoletto¹²², V. Bortolotto^{62a}, D. Boscherini^{22a}, M. Bosman¹³, J.D. Bossio Sola²⁹, J. Boudreau¹²⁷, E.V. Bouhova-Thacker⁷⁵, D. Boumediene³⁷, C. Bourdarios¹¹⁹, S.K. Boutle⁵⁶, A. Boveia¹¹³, J. Boyd³², I.R. Boyko⁶⁸, A.J. Bozson⁸⁰, J. Bracinik¹⁹, A. Brandt⁸, G. Brandt⁵⁷, O. Brandt^{60a}, F. Braren⁴⁵, U. Bratzler¹⁵⁸, B. Brau⁸⁹, J.E. Brau¹¹⁸, W.D. Breaden Madden⁵⁶, K. Brendlinger⁴⁵, A.J. Brennan⁹¹, L. Brenner¹⁰⁹, R. Brenner¹⁶⁸, S. Bressler¹⁷⁵, D.L. Briglin¹⁹, T.M. Bristow⁴⁹, D. Britton⁵⁶, D. Britzger⁴⁵, F.M. Brochu³⁰, I. Brock²³, R. Brock⁹³, G. Brooijmans³⁸, T. Brooks⁸⁰, W.K. Brooks^{34b}, J. Brosamer¹⁶, E. Brost¹¹⁰, J.H. Broughton¹⁹, P.A. Bruckman de Renstrom⁴², D. Bruncko^{146b}, A. Bruni^{22a}, G. Bruni^{22a}, L.S. Bruni¹⁰⁹, S. Bruno^{135a,135b}, B.H. Brunt³⁰, M. Bruschi^{22a}, N. Bruscino¹²⁷, P. Bryant³³, L. Bryngemark⁴⁵, T. Buanes¹⁵, Q. Buat¹⁴⁴, P. Buchholz¹⁴³, A.G. Buckley⁵⁶, I.A. Budagov⁶⁸, F. Buehrer⁵¹, M.K. Bugge¹²¹, O. Bulekov¹⁰⁰, D. Bullock⁸, T.J. Burch¹¹⁰, S. Burdin⁷⁷, C.D. Burgard¹⁰⁹, A.M. Burger⁵, B. Burghgrave¹¹⁰, K. Burka⁴², S. Burke¹³³, I. Burmeister⁴⁶, J.T.P. Burr¹²², D. Büscher⁵¹, V. Büscher⁸⁶, P. Bussey⁵⁶, J.M. Butler²⁴, C.M. Buttar⁵⁶, J.M. Butterworth⁸¹, P. Butti³², W. Buttinger²⁷, A. Buzatu¹⁵³, A.R. Buzykaev^{111,c}, S. Cabrera Urbán¹⁷⁰, D. Caforio¹³⁰, H. Cai¹⁶⁹, V.M. Cairo^{40a,40b}, O. Cakir^{4a}, N. Calace⁵², P. Calafiura¹⁶, A. Calandri⁸⁸, G. Calderini⁸³, P. Calfayan⁶⁴, G. Callea^{40a,40b}, L.P. Caloba^{26a}, S. Calvente Lopez⁸⁵, D. Calvet³⁷, S. Calvet³⁷, T.P. Calvet⁸⁸, R. Camacho Toro³³, S. Camarda³², P. Camarri^{135a,135b}, D. Cameron¹²¹, R. Caminal Armadans¹⁶⁹, C. Camincher⁵⁸, S. Campana³², M. Campanelli⁸¹, A. Camplani^{94a,94b}, A. Campoverde¹⁴³, V. Canale^{106a,106b}, M. Cano Bret^{36c}, J. Cantero¹¹⁶, T. Cao¹⁵⁵, M.D.M. Capeans Garrido³², I. Caprini^{28b}, M. Caprini^{28b}, M. Capua^{40a,40b}, R.M. Carbone³⁸, R. Cardarelli^{135a}, F. Cardillo⁵¹, I. Carli¹³¹, T. Carli³², G. Carlino^{106a}, B.T. Carlson¹²⁷, L. Carminati^{94a,94b}, R.M.D. Carney^{148a,148b}, S. Caron¹⁰⁸, E. Carquin^{34b}, S. Carrá^{94a,94b}, G.D. Carrillo-Montoya³², D. Casadei¹⁹, M.P. Casado^{13,j}, A.F. Casha¹⁶¹, M. Casolino¹³, D.W. Casper¹⁶⁶, R. Castelijns¹⁰⁹, V. Castillo Gimenez¹⁷⁰, N.F. Castro^{128a,k}, A. Catinaccio³², J.R. Catmore¹²¹, A. Cattai³², J. Caudron²³, V. Cavaliere¹⁶⁹, E. Cavallaro¹³, D. Cavalli^{94a}, M. Cavalli-Sforza¹³, V. Cavasinni^{126a,126b}, E. Celebi^{20d}, F. Ceradini^{136a,136b}, L. Cerda Alberich¹⁷⁰, A.S. Cerqueira^{26b}, A. Cerri¹⁵¹, L. Cerrito^{135a,135b}, F. Cerutti¹⁶, A. Cervelli^{22a,22b}, S.A. Cetin^{20d}, A. Chafaq^{137a}, D. Chakraborty¹¹⁰, S.K. Chan⁵⁹, W.S. Chan¹⁰⁹, Y.L. Chan^{62a}, P. Chang¹⁶⁹, J.D. Chapman³⁰, D.G. Charlton¹⁹, C.C. Chau³¹, C.A. Chavez Barajas¹⁵¹, S. Che¹¹³, S. Cheatham^{167a,167c}, A. Chegwidden⁹³, S. Chekanov⁶, S.V. Chekulaev^{163a}, G.A. Chelkov^{68,l}, M.A. Chelstowska³², C. Chen^{36a}, C. Chen⁶⁷, H. Chen²⁷, J. Chen^{36a}, S. Chen^{35b}, S. Chen¹⁵⁷, X. Chen^{35c,m}, Y. Chen⁷⁰, H.C. Cheng⁹², H.J. Cheng^{35a,35d}, A. Cheplakov⁶⁸, E. Cheremushkina¹³², R. Cherkouhi El Moursli^{137e}, E. Cheu⁷, K. Cheung⁶³, L. Chevalier¹³⁸, V. Chiarella⁵⁰, G. Chiarelli^{126a}, G. Chiodini^{76a}, A.S. Chisholm³², A. Chitan^{28b}, Y.H. Chiu¹⁷², M.V. Chizhov⁶⁸, K. Choi⁶⁴, A.R. Chomont³⁷, S. Chouridou¹⁵⁶, Y.S. Chow^{62a}, V. Christodoulou⁸¹, M.C. Chu^{62a}, J. Chudoba¹²⁹, A.J. Chuinard⁹⁰, J.J. Chwastowski⁴², L. Chytka¹¹⁷, A.K. Ciftci^{4a}, D. Cinca⁴⁶, V. Cindro⁷⁸, I.A. Cioara²³, A. Ciochio¹⁶, F. Ciotto^{106a,106b}, Z.H. Citron¹⁷⁵, M. Citterio^{94a}, M. Ciubancan^{28b}, A. Clark⁵², B.L. Clark⁵⁹, M.R. Clark³⁸, P.J. Clark⁴⁹, R.N. Clarke¹⁶, C. Clement^{148a,148b}, Y. Coadou⁸⁸, M. Cobal^{167a,167c}, A. Coccaro⁵², J. Cochran⁶⁷, L. Colasurdo¹⁰⁸, B. Cole³⁸, A.P. Colijn¹⁰⁹, J. Collot⁵⁸, T. Colombo¹⁶⁶, P. Conde Muiño^{128a,128b}, E. Coniavitis⁵¹, S.H. Connell^{147b}, I.A. Connelly⁸⁷, S. Constantinescu^{28b}, G. Conti³², F. Conventi^{106a,n}, M. Cooke¹⁶, A.M. Cooper-Sarkar¹²², F. Cormier¹⁷¹, K.J.R. Cormier¹⁶¹, M. Corradi^{134a,134b}, F. Corriveau^{90,o}, A. Cortes-Gonzalez³², G. Costa^{94a}, M.J. Costa¹⁷⁰, D. Costanzo¹⁴¹, G. Cottin³⁰, G. Cowan⁸⁰, B.E. Cox⁸⁷, K. Cranmer¹¹², S.J. Crawley⁵⁶, R.A. Creager¹²⁴, G. Cree³¹, S. Crépe-Renaudin⁵⁸, F. Crescioli⁸³, W.A. Cribbs^{148a,148b}, M. Cristinziani²³, V. Croft¹¹², G. Crosetti^{40a,40b}, A. Cueto⁸⁵, T. Cuhadar Donszelmann¹⁴¹, A.R. Cukierman¹⁴⁵, J. Cummings¹⁷⁹, M. Curatolo⁵⁰, J. Cúth⁸⁶, S. Czekaierda⁴², P. Czodrowski³², G. D'amen^{22a,22b}, S. D'Auria⁵⁶, L. D'eraimo⁸³, M. D'Onofrio⁷⁷, M.J. Da Cunha Sargedadas De Sousa^{128a,128b}, C. Da Via⁸⁷, W. Dabrowski^{41a}, T. Dado^{146a}, T. Dai⁹²,

O. Dale¹⁵, F. Dallaire⁹⁷, C. Dallapiccola⁸⁹, M. Dam³⁹, J.R. Dandoy¹²⁴, M.F. Daneri²⁹, N.P. Dang¹⁷⁶, A.C. Daniells¹⁹, N.S. Dann⁸⁷, M. Danninger¹⁷¹, M. Dano Hoffmann¹³⁸, V. Dao¹⁵⁰, G. Darbo^{53a}, S. Darmora⁸, J. Dassoulas³, A. Dattagupta¹¹⁸, T. Daubney⁴⁵, W. Davey²³, C. David⁴⁵, T. Davidek¹³¹, D.R. Davis⁴⁸, P. Davison⁸¹, E. Dawe⁹¹, I. Dawson¹⁴¹, K. De⁸, R. de Asmundis^{106a}, A. De Benedetti¹¹⁵, S. De Castro^{22a,22b}, S. De Cecco⁸³, N. De Groot¹⁰⁸, P. de Jong¹⁰⁹, H. De la Torre⁹³, F. De Lorenzi⁶⁷, A. De Maria⁵⁷, D. De Pedis^{134a}, A. De Salvo^{134a}, U. De Sanctis^{135a,135b}, A. De Santo¹⁵¹, K. De Vasconcelos Corga⁸⁸, J.B. De Vivie De Regie¹¹⁹, R. Debbe²⁷, C. Debenedetti¹³⁹, D.V. Dedovich⁶⁸, N. Dehghanian³, I. Deigaard¹⁰⁹, M. Del Gaudio^{40a,40b}, J. Del Peso⁸⁵, D. Delgove¹¹⁹, F. Deliot¹³⁸, C.M. Delitzsch⁷, A. Dell'Acqua³², L. Dell'Asta²⁴, M. Dell'Orso^{126a,126b}, M. Della Pietra^{106a,106b}, D. della Volpe⁵², M. Delmastro⁵, C. Delporte¹¹⁹, P.A. Delsart⁵⁸, D.A. DeMarco¹⁶¹, S. Demers¹⁷⁹, M. Demichev⁶⁸, A. Demilly⁸³, S.P. Denisov¹³², D. Denysiuk¹³⁸, D. Derendarz⁴², J.E. Derkaoui^{137d}, F. Derue⁸³, P. Dervan⁷⁷, K. Desch²³, C. Deterre⁴⁵, K. Dette¹⁶¹, M.R. Devesa²⁹, P.O. Deviveiros³², A. Dewhurst¹³³, S. Dhaliwal²⁵, F.A. Di Bello⁵², A. Di Ciaccio^{135a,135b}, L. Di Ciaccio⁵, W.K. Di Clemente¹²⁴, C. Di Donato^{106a,106b}, A. Di Girolamo³², B. Di Girolamo³², B. Di Micco^{136a,136b}, R. Di Nardo³², K.F. Di Petrillo⁵⁹, A. Di Simone⁵¹, R. Di Sipio¹⁶¹, D. Di Valentino³¹, C. Diaconu⁸⁸, M. Diamond¹⁶¹, F.A. Dias³⁹, M.A. Diaz^{34a}, J. Dickinson¹⁶, E.B. Diehl⁹², J. Dietrich¹⁷, S. Díez Cornell⁴⁵, A. Dimitrievska¹⁴, J. Dingfelder²³, P. Dita^{28b}, S. Dita^{28b}, F. Dittus³², F. Djama⁸⁸, T. Djobava^{54b}, J.I. Djuvsland^{60a}, M.A.B. do Vale^{26c}, D. Dobos³², M. Dobre^{28b}, D. Dodsworth²⁵, C. Doglioni⁸⁴, J. Dolejsi¹³¹, Z. Dolezal¹³¹, M. Donadelli^{26d}, S. Donati^{126a,126b}, P. Dondero^{123a,123b}, J. Donini³⁷, J. Dopke¹³³, A. Doria^{106a}, M.T. Dova⁷⁴, A.T. Doyle⁵⁶, E. Drechsler⁵⁷, M. Dris¹⁰, Y. Du^{36b}, J. Duarte-Campderros¹⁵⁵, F. Dubinin⁹⁸, A. Dubreuil⁵², E. Duchovni¹⁷⁵, G. Duckeck¹⁰², A. Ducourthial⁸³, O.A. Ducu^{97,p}, D. Duda¹⁰⁹, A. Dudarev³², A.Ch. Dudder⁸⁶, E.M. Duffield¹⁶, L. Duflost¹¹⁹, M. Dührssen³², C. Dulsen¹⁷⁸, M. Dumancic¹⁷⁵, A.E. Dumitriu^{28b}, A.K. Duncan⁵⁶, M. Dunford^{60a}, A. Duperrin⁸⁸, H. Duran Yildiz^{4a}, M. Düren⁵⁵, A. Durglishvili^{54b}, D. Duschinger⁴⁷, B. Dutta⁴⁵, D. Duvnjak¹, M. Dyndal⁴⁵, B.S. Dziedzic⁴², C. Eckardt⁴⁵, K.M. Ecker¹⁰³, R.C. Edgar⁹², T. Eifert³², G. Eigen¹⁵, K. Einsweiler¹⁶, T. Ekelof¹⁶⁸, M. El Kacimi^{137c}, R. El Kosseifi⁸⁸, V. Ellajosyula⁸⁸, M. Ellert¹⁶⁸, S. Elles⁵, F. Ellinghaus¹⁷⁸, A.A. Elliot¹⁷², N. Ellis³², J. Elmsheuser²⁷, M. Elsing³², D. Emelianov¹³³, Y. Enari¹⁵⁷, J.S. Ennis¹⁷³, M.B. Epland⁴⁸, J. Erdmann⁴⁶, A. Ereditato¹⁸, M. Ernst²⁷, S. Errede¹⁶⁹, M. Escalier¹¹⁹, C. Escobar¹⁷⁰, B. Esposito⁵⁰, O. Estrada Pastor¹⁷⁰, A.I. Etievre¹³⁸, E. Etzion¹⁵⁵, H. Evans⁶⁴, A. Ezhilov¹²⁵, M. Ezzi^{137e}, F. Fabbri^{22a,22b}, L. Fabbri^{22a,22b}, V. Fabiani¹⁰⁸, G. Facini⁸¹, R.M. Fakhruddinov¹³², S. Falciano^{134a}, R.J. Falla⁸¹, J. Faltova³², Y. Fang^{35a}, M. Fanti^{94a,94b}, A. Farbin⁸, A. Farilla^{136a}, C. Farina¹²⁷, E.M. Farina^{123a,123b}, T. Farooque⁹³, S. Farrell¹⁶, S.M. Farrington¹⁷³, P. Farthouat³², F. Fassi^{137e}, P. Fassnacht³², D. Fassoulitis⁹, M. Faucci Giannelli⁴⁹, A. Favareto^{53a,53b}, W.J. Fawcett¹²², L. Fayard¹¹⁹, O.L. Fedin^{125,q}, W. Fedorko¹⁷¹, S. Feigl¹²¹, L. Feligioni⁸⁸, C. Feng^{36b}, E.J. Feng³², M.J. Fenton⁵⁶, A.B. Fenyuk¹³², L. Feremenga⁸, P. Fernandez Martinez¹⁷⁰, J. Ferrando⁴⁵, A. Ferrari¹⁶⁸, P. Ferrari¹⁰⁹, R. Ferrari^{123a}, D.E. Ferreira de Lima^{60b}, A. Ferrer¹⁷⁰, D. Ferrere⁵², C. Ferretti⁹², F. Fiedler⁸⁶, A. Filipčič⁷⁸, M. Filipuzzi⁴⁵, F. Filthaut¹⁰⁸, M. Fincke-Keeler¹⁷², K.D. Finelli²⁴, M.C.N. Fiolhais^{128a,128c,r}, L. Fiorini¹⁷⁰, A. Fischer², C. Fischer¹³, J. Fischer¹⁷⁸, W.C. Fisher⁹³, N. Flaschel⁴⁵, I. Fleck¹⁴³, P. Fleischmann⁹², R.R.M. Fletcher¹²⁴, T. Flick¹⁷⁸, B.M. Flierl¹⁰², L.R. Flores Castillo^{62a}, M.J. Flowerdew¹⁰³, G.T. Forcolin⁸⁷, A. Formica¹³⁸, F.A. Förster¹³, A. Forti⁸⁷, A.G. Foster¹⁹, D. Fournier¹¹⁹, H. Fox⁷⁵, S. Fracchia¹⁴¹, P. Francavilla^{126a,126b}, M. Franchini^{22a,22b}, S. Franchino^{60a}, D. Francis³², L. Franconi¹²¹, M. Franklin⁵⁹, M. Frate¹⁶⁶, M. Fraternali^{123a,123b}, D. Freeborn⁸¹, S.M. Fressard-Batraneanu³², B. Freund⁹⁷, D. Froidevaux³², J.A. Frost¹²², C. Fukunaga¹⁵⁸, T. Fusayasu¹⁰⁴, J. Fuster¹⁷⁰, O. Gabizon¹⁵⁴, A. Gabrielli^{22a,22b}, A. Gabrielli¹⁶, G.P. Gach^{41a}, S. Gadatsch³², S. Gadomski⁸⁰, G. Gagliardi^{53a,53b}, L.G. Gagnon⁹⁷, C. Galea¹⁰⁸, B. Galhardo^{128a,128c}, E.J. Gallas¹²², B.J. Gallop¹³³, P. Gallus¹³⁰, G. Galster³⁹, K.K. Gan¹¹³, S. Ganguly³⁷, Y. Gao⁷⁷, Y.S. Gao^{145,g}, F.M. Garay Walls^{34a}, C. García¹⁷⁰, J.E. García Navarro¹⁷⁰, J.A. García Pascual^{35a}, M. Garcia-Sciveres¹⁶, R.W. Gardner³³, N. Garelli¹⁴⁵, V. Garonne¹²¹, A. Gascon Bravo⁴⁵, K. Gasnikova⁴⁵, C. Gatti⁵⁰, A. Gaudiello^{53a,53b}, G. Gaudio^{123a}, I.L. Gavrilenko⁹⁸, C. Gay¹⁷¹, G. Gaycken²³, E.N. Gazis¹⁰, C.N.P. Gee¹³³, J. Geisen⁵⁷, M. Geisen⁸⁶, M.P. Geisler^{60a}, K. Gellerstedt^{148a,148b}, C. Gemme^{53a}, M.H. Genest⁵⁸, C. Geng⁹², S. Gentile^{134a,134b}, C. Gentsos¹⁵⁶, S. George⁸⁰, D. Gerbaudo¹³, G. Geßner⁴⁶, S. Ghasemi¹⁴³, M. Ghneimat²³, B. Giacobbe^{22a}, S. Giagu^{134a,134b}, N. Giangiacomi^{22a,22b},

P. Giannetti ^{126a}, S.M. Gibson ⁸⁰, M. Gignac ¹⁷¹, M. Gilchriese ¹⁶, D. Gillberg ³¹, G. Gilles ¹⁷⁸, D.M. Gingrich ^{3,d}, M.P. Giordani ^{167a,167c}, F.M. Giorgi ^{22a}, P.F. Giraud ¹³⁸, P. Giromini ⁵⁹, G. Giugliarelli ^{167a,167c}, D. Giugni ^{94a}, F. Giuli ¹²², C. Giuliani ¹⁰³, M. Giulini ^{60b}, B.K. Gjelsten ¹²¹, S. Gkaitatzis ¹⁵⁶, I. Gkialas ^{9,s}, E.L. Gkoukousis ¹³, P. Gkoutoumis ¹⁰, L.K. Gladilin ¹⁰¹, C. Glasman ⁸⁵, J. Glatzer ¹³, P.C.F. Glaysheer ⁴⁵, A. Glazov ⁴⁵, M. Goblirsch-Kolb ²⁵, J. Godlewski ⁴², S. Goldfarb ⁹¹, T. Golling ⁵², D. Golubkov ¹³², A. Gomes ^{128a,128b,128d}, R. Gonçalo ^{128a}, R. Goncalves Gama ^{26a}, J. Goncalves Pinto Firmino Da Costa ¹³⁸, G. Gonella ⁵¹, L. Gonella ¹⁹, A. Gongadze ⁶⁸, J.L. Gonski ⁵⁹, S. González de la Hoz ¹⁷⁰, S. Gonzalez-Sevilla ⁵², L. Goossens ³², P.A. Gorbounov ⁹⁹, H.A. Gordon ²⁷, I. Gorelov ¹⁰⁷, B. Gorini ³², E. Gorini ^{76a,76b}, A. Gorišek ⁷⁸, A.T. Goshaw ⁴⁸, C. Gössling ⁴⁶, M.I. Gostkin ⁶⁸, C.A. Gottardo ²³, C.R. Goudet ¹¹⁹, D. Goujdami ^{137c}, A.G. Goussiou ¹⁴⁰, N. Govender ^{147b,t}, E. Gozani ¹⁵⁴, I. Grabowska-Bold ^{41a}, P.O.J. Gradin ¹⁶⁸, J. Gramling ¹⁶⁶, E. Gramstad ¹²¹, S. Grancagnolo ¹⁷, V. Gratchev ¹²⁵, P.M. Gravila ^{28f}, C. Gray ⁵⁶, H.M. Gray ¹⁶, Z.D. Greenwood ^{82,u}, C. Grefe ²³, K. Gregersen ⁸¹, I.M. Gregor ⁴⁵, P. Grenier ¹⁴⁵, K. Grevtsov ⁵, J. Griffiths ⁸, A.A. Grillo ¹³⁹, K. Grimm ⁷⁵, S. Grinstein ^{13,v}, Ph. Gris ³⁷, J.-F. Grivaz ¹¹⁹, S. Groh ⁸⁶, E. Gross ¹⁷⁵, J. Grosse-Knetter ⁵⁷, G.C. Grossi ⁸², Z.J. Grout ⁸¹, A. Grummer ¹⁰⁷, L. Guan ⁹², W. Guan ¹⁷⁶, J. Guenther ³², F. Guescini ^{163a}, D. Guest ¹⁶⁶, O. Gueta ¹⁵⁵, B. Gui ¹¹³, E. Guido ^{53a,53b}, T. Guillemain ⁵, S. Guindon ³², U. Gul ⁵⁶, C. Gumpert ³², J. Guo ^{36c}, W. Guo ⁹², Y. Guo ^{36a,w}, R. Gupta ⁴³, S. Gurbuz ^{20a}, G. Gustavino ¹¹⁵, B.J. Gutelman ¹⁵⁴, P. Gutierrez ¹¹⁵, N.G. Gutierrez Ortiz ⁸¹, C. Gutsche ⁸¹, C. Guyot ¹³⁸, M.P. Guzik ^{41a}, C. Gwenlan ¹²², C.B. Gwilliam ⁷⁷, A. Haas ¹¹², C. Haber ¹⁶, H.K. Hadavand ⁸, N. Haddad ^{137e}, A. Hadeef ⁸⁸, S. Hageböck ²³, M. Hagihara ¹⁶⁴, H. Hakobyan ^{180,*}, M. Haleem ⁴⁵, J. Haley ¹¹⁶, G. Halladjian ⁹³, G.D. Hallewell ⁸⁸, K. Hamacher ¹⁷⁸, P. Hamal ¹¹⁷, K. Hamano ¹⁷², A. Hamilton ^{147a}, G.N. Hamity ¹⁴¹, P.G. Hamnett ⁴⁵, L. Han ^{36a}, S. Han ^{35a,35d}, K. Hanagaki ^{69,x}, K. Hanawa ¹⁵⁷, M. Hance ¹³⁹, D.M. Handl ¹⁰², B. Haney ¹²⁴, P. Hanke ^{60a}, J.B. Hansen ³⁹, J.D. Hansen ³⁹, M.C. Hansen ²³, P.H. Hansen ³⁹, K. Hara ¹⁶⁴, A.S. Hard ¹⁷⁶, T. Harenberg ¹⁷⁸, F. Hariri ¹¹⁹, S. Harkusha ⁹⁵, P.F. Harrison ¹⁷³, N.M. Hartmann ¹⁰², Y. Hasegawa ¹⁴², A. Hasib ⁴⁹, S. Hassani ¹³⁸, S. Haug ¹⁸, R. Hauser ⁹³, L. Hauswald ⁴⁷, L.B. Havener ³⁸, M. Havranek ¹³⁰, C.M. Hawkes ¹⁹, R.J. Hawking ³², D. Hayakawa ¹⁵⁹, D. Hayden ⁹³, C.P. Hays ¹²², J.M. Hays ⁷⁹, H.S. Hayward ⁷⁷, S.J. Haywood ¹³³, S.J. Head ¹⁹, T. Heck ⁸⁶, V. Hedberg ⁸⁴, L. Heelan ⁸, S. Heer ²³, K.K. Heidegger ⁵¹, S. Heim ⁴⁵, T. Heim ¹⁶, B. Heinemann ^{45,y}, J.J. Heinrich ¹⁰², L. Heinrich ¹¹², C. Heinz ⁵⁵, J. Hejbal ¹²⁹, L. Helary ³², A. Held ¹⁷¹, S. Hellman ^{148a,148b}, C. Helsens ³², R.C.W. Henderson ⁷⁵, Y. Heng ¹⁷⁶, S. Henkelmann ¹⁷¹, A.M. Henriques Correia ³², S. Henrot-Versille ¹¹⁹, G.H. Herbert ¹⁷, H. Herde ²⁵, V. Herget ¹⁷⁷, Y. Hernández Jiménez ^{147c}, H. Herr ⁸⁶, G. Herten ⁵¹, R. Hertenberger ¹⁰², L. Hervas ³², T.C. Herwig ¹²⁴, G.G. Hesketh ⁸¹, N.P. Hessey ^{163a}, J.W. Hetherly ⁴³, S. Higashino ⁶⁹, E. Higón-Rodríguez ¹⁷⁰, K. Hildebrand ³³, E. Hill ¹⁷², J.C. Hill ³⁰, K.H. Hiller ⁴⁵, S.J. Hillier ¹⁹, M. Hils ⁴⁷, I. Hinchliffe ¹⁶, M. Hirose ⁵¹, D. Hirschbuehl ¹⁷⁸, B. Hiti ⁷⁸, O. Hladik ¹²⁹, D.R. Hlaluku ^{147c}, X. Hoad ⁴⁹, J. Hobbs ¹⁵⁰, N. Hod ^{163a}, M.C. Hodgkinson ¹⁴¹, P. Hodgson ¹⁴¹, A. Hoecker ³², M.R. Hoferkamp ¹⁰⁷, F. Hoenig ¹⁰², D. Hohn ²³, T.R. Holmes ³³, M. Holzbock ¹⁰², M. Homann ⁴⁶, S. Honda ¹⁶⁴, T. Honda ⁶⁹, T.M. Hong ¹²⁷, B.H. Hooberman ¹⁶⁹, W.H. Hopkins ¹¹⁸, Y. Horii ¹⁰⁵, A.J. Horton ¹⁴⁴, J.-Y. Hostachy ⁵⁸, A. Hostiuc ¹⁴⁰, S. Hou ¹⁵³, A. Hoummada ^{137a}, J. Howarth ⁸⁷, J. Hoya ⁷⁴, M. Hrabovsky ¹¹⁷, J. Hrdinka ³², I. Hristova ¹⁷, J. Hrivnac ¹¹⁹, T. Hryn'ova ⁵, A. Hrynevich ⁹⁶, P.J. Hsu ⁶³, S.-C. Hsu ¹⁴⁰, Q. Hu ²⁷, S. Hu ^{36c}, Y. Huang ^{35a}, Z. Hubacek ¹³⁰, F. Hubaut ⁸⁸, F. Huegging ²³, T.B. Huffman ¹²², E.W. Hughes ³⁸, M. Huhtinen ³², R.F.H. Hunter ³¹, P. Huo ¹⁵⁰, N. Huseynov ^{68,b}, J. Huston ⁹³, J. Huth ⁵⁹, R. Hyneman ⁹², G. Iacobucci ⁵², G. Iakovidis ²⁷, I. Ibragimov ¹⁴³, L. Iconomidou-Fayard ¹¹⁹, Z. Idrissi ^{137e}, P. Iengo ³², O. Igonkina ^{109,z}, T. Iizawa ¹⁷⁴, Y. Ikegami ⁶⁹, M. Ikeno ⁶⁹, Y. Ilchenko ^{11,aa}, D. Iliadis ¹⁵⁶, N. Ilic ¹⁴⁵, F. Iltzsche ⁴⁷, G. Introzzi ^{123a,123b}, P. Ioannou ^{9,*}, M. Iodice ^{136a}, K. Iordanidou ³⁸, V. Ippolito ⁵⁹, M.F. Isacson ¹⁶⁸, N. Ishijima ¹²⁰, M. Ishino ¹⁵⁷, M. Ishitsuka ¹⁵⁹, C. Issever ¹²², S. Istin ^{20a}, F. Ito ¹⁶⁴, J.M. Iturbe Ponce ^{62a}, R. Iuppa ^{162a,162b}, H. Iwasaki ⁶⁹, J.M. Izen ⁴⁴, V. Izzo ^{106a}, S. Jabbar ³, P. Jackson ¹, R.M. Jacobs ²³, V. Jain ², K.B. Jakobi ⁸⁶, K. Jakobs ⁵¹, S. Jakobsen ⁶⁵, T. Jakoubek ¹²⁹, D.O. Jamin ¹¹⁶, D.K. Jana ⁸², R. Jansky ⁵², J. Janssen ²³, M. Janus ⁵⁷, P.A. Janus ^{41a}, G. Jarlskog ⁸⁴, N. Javadov ^{68,b}, T. Javůrek ⁵¹, M. Javurkova ⁵¹, F. Jeanneau ¹³⁸, L. Jeanty ¹⁶, J. Jejelava ^{54a,ab}, A. Jelinskas ¹⁷³, P. Jenni ^{51,ac}, C. Jeske ¹⁷³, S. Jézéquel ⁵, H. Ji ¹⁷⁶, J. Jia ¹⁵⁰, H. Jiang ⁶⁷, Y. Jiang ^{36a}, Z. Jiang ¹⁴⁵, S. Jiggins ⁸¹, J. Jimenez Pena ¹⁷⁰, S. Jin ^{35b}, A. Jinaru ^{28b}, O. Jinnouchi ¹⁵⁹, H. Jivan ^{147c}, P. Johansson ¹⁴¹, K.A. Johns ⁷, C.A. Johnson ⁶⁴, W.J. Johnson ¹⁴⁰, K. Jon-And ^{148a,148b}, R.W.L. Jones ⁷⁵, S.D. Jones ¹⁵¹, S. Jones ⁷, T.J. Jones ⁷⁷, J. Jongmanns ^{60a},

P.M. Jorge^{128a,128b}, J. Jovicevic^{163a}, X. Ju¹⁷⁶, A. Juste Rozas^{13,v}, M.K. Köhler¹⁷⁵, A. Kaczmarzka⁴², M. Kado¹¹⁹, H. Kagan¹¹³, M. Kagan¹⁴⁵, S.J. Kahn⁸⁸, T. Kaji¹⁷⁴, E. Kajomovitz¹⁵⁴, C.W. Kalderon⁸⁴, A. Kaluza⁸⁶, S. Kama⁴³, A. Kamenshchikov¹³², N. Kanaya¹⁵⁷, L. Kanjir⁷⁸, V.A. Kantserov¹⁰⁰, J. Kanzaki⁶⁹, B. Kaplan¹¹², L.S. Kaplan¹⁷⁶, D. Kar^{147c}, K. Karakostas¹⁰, N. Karastathis¹⁰, M.J. Kareem^{163b}, E. Karentzos¹⁰, S.N. Karpov⁶⁸, Z.M. Karpova⁶⁸, K. Karthik¹¹², V. Kartvelishvili⁷⁵, A.N. Karyukhin¹³², K. Kasahara¹⁶⁴, L. Kashif¹⁷⁶, R.D. Kass¹¹³, A. Kastanas¹⁴⁹, Y. Kataoka¹⁵⁷, C. Kato¹⁵⁷, A. Katre⁵², J. Katzy⁴⁵, K. Kawade⁷⁰, K. Kawagoe⁷³, T. Kawamoto¹⁵⁷, G. Kawamura⁵⁷, E.F. Kay⁷⁷, V.F. Kazanin^{111,c}, R. Keeler¹⁷², R. Kehoe⁴³, J.S. Keller³¹, E. Kellermann⁸⁴, J.J. Kempster⁸⁰, J. Kendrick¹⁹, H. Keoshkerian¹⁶¹, O. Kepka¹²⁹, B.P. Kerševan⁷⁸, S. Kersten¹⁷⁸, R.A. Keyes⁹⁰, M. Khader¹⁶⁹, F. Khalil-zada¹², A. Khanov¹¹⁶, A.G. Kharlamov^{111,c}, T. Kharlamova^{111,c}, A. Khodinov¹⁶⁰, T.J. Khoo⁵², V. Khovanskiy^{99,*}, E. Khramov⁶⁸, J. Khubua^{54b,ad}, S. Kido⁷⁰, C.R. Kilby⁸⁰, H.Y. Kim⁸, S.H. Kim¹⁶⁴, Y.K. Kim³³, N. Kimura¹⁵⁶, O.M. Kind¹⁷, B.T. King⁷⁷, D. Kirchmeier⁴⁷, J. Kirk¹³³, A.E. Kiryunin¹⁰³, T. Kishimoto¹⁵⁷, D. Kisielewska^{41a}, V. Kitali⁴⁵, O. Kivernyk⁵, E. Kladiva^{146b}, T. Klapdor-Kleingrothaus⁵¹, M.H. Klein⁹², M. Klein⁷⁷, U. Klein⁷⁷, K. Kleinknecht⁸⁶, P. Klimek¹¹⁰, A. Klimentov²⁷, R. Klingenberg^{46,*}, T. Klingl²³, T. Klioutchnikova³², F.F. Klitzner¹⁰², E.-E. Kluge^{60a}, P. Kluit¹⁰⁹, S. Kluth¹⁰³, E. Kneringer⁶⁵, E.B.F.G. Knoops⁸⁸, A. Knue¹⁰³, A. Kobayashi¹⁵⁷, D. Kobayashi⁷³, T. Kobayashi¹⁵⁷, M. Kobel⁴⁷, M. Kocian¹⁴⁵, P. Kodys¹³¹, T. Koffas³¹, E. Koffeman¹⁰⁹, N.M. Köhler¹⁰³, T. Koi¹⁴⁵, M. Kolb^{60b}, I. Koletsou⁵, T. Kondo⁶⁹, N. Kondrashova^{36c}, K. Köneke⁵¹, A.C. König¹⁰⁸, T. Kono^{69,ae}, R. Konoplich^{112,af}, N. Konstantinidis⁸¹, B. Konya⁸⁴, R. Kopeliansky⁶⁴, S. Koperny^{41a}, A.K. Kopp⁵¹, K. Korcyl⁴², K. Kordas¹⁵⁶, A. Korn⁸¹, A.A. Korol^{111,c}, I. Korolkov¹³, E.V. Korolkova¹⁴¹, O. Kortner¹⁰³, S. Kortner¹⁰³, T. Kosek¹³¹, V.V. Kostyukhin²³, A. Kotwal⁴⁸, A. Koulouris¹⁰, A. Kourkoulouli-Charalampidi^{123a,123b}, C. Kourkoulouli⁹, E. Kourlitis¹⁴¹, V. Kouskoura²⁷, A.B. Kowalewska⁴², R. Kowalewski¹⁷², T.Z. Kowalski^{41a}, C. Kozakai¹⁵⁷, W. Kozanecki¹³⁸, A.S. Kozhin¹³², V.A. Kramarenko¹⁰¹, G. Kramberger⁷⁸, D. Krasnopevtsev¹⁰⁰, M.W. Krasny⁸³, A. Krasznahorkay³², D. Krauss¹⁰³, J.A. Kremer^{41a}, J. Kretzschmar⁷⁷, K. Kreutzfeldt⁵⁵, P. Krieger¹⁶¹, K. Krizka¹⁶, K. Kroeninger⁴⁶, H. Kroha¹⁰³, J. Kroll¹²⁹, J. Kroll¹²⁴, J. Kroseberg²³, J. Krstic¹⁴, U. Kruchonak⁶⁸, H. Krüger²³, N. Krumnack⁶⁷, M.C. Kruse⁴⁸, T. Kubota⁹¹, H. Kucuk⁸¹, S. Kuday^{4b}, J.T. Kuechler¹⁷⁸, S. Kuehn³², A. Kugel^{60a}, F. Kuger¹⁷⁷, T. Kuhl⁴⁵, V. Kukhtin⁶⁸, R. Kukla⁸⁸, Y. Kulchitsky⁹⁵, S. Kuleshov^{34b}, Y.P. Kulinich¹⁶⁹, M. Kuna^{134a,134b}, T. Kunigo⁷¹, A. Kupco¹²⁹, T. Kupfer⁴⁶, O. Kuprash¹⁵⁵, H. Kurashige⁷⁰, L.L. Kurchaninov^{163a}, Y.A. Kurochkin⁹⁵, M.G. Kurth^{35a,35d}, E.S. Kuwertz¹⁷², M. Kuze¹⁵⁹, J. Kvita¹¹⁷, T. Kwan¹⁷², D. Kyriazopoulos¹⁴¹, A. La Rosa¹⁰³, J.L. La Rosa Navarro^{26d}, L. La Rotonda^{40a,40b}, F. La Ruffa^{40a,40b}, C. Lacasta¹⁷⁰, F. Lacava^{134a,134b}, J. Lacey⁴⁵, D.P.J. Lack⁸⁷, H. Lacker¹⁷, D. Lacour⁸³, E. Ladygin⁶⁸, R. Lafaye⁵, B. Laforge⁸³, T. Lagouri¹⁷⁹, S. Lai⁵⁷, S. Lammers⁶⁴, W. Lampl⁷, E. Lançon²⁷, U. Landgraf⁵¹, M.P.J. Landon⁷⁹, M.C. Lanfermann⁵², V.S. Lang⁴⁵, J.C. Lange¹³, R.J. Langenberg³², A.J. Lankford¹⁶⁶, F. Lanni²⁷, K. Lantzsch²³, A. Lanza^{123a}, A. Lapertosa^{53a,53b}, S. Laplace⁸³, J.F. Laporte¹³⁸, T. Lari^{94a}, F. Lasagni Manghi^{22a,22b}, M. Lassnig³², T.S. Lau^{62a}, P. Laurelli⁵⁰, W. Lavrijsen¹⁶, A.T. Law¹³⁹, P. Laycock⁷⁷, T. Lazovich⁵⁹, M. Lazzaroni^{94a,94b}, B. Le⁹¹, O. Le Dortz⁸³, E. Le Guirriec⁸⁸, E.P. Le Quilleuc¹³⁸, M. LeBlanc¹⁷², T. LeCompte⁶, F. Ledroit-Guillon⁵⁸, C.A. Lee²⁷, G.R. Lee^{34a}, S.C. Lee¹⁵³, L. Lee⁵⁹, B. Lefebvre⁹⁰, G. Lefebvre⁸³, M. Lefebvre¹⁷², F. Legger¹⁰², C. Leggett¹⁶, G. Lehmann Miotto³², X. Lei⁷, W.A. Leight⁴⁵, M.A.L. Leite^{26d}, R. Leitner¹³¹, D. Lellouch¹⁷⁵, B. Lemmer⁵⁷, K.J.C. Leney⁸¹, T. Lenz²³, B. Lenzi³², R. Leone⁷, S. Leone^{126a}, C. Leonidopoulos⁴⁹, G. Lerner¹⁵¹, C. Leroy⁹⁷, R. Les¹⁶¹, A.A.J. Lesage¹³⁸, C.G. Lester³⁰, M. Levchenko¹²⁵, J. Levêque⁵, D. Levin⁹², L.J. Levinson¹⁷⁵, M. Levy¹⁹, D. Lewis⁷⁹, C. Li^{36a}, B. Li^{36a,w}, H. Li¹⁵⁰, L. Li^{36c}, Q. Li^{35a,35d}, Q. Li^{36a}, S. Li⁴⁸, X. Li^{36c}, Y. Li¹⁴³, Z. Liang^{35a}, B. Liberti^{135a}, A. Liblong¹⁶¹, K. Lie^{62c}, J. Liebal²³, W. Liebig¹⁵, A. Limosani¹⁵², C.Y. Lin³⁰, K. Lin⁹³, S.C. Lin¹⁸², T.H. Lin⁸⁶, R.A. Linck⁶⁴, B.E. Lindquist¹⁵⁰, A.E. Lioni⁵², E. Lipeles¹²⁴, A. Lipniacka¹⁵, M. Lisovyi^{60b}, T.M. Liss^{169,ag}, A. Lister¹⁷¹, A.M. Litke¹³⁹, B. Liu⁶⁷, H. Liu⁹², H. Liu²⁷, J.K.K. Liu¹²², J. Liu^{36b}, J.B. Liu^{36a}, K. Liu⁸⁸, L. Liu¹⁶⁹, M. Liu^{36a}, Y.L. Liu^{36a}, Y. Liu^{36a}, M. Livan^{123a,123b}, A. Lleres⁵⁸, J. Llorente Merino^{35a}, S.L. Lloyd⁷⁹, C.Y. Lo^{62b}, F. Lo Sterzo⁴³, E.M. Lobodzinska⁴⁵, P. Loch⁷, F.K. Loebinger⁸⁷, A. Loesle⁵¹, K.M. Loew²⁵, T. Lohse¹⁷, K. Lohwasser¹⁴¹, M. Lokajicek¹²⁹, B.A. Long²⁴, J.D. Long¹⁶⁹, R.E. Long⁷⁵, L. Longo^{76a,76b}, K.A. Looper¹¹³, J.A. Lopez^{34b}, I. Lopez Paz¹³, A. Lopez Solis⁸³, J. Lorenz¹⁰², N. Lorenzo Martinez⁵, M. Losada²¹, P.J. Lösel¹⁰², X. Lou^{35a}, A. Lounis¹¹⁹, J. Love⁶, P.A. Love⁷⁵, H. Lu^{62a}, N. Lu⁹², Y.J. Lu⁶³, H.J. Lubatti¹⁴⁰, C. Luci^{134a,134b}, A. Lucotte⁵⁸, C. Luedtke⁵¹, F. Luehring⁶⁴, W. Lukas⁶⁵, L. Luminari^{134a},

O. Lundberg^{148a,148b}, B. Lund-Jensen¹⁴⁹, M.S. Lutz⁸⁹, P.M. Luzi⁸³, D. Lynn²⁷, R. Lysak¹²⁹, E. Lytken⁸⁴, F. Lyu^{35a}, V. Lyubushkin⁶⁸, H. Ma²⁷, L.L. Ma^{36b}, Y. Ma^{36b}, G. Maccarrone⁵⁰, A. Macchiolo¹⁰³, C.M. Macdonald¹⁴¹, B. Maček⁷⁸, J. Machado Miguens^{124,128b}, D. Madaffari¹⁷⁰, R. Madar³⁷, W.F. Mader⁴⁷, A. Madsen⁴⁵, N. Madysa⁴⁷, J. Maeda⁷⁰, S. Maeland¹⁵, T. Maeno²⁷, A.S. Maevskiy¹⁰¹, V. Magerl⁵¹, C. Maiani¹¹⁹, C. Maidantchik^{26a}, T. Maier¹⁰², A. Maio^{128a,128b,128d}, O. Majersky^{146a}, S. Majewski¹¹⁸, Y. Makida⁶⁹, N. Makovec¹¹⁹, B. Malaescu⁸³, Pa. Malecki⁴², V.P. Maleev¹²⁵, F. Malek⁵⁸, U. Mallik⁶⁶, D. Malon⁶, C. Malone³⁰, S. Maltezos¹⁰, S. Malyukov³², J. Mamuzic¹⁷⁰, G. Mancini⁵⁰, I. Mandić⁷⁸, J. Maneira^{128a,128b}, L. Manhaes de Andrade Filho^{26b}, J. Manjarres Ramos⁴⁷, K.H. Mankinen⁸⁴, A. Mann¹⁰², A. Manousos³², B. Mansoulie¹³⁸, J.D. Mansour^{35a}, R. Mantifel⁹⁰, M. Mantoani⁵⁷, S. Manzoni^{94a,94b}, L. Mapelli³², G. Marceca²⁹, L. March⁵², L. Marchese¹²², G. Marchiori⁸³, M. Marcisovsky¹²⁹, C.A. Marin Tobon³², M. Marjanovic³⁷, D.E. Marley⁹², F. Marroquim^{26a}, S.P. Marsden⁸⁷, Z. Marshall¹⁶, M.U.F. Martensson¹⁶⁸, S. Marti-Garcia¹⁷⁰, C.B. Martin¹¹³, T.A. Martin¹⁷³, V.J. Martin⁴⁹, B. Martin dit Latour¹⁵, M. Martinez^{13,v}, V.I. Martinez Outschoorn¹⁶⁹, S. Martin-Haugh¹³³, V.S. Martoiu^{28b}, A.C. Martyniuk⁸¹, A. Marzin³², L. Masetti⁸⁶, T. Mashimo¹⁵⁷, R. Mashinistov⁹⁸, J. Masik⁸⁷, A.L. Maslennikov^{111,c}, L.H. Mason⁹¹, L. Massa^{135a,135b}, P. Mastrandrea⁵, A. Mastroberardino^{40a,40b}, T. Masubuchi¹⁵⁷, P. Mättig¹⁷⁸, J. Maurer^{28b}, S.J. Maxfield⁷⁷, D.A. Maximov^{111,c}, R. Mazini¹⁵³, I. Maznas¹⁵⁶, S.M. Mazza^{94a,94b}, N.C. Mc Fadden¹⁰⁷, G. Mc Goldrick¹⁶¹, S.P. Mc Kee⁹², A. McCarn⁹², R.L. McCarthy¹⁵⁰, T.G. McCarthy¹⁰³, L.I. McClymont⁸¹, E.F. McDonald⁹¹, J.A. Mcfayden³², G. Mchedlidze⁵⁷, S.J. McMahon¹³³, P.C. McNamara⁹¹, C.J. McNicol¹⁷³, R.A. McPherson^{172,o}, S. Meehan¹⁴⁰, T.J. Megy⁵¹, S. Mehlhase¹⁰², A. Mehta⁷⁷, T. Meideck⁵⁸, K. Meier^{60a}, B. Meirose⁴⁴, D. Melini^{170,ah}, B.R. Mellado Garcia^{147c}, J.D. Mellenthin⁵⁷, M. Melo^{146a}, F. Meloni¹⁸, A. Melzer²³, S.B. Menary⁸⁷, L. Meng⁷⁷, X.T. Meng⁹², A. Mengarelli^{22a,22b}, S. Menke¹⁰³, E. Meoni^{40a,40b}, S. Mergelmeyer¹⁷, C. Merlassino¹⁸, P. Mermod⁵², L. Merola^{106a,106b}, C. Meroni^{94a}, F.S. Merritt³³, A. Messina^{134a,134b}, J. Metcalfe⁶, A.S. Mete¹⁶⁶, C. Meyer¹²⁴, J.-P. Meyer¹³⁸, J. Meyer¹⁰⁹, H. Meyer Zu Theenhausen^{60a}, F. Miano¹⁵¹, R.P. Middleton¹³³, S. Miglioranza^{53a,53b}, L. Mijović⁴⁹, G. Mikenberg¹⁷⁵, M. Mikestikova¹²⁹, M. Mikuž⁷⁸, M. Milesi⁹¹, A. Milic¹⁶¹, D.A. Millar⁷⁹, D.W. Miller³³, C. Mills⁴⁹, A. Milov¹⁷⁵, D.A. Milstead^{148a,148b}, A.A. Minaenko¹³², Y. Minami¹⁵⁷, I.A. Minashvili^{54b}, A.I. Mincer¹¹², B. Mindur^{41a}, M. Mineev⁶⁸, Y. Minegishi¹⁵⁷, Y. Ming¹⁷⁶, L.M. Mir¹³, A. Mirto^{76a,76b}, K.P. Mistry¹²⁴, T. Mitani¹⁷⁴, J. Mitrevski¹⁰², V.A. Mitsou¹⁷⁰, A. Miucci¹⁸, P.S. Miyagawa¹⁴¹, A. Mizukami⁶⁹, J.U. Mjörnmark⁸⁴, T. Mkrtchyan¹⁸⁰, M. Mlynarikova¹³¹, T. Moa^{148a,148b}, K. Mochizuki⁹⁷, P. Mogg⁵¹, S. Mohapatra³⁸, S. Molander^{148a,148b}, R. Moles-Valls²³, M.C. Mondragon⁹³, K. Mönig⁴⁵, J. Monk³⁹, E. Monnier⁸⁸, A. Montalbano¹⁵⁰, J. Montejo Berlingen³², F. Monticelli⁷⁴, S. Monzani^{94a}, R.W. Moore³, N. Morange¹¹⁹, D. Moreno²¹, M. Moreno Llácer³², P. Morettini^{53a}, S. Morgenstern³², D. Mori¹⁴⁴, T. Mori¹⁵⁷, M. Morii⁵⁹, M. Morinaga¹⁷⁴, V. Morisbak¹²¹, A.K. Morley³², G. Mornacchi³², J.D. Morris⁷⁹, L. Morvaj¹⁵⁰, P. Moschovakos¹⁰, M. Mosidze^{54b}, H.J. Moss¹⁴¹, J. Moss^{145,ai}, K. Motohashi¹⁵⁹, R. Mount¹⁴⁵, E. Mountricha²⁷, E.J.W. Moyse⁸⁹, S. Muanza⁸⁸, F. Mueller¹⁰³, J. Mueller¹²⁷, R.S.P. Mueller¹⁰², D. Muenstermann⁷⁵, P. Mullen⁵⁶, G.A. Mullier¹⁸, F.J. Munoz Sanchez⁸⁷, W.J. Murray^{173,133}, H. Musheghyan³², M. Muškinja⁷⁸, A.G. Myagkov^{132,aj}, M. Myska¹³⁰, B.P. Nachman¹⁶, O. Nackenhorst⁵², K. Nagai¹²², R. Nagai^{69,ae}, K. Nagano⁶⁹, Y. Nagasaka⁶¹, K. Nagata¹⁶⁴, M. Nagel⁵¹, E. Nagy⁸⁸, A.M. Nairz³², Y. Nakahama¹⁰⁵, K. Nakamura⁶⁹, T. Nakamura¹⁵⁷, I. Nakano¹¹⁴, R.F. Naranjo Garcia⁴⁵, R. Narayan¹¹, D.I. Narrias Villar^{60a}, I. Naryshkin¹²⁵, T. Naumann⁴⁵, G. Navarro²¹, R. Nayyar⁷, H.A. Neal⁹², P.Yu. Nechaeva⁹⁸, T.J. Neep¹³⁸, A. Negri^{123a,123b}, M. Negrini^{22a}, S. Nektarijevic¹⁰⁸, C. Nellist⁵⁷, A. Nelson¹⁶⁶, M.E. Nelson¹²², S. Nemecek¹²⁹, P. Nemethy¹¹², M. Nessi^{32,ak}, M.S. Neubauer¹⁶⁹, M. Neumann¹⁷⁸, P.R. Newman¹⁹, T.Y. Ng^{62c}, Y.S. Ng¹⁷, T. Nguyen Manh⁹⁷, R.B. Nickerson¹²², R. Nicolaidou¹³⁸, J. Nielsen¹³⁹, N. Nikiforou¹¹, V. Nikolaenko^{132,aj}, I. Nikolic-Audit⁸³, K. Nikolopoulos¹⁹, P. Nilsson²⁷, Y. Ninomiya⁶⁹, A. Nisati^{134a}, N. Nishu^{36c}, R. Nisius¹⁰³, I. Nitsche⁴⁶, T. Nitta¹⁷⁴, T. Nobe¹⁵⁷, Y. Noguchi⁷¹, M. Nomachi¹²⁰, I. Nomidis³¹, M.A. Nomura²⁷, T. Nooney⁷⁹, M. Nordberg³², N. Norjoharuddeen¹²², O. Novgorodova⁴⁷, M. Nozaki⁶⁹, L. Nozka¹¹⁷, K. Ntekas¹⁶⁶, E. Nurse⁸¹, F. Nuti⁹¹, K. O'Connor²⁵, D.C. O'Neil¹⁴⁴, A.A. O'Rourke⁴⁵, V. O'Shea⁵⁶, F.G. Oakham^{31,d}, H. Oberlack¹⁰³, T. Obermann²³, J. Ocariz⁸³, A. Ochi⁷⁰, I. Ochoa³⁸, J.P. Ochoa-Ricoux^{34a}, S. Oda⁷³, S. Odaka⁶⁹, A. Oh⁸⁷, S.H. Oh⁴⁸, C.C. Ohm¹⁴⁹, H. Ohman¹⁶⁸, H. Oide^{53a,53b}, H. Okawa¹⁶⁴, Y. Okumura¹⁵⁷,

T. Okuyama⁶⁹, A. Olariu^{28b}, L.F. Oleiro Seabra^{128a}, S.A. Olivares Pino^{34a}, D. Oliveira Damazio²⁷, M.J.R. Olsson³³, A. Olszewski⁴², J. Olszowska⁴², A. Onofre^{128a,128e}, K. Onogi¹⁰⁵, P.U.E. Onyisi^{11,aa}, H. Oppen¹²¹, M.J. Oreglia³³, Y. Oren¹⁵⁵, D. Orestano^{136a,136b}, N. Orlando^{62b}, R.S. Orr¹⁶¹, B. Osculati^{53a,53b,*}, R. Ospanov^{36a}, G. Otero y Garzon²⁹, H. Otono⁷³, M. Ouchrif^{137d}, F. Ould-Saada¹²¹, A. Ouraou¹³⁸, K.P. Oussoren¹⁰⁹, Q. Ouyang^{35a}, M. Owen⁵⁶, R.E. Owen¹⁹, V.E. Ozcan^{20a}, N. Ozturk⁸, K. Pachal¹⁴⁴, A. Pacheco Pages¹³, L. Pacheco Rodriguez¹³⁸, C. Padilla Aranda¹³, S. Pagan Griso¹⁶, M. Paganini¹⁷⁹, F. Paige²⁷, G. Palacino⁶⁴, S. Palazzo^{40a,40b}, S. Palestini³², M. Palka^{41b}, D. Pallin³⁷, E.St. Panagiotopoulou¹⁰, I. Panagoulas¹⁰, C.E. Pandini⁵², J.G. Panduro Vazquez⁸⁰, P. Pani³², S. Panitkin²⁷, D. Pantea^{28b}, L. Paolozzi⁵², Th.D. Papadopoulou¹⁰, K. Papageorgiou^{9,s}, A. Paramonov⁶, D. Paredes Hernandez¹⁷⁹, A.J. Parker⁷⁵, M.A. Parker³⁰, K.A. Parker⁴⁵, F. Parodi^{53a,53b}, J.A. Parsons³⁸, U. Parzefall⁵¹, V.R. Pascuzzi¹⁶¹, J.M. Pasner¹³⁹, E. Pasqualucci^{134a}, S. Passaggio^{53a}, Fr. Pastore⁸⁰, S. Pataria⁸⁶, J.R. Pater⁸⁷, T. Pauly³², B. Pearson¹⁰³, S. Pedraza Lopez¹⁷⁰, R. Pedro^{128a,128b}, S.V. Peleganchuk^{111,c}, O. Penc¹²⁹, C. Peng^{35a,35d}, H. Peng^{36a}, J. Penwell⁶⁴, B.S. Peralva^{26b}, M.M. Perego¹³⁸, D.V. Perepelitsa²⁷, F. Peri¹⁷, L. Perini^{94a,94b}, H. Pernegger³², S. Perrella^{106a,106b}, R. Peschke⁴⁵, V.D. Peshekhonov^{68,*}, K. Peters⁴⁵, R.F.Y. Peters⁸⁷, B.A. Petersen³², T.C. Petersen³⁹, E. Petit⁵⁸, A. Petridis¹, C. Petridou¹⁵⁶, P. Petroff¹¹⁹, E. Petrolo^{134a}, M. Petrov¹²², F. Petrucci^{136a,136b}, N.E. Pettersson⁸⁹, A. Peyaud¹³⁸, R. Pezoa^{34b}, F.H. Phillips⁹³, P.W. Phillips¹³³, G. Piacquadio¹⁵⁰, E. Pianori¹⁷³, A. Picazio⁸⁹, M.A. Pickering¹²², R. Piegaia²⁹, J.E. Pilcher³³, A.D. Pilkington⁸⁷, M. Pinamonti^{135a,135b}, J.L. Pinfold³, H. Pirumov⁴⁵, M. Pitt¹⁷⁵, L. Plazak^{146a}, M.-A. Pleier²⁷, V. Pleskot⁸⁶, E. Plotnikova⁶⁸, D. Pluth⁶⁷, P. Podberezko¹¹¹, R. Poettgen⁸⁴, R. Poggi^{123a,123b}, L. Poggioli¹¹⁹, I. Pogrebnyak⁹³, D. Pohl²³, I. Pokharel⁵⁷, G. Polesello^{123a}, A. Poley⁴⁵, A. Policicchio^{40a,40b}, R. Polifka³², A. Polini^{22a}, C.S. Pollard⁵⁶, V. Polychronakos²⁷, K. Pommès³², D. Ponomarenko¹⁰⁰, L. Pontecorvo^{134a}, G.A. Popeneciu^{28d}, D.M. Portillo Quintero⁸³, S. Pospisil¹³⁰, K. Potamianos⁴⁵, I.N. Potrap⁶⁸, C.J. Potter³⁰, H. Potti¹¹, T. Poulsen⁸⁴, J. Poveda³², M.E. Pozo Astigarraga³², P. Pralavorio⁸⁸, A. Pranko¹⁶, S. Prell⁶⁷, D. Price⁸⁷, M. Primavera^{76a}, S. Prince⁹⁰, N. Proklova¹⁰⁰, K. Prokofiev^{62c}, F. Prokoshin^{34b}, S. Protopopescu²⁷, J. Proudfoot⁶, M. Przybycien^{41a}, A. Puri¹⁶⁹, P. Puzo¹¹⁹, J. Qian⁹², G. Qin⁵⁶, Y. Qin⁸⁷, A. Quadt⁵⁷, M. Queitsch-Maitland⁴⁵, D. Quilty⁵⁶, S. Raddum¹²¹, V. Radeka²⁷, V. Radescu¹²², S.K. Radhakrishnan¹⁵⁰, P. Radloff¹¹⁸, P. Rados⁹¹, F. Ragusa^{94a,94b}, G. Rahal¹⁸¹, J.A. Raine⁸⁷, S. Rajagopalan²⁷, C. Rangel-Smith¹⁶⁸, T. Rashid¹¹⁹, S. Raspopov⁵, M.G. Ratti^{94a,94b}, D.M. Rauch⁴⁵, F. Rauscher¹⁰², S. Rave⁸⁶, I. Ravinovich¹⁷⁵, J.H. Rawling⁸⁷, M. Raymond³², A.L. Read¹²¹, N.P. Readioff⁵⁸, M. Reale^{76a,76b}, D.M. Rebuzzi^{123a,123b}, A. Redelbach¹⁷⁷, G. Redlinger²⁷, R. Reece¹³⁹, R.G. Reed^{147c}, K. Reeves⁴⁴, L. Rehnisch¹⁷, J. Reichert¹²⁴, A. Reiss⁸⁶, C. Rembser³², H. Ren^{35a,35d}, M. Rescigno^{134a}, S. Resconi^{94a}, E.D. Resseguie¹²⁴, S. Rettie¹⁷¹, E. Reynolds¹⁹, O.L. Rezanova^{111,c}, P. Reznicek¹³¹, R. Rezvani⁹⁷, R. Richter¹⁰³, S. Richter⁸¹, E. Richter-Was^{41b}, O. Ricken²³, M. Ridet⁸³, P. Rieck¹⁰³, C.J. Riegel¹⁷⁸, J. Rieger⁵⁷, O. Rifki¹¹⁵, M. Rijssenbeek¹⁵⁰, A. Rimoldi^{123a,123b}, M. Rimoldi¹⁸, L. Rinaldi^{22a}, G. Ripellino¹⁴⁹, B. Ristić³², E. Ritsch³², I. Riu¹³, F. Rizatdinova¹¹⁶, E. Rizvi⁷⁹, C. Rizzi¹³, R.T. Roberts⁸⁷, S.H. Robertson^{90,o}, A. Robichaud-Veronneau⁹⁰, D. Robinson³⁰, J.E.M. Robinson⁴⁵, A. Robson⁵⁶, E. Rocco⁸⁶, C. Roda^{126a,126b}, Y. Rodina^{88,al}, S. Rodriguez Bosca¹⁷⁰, A. Rodriguez Perez¹³, D. Rodriguez Rodriguez¹⁷⁰, S. Roe³², C.S. Rogan⁵⁹, O. Røhne¹²¹, J. Roloff⁵⁹, A. Romaniouk¹⁰⁰, M. Romano^{22a,22b}, S.M. Romano Saez³⁷, E. Romero Adam¹⁷⁰, N. Rompotis⁷⁷, M. Ronzani⁵¹, L. Roos⁸³, S. Rosati^{134a}, K. Rosbach⁵¹, P. Rose¹³⁹, N.-A. Rosien⁵⁷, E. Rossi^{106a,106b}, L.P. Rossi^{53a}, J.H.N. Rosten³⁰, R. Rosten¹⁴⁰, M. Rotaru^{28b}, J. Rothberg¹⁴⁰, D. Rousseau¹¹⁹, D. Roy^{147c}, A. Rozanov⁸⁸, Y. Rozen¹⁵⁴, X. Ruan^{147c}, F. Rubbo¹⁴⁵, F. Rühr⁵¹, A. Ruiz-Martinez³¹, Z. Rurikova⁵¹, N.A. Rusakovich⁶⁸, H.L. Russell⁹⁰, J.P. Rutherford⁷, N. Ruthmann³², E.M. Rüttinger⁴⁵, Y.F. Ryabov¹²⁵, M. Rybar¹⁶⁹, G. Rybkin¹¹⁹, S. Ryu⁶, A. Ryzhov¹³², G.F. Rzehorz⁵⁷, A.F. Saavedra¹⁵², G. Sabato¹⁰⁹, S. Sacerdoti²⁹, H.F.W. Sadrozinski¹³⁹, R. Sadykov⁶⁸, F. Safai Tehrani^{134a}, P. Saha¹¹⁰, M. Sahinsoy^{60a}, M. Saimpert⁴⁵, M. Saito¹⁵⁷, T. Saito¹⁵⁷, H. Sakamoto¹⁵⁷, Y. Sakurai¹⁷⁴, G. Salamanna^{136a,136b}, J.E. Salazar Loyola^{34b}, D. Salek¹⁰⁹, P.H. Sales De Bruin¹⁶⁸, D. Salihagic¹⁰³, A. Salnikov¹⁴⁵, J. Salt¹⁷⁰, D. Salvatore^{40a,40b}, F. Salvatore¹⁵¹, A. Salvucci^{62a,62b,62c}, A. Salzburger³², D. Sammel⁵¹, D. Sampsonidis¹⁵⁶, D. Sampsonidou¹⁵⁶, J. Sánchez¹⁷⁰, V. Sanchez Martinez¹⁷⁰, A. Sanchez Pineda^{167a,167c}, H. Sandaker¹²¹, R.L. Sandbach⁷⁹, C.O. Sander⁴⁵, M. Sandhoff¹⁷⁸, C. Sandoval²¹, D.P.C. Sankey¹³³, M. Sannino^{53a,53b}, Y. Sano¹⁰⁵, A. Sansoni⁵⁰, C. Santoni³⁷, H. Santos^{128a}, I. Santoyo Castillo¹⁵¹, A. Sapronov⁶⁸,

J.G. Saraiva^{128a,128d}, B. Sarrazin²³, O. Sasaki⁶⁹, K. Sato¹⁶⁴, E. Sauvan⁵, G. Savage⁸⁰, P. Savard^{161,d}, N. Savic¹⁰³, C. Sawyer¹³³, L. Sawyer^{82,u}, J. Saxon³³, C. Sbarra^{22a}, A. Sbrizzi^{22a,22b}, T. Scanlon⁸¹, D.A. Scannicchio¹⁶⁶, J. Schaarschmidt¹⁴⁰, P. Schacht¹⁰³, B.M. Schachtner¹⁰², D. Schaefer³³, L. Schaefer¹²⁴, R. Schaefer⁴⁵, J. Schaeffer⁸⁶, S. Schaepe³², S. Schaezel^{60b}, U. Schäfer⁸⁶, A.C. Schaffer¹¹⁹, D. Schaile¹⁰², R.D. Schamberger¹⁵⁰, V.A. Schegelsky¹²⁵, D. Scheirich¹³¹, F. Schenck¹⁷, M. Schernau¹⁶⁶, C. Schiavi^{53a,53b}, S. Schier¹³⁹, L.K. Schildgen²³, C. Schillo⁵¹, M. Schioppa^{40a,40b}, S. Schlenker³², K.R. Schmidt-Sommerfeld¹⁰³, K. Schmieden³², C. Schmitt⁸⁶, S. Schmitt⁴⁵, S. Schmitz⁸⁶, U. Schnoor⁵¹, L. Schoeffel¹³⁸, A. Schoening^{60b}, B.D. Schoenrock⁹³, E. Schopf²³, M. Schott⁸⁶, J.F.P. Schouwenger¹⁰⁸, J. Schovancova³², S. Schramm⁵², N. Schuh⁸⁶, A. Schulte⁸⁶, M.J. Schultens²³, H.-C. Schultz-Coulon^{60a}, H. Schulz¹⁷, M. Schumacher⁵¹, B.A. Schumm¹³⁹, Ph. Schune¹³⁸, A. Schwartzman¹⁴⁵, T.A. Schwarz⁹², H. Schweiger⁸⁷, Ph. Schwemling¹³⁸, R. Schwienhorst⁹³, J. Schwindling¹³⁸, A. Sciandra²³, G. Sciolla²⁵, M. Scornajenghi^{40a,40b}, F. Scuri^{126a}, F. Scutti⁹¹, J. Searcy⁹², P. Seema²³, S.C. Seidel¹⁰⁷, A. Seiden¹³⁹, J.M. Seixas^{26a}, G. Sekhniaidze^{106a}, K. Sekhon⁹², S.J. Sekula⁴³, N. Semprini-Cesari^{22a,22b}, S. Senkin³⁷, C. Serfon¹²¹, L. Serin¹¹⁹, L. Serkin^{167a,167b}, M. Sessa^{136a,136b}, R. Seuster¹⁷², H. Severini¹¹⁵, T. Šfiligoi⁷⁸, F. Sforza¹⁶⁵, A. Sfyrly⁵², E. Shabalina⁵⁷, N.W. Shaikh^{148a,148b}, L.Y. Shan^{35a}, R. Shang¹⁶⁹, J.T. Shank²⁴, M. Shapiro¹⁶, P.B. Shatalov⁹⁹, K. Shaw^{167a,167b}, S.M. Shaw⁸⁷, A. Shcherbakova^{148a,148b}, C.Y. Shehu¹⁵¹, Y. Shen¹¹⁵, N. Sherafati³¹, A.D. Sherman²⁴, P. Sherwood⁸¹, L. Shi^{153,am}, S. Shimizu⁷⁰, C.O. Shimmin¹⁷⁹, M. Shimojima¹⁰⁴, I.P.J. Shipsey¹²², S. Shirabe⁷³, M. Shiyakova^{68,an}, J. Shlomi¹⁷⁵, A. Shmeleva⁹⁸, D. Shoaleh Saadi⁹⁷, M.J. Shochet³³, S. Shojaii^{94a,94b}, D.R. Shope¹¹⁵, S. Shrestha¹¹³, E. Shulga¹⁰⁰, M.A. Shupe⁷, P. Sicho¹²⁹, A.M. Sickles¹⁶⁹, P.E. Sidebo¹⁴⁹, E. Sideras Haddad^{147c}, O. Sidiropoulou¹⁷⁷, A. Sidoti^{22a,22b}, F. Siegert⁴⁷, Dj. Sijacki¹⁴, J. Silva^{128a,128d}, S.B. Silverstein^{148a}, V. Simak¹³⁰, L. Simic⁶⁸, S. Simion¹¹⁹, E. Simioni⁸⁶, B. Simmons⁸¹, M. Simon⁸⁶, P. Sinervo¹⁶¹, N.B. Sinev¹¹⁸, M. Sioli^{22a,22b}, G. Siragusa¹⁷⁷, I. Siral⁹², S.Yu. Sivoklov¹⁰¹, J. Sjölin^{148a,148b}, M.B. Skinner⁷⁵, P. Skubic¹¹⁵, M. Slater¹⁹, T. Slavicek¹³⁰, M. Slawinska⁴², K. Sliwa¹⁶⁵, R. Slovak¹³¹, V. Smakhtin¹⁷⁵, B.H. Smart⁵, J. Smiesko^{146a}, N. Smirnov¹⁰⁰, S.Yu. Smirnov¹⁰⁰, Y. Smirnov¹⁰⁰, L.N. Smirnova^{101,ao}, O. Smirnova⁸⁴, J.W. Smith⁵⁷, M.N.K. Smith³⁸, R.W. Smith³⁸, M. Smizanska⁷⁵, K. Smolek¹³⁰, A.A. Snesarev⁹⁸, I.M. Snyder¹¹⁸, S. Snyder²⁷, R. Sobie^{172,o}, F. Socher⁴⁷, A. Soffer¹⁵⁵, A. Søgaard⁴⁹, D.A. Soh¹⁵³, G. Sokhrannyi⁷⁸, C.A. Solans Sanchez³², M. Solar¹³⁰, E.Yu. Soldatov¹⁰⁰, U. Soldevila¹⁷⁰, A.A. Solodkov¹³², A. Soloshenko⁶⁸, O.V. Solovyanov¹³², V. Solovyev¹²⁵, P. Sommer¹⁴¹, H. Son¹⁶⁵, A. Sopczak¹³⁰, D. Sosa^{60b}, C.L. Sotiropoulou^{126a,126b}, S. Sottocornola^{123a,123b}, R. Soualah^{167a,167c}, A.M. Soukharev^{111,c}, D. South⁴⁵, B.C. Sowden⁸⁰, S. Spagnolo^{76a,76b}, M. Spalla^{126a,126b}, M. Spangenberg¹⁷³, F. Spanò⁸⁰, D. Sperlich¹⁷, F. Spettel¹⁰³, T.M. Spieker^{60a}, R. Spighi^{22a}, G. Spigo³², L.A. Spiller⁹¹, M. Spousta¹³¹, R.D. St. Denis^{56,*}, A. Stabile^{94a,94b}, R. Stamen^{60a}, S. Stamm¹⁷, E. Stanecka⁴², R.W. Stanek⁶, C. Stancu^{136a}, M.M. Stanitzki⁴⁵, B.S. Stapf¹⁰⁹, S. Stapnes¹²¹, E.A. Starchenko¹³², G.H. Stark³³, J. Stark⁵⁸, S.H. Stark³⁹, P. Staroba¹²⁹, P. Starovoitov^{60a}, S. Stärz³², R. Staszewski⁴², M. Stegler⁴⁵, P. Steinberg²⁷, B. Stelzer¹⁴⁴, H.J. Stelzer³², O. Stelzer-Chilton^{163a}, H. Stenzel⁵⁵, T.J. Stevenson⁷⁹, G.A. Stewart⁵⁶, M.C. Stockton¹¹⁸, M. Stoebe⁹⁰, G. Stoica^{28b}, P. Stolte⁵⁷, S. Stonjek¹⁰³, A.R. Stradling⁸, A. Straessner⁴⁷, M.E. Stramaglia¹⁸, J. Strandberg¹⁴⁹, S. Strandberg^{148a,148b}, M. Strauss¹¹⁵, P. Strizenec^{146b}, R. Ströhmer¹⁷⁷, D.M. Strom¹¹⁸, R. Stroynowski⁴³, A. Strubig⁴⁹, S.A. Stucci²⁷, B. Stugu¹⁵, N.A. Styles⁴⁵, D. Su¹⁴⁵, J. Su¹²⁷, S. Suchek^{60a}, Y. Sugaya¹²⁰, M. Suk¹³⁰, V.V. Sulin⁹⁸, DMS Sultan^{162a,162b}, S. Sultansoy^{4c}, T. Sumida⁷¹, S. Sun⁵⁹, X. Sun³, K. Suruliz¹⁵¹, C.J.E. Suster¹⁵², M.R. Sutton¹⁵¹, S. Suzuki⁶⁹, M. Svatos¹²⁹, M. Swiatkowski³³, S.P. Swift², I. Sykora^{146a}, T. Sykora¹³¹, D. Ta⁵¹, K. Tackmann⁴⁵, J. Taenzer¹⁵⁵, A. Taffard¹⁶⁶, R. Tafirout^{163a}, E. Tahirovic⁷⁹, N. Taiblum¹⁵⁵, H. Takai²⁷, R. Takashima⁷², E.H. Takasugi¹⁰³, K. Takeda⁷⁰, T. Takeshita¹⁴², Y. Takubo⁶⁹, M. Talby⁸⁸, A.A. Talyshev^{111,c}, J. Tanaka¹⁵⁷, M. Tanaka¹⁵⁹, R. Tanaka¹¹⁹, S. Tanaka⁶⁹, R. Tanioka⁷⁰, B.B. Tannenwald¹¹³, S. Tapia Araya^{34b}, S. Tapprogge⁸⁶, S. Tarem¹⁵⁴, G.F. Tartarelli^{94a}, P. Tas¹³¹, M. Tasevsky¹²⁹, T. Tashiro⁷¹, E. Tassi^{40a,40b}, A. Tavares Delgado^{128a,128b}, Y. Tayalati^{137e}, A.C. Taylor¹⁰⁷, A.J. Taylor⁴⁹, G.N. Taylor⁹¹, P.T.E. Taylor⁹¹, W. Taylor^{163b}, P. Teixeira-Dias⁸⁰, D. Temple¹⁴⁴, H. Ten Kate³², P.K. Teng¹⁵³, J.J. Teoh¹²⁰, F. Tepel¹⁷⁸, S. Terada⁶⁹, K. Terashi¹⁵⁷, J. Terron⁸⁵, S. Terzo¹³, M. Testa⁵⁰, R.J. Teuscher^{161,o}, S.J. Thais¹⁷⁹, T. Theveniaux-Pelzer⁸⁸, F. Thiele³⁹, J.P. Thomas¹⁹, J. Thomas-Wilsker⁸⁰, P.D. Thompson¹⁹, A.S. Thompson⁵⁶, L.A. Thomsen¹⁷⁹, E. Thomson¹²⁴, Y. Tian³⁸, M.J. Tibbetts¹⁶, R.E. Ticse Torres⁵⁷, V.O. Tikhomirov^{98,ap}, Yu.A. Tikhonov^{111,c}, S. Timoshenko¹⁰⁰,

P. Tipton¹⁷⁹, S. Tisserant⁸⁸, K. Todome¹⁵⁹, S. Todorova-Nova⁵, S. Todt⁴⁷, J. Tojo⁷³, S. Tokár^{146a}, K. Tokushuku⁶⁹, E. Tolley¹¹³, L. Tomlinson⁸⁷, M. Tomoto¹⁰⁵, L. Tompkins^{145,ar}, K. Toms¹⁰⁷, B. Tong⁵⁹, P. Tornambe⁵¹, E. Torrence¹¹⁸, H. Torres⁴⁷, E. Torró Pastor¹⁴⁰, J. Toth^{88,ar}, F. Touchard⁸⁸, D.R. Tovey¹⁴¹, C.J. Treado¹¹², T. Trefzger¹⁷⁷, F. Tresoldi¹⁵¹, A. Tricoli²⁷, I.M. Trigger^{163a}, S. Trincaz-Duvoid⁸³, M.F. Tripiana¹³, W. Trischuk¹⁶¹, B. Trocmé⁵⁸, A. Trofymov⁴⁵, C. Troncon^{94a}, M. Trotter-McDonald¹⁶, M. Trovatelli¹⁷², L. Truong^{147b}, M. Trzebinski⁴², A. Trzupek⁴², K.W. Tsang^{62a}, J.C.-L. Tseng¹²², P.V. Tsiarashka⁹⁵, N. Tsirintanis⁹, S. Tsiskaridze¹³, V. Tsiskaridze⁵¹, E.G. Tskhadadze^{54a}, I.I. Tsukerman⁹⁹, V. Tsulaia¹⁶, S. Tsuno⁶⁹, D. Tsybychev¹⁵⁰, Y. Tu^{62b}, A. Tudorache^{28b}, V. Tudorache^{28b}, T.T. Tulbure^{28a}, A.N. Tuna⁵⁹, S. Turchikhin⁶⁸, D. Turgeman¹⁷⁵, I. Turk Cakir^{4b,as}, R. Turra^{94a}, P.M. Tuts³⁸, G. Ucchielli^{22a,22b}, I. Ueda⁶⁹, M. Ughetto^{148a,148b}, F. Ukegawa¹⁶⁴, G. Unal³², A. Undrus²⁷, G. Unel¹⁶⁶, F.C. Ungaro⁹¹, Y. Unno⁶⁹, K. Uno¹⁵⁷, C. Unverdorben¹⁰², J. Urban^{146b}, P. Urquijo⁹¹, P. Urrejola⁸⁶, G. Usai⁸, J. Usui⁶⁹, L. Vacavant⁸⁸, V. Vacek¹³⁰, B. Vachon⁹⁰, K.O.H. Vadla¹²¹, A. Vaidya⁸¹, C. Valderanis¹⁰², E. Valdes Santurio^{148a,148b}, M. Valente⁵², S. Valentini^{22a,22b}, A. Valero¹⁷⁰, L. Valéry¹³, S. Valkar¹³¹, A. Vallier⁵, J.A. Valls Ferrer¹⁷⁰, W. Van Den Wollenberg¹⁰⁹, H. van der Graaf¹⁰⁹, P. van Gemmeren⁶, J. Van Nieuwkoop¹⁴⁴, I. van Vulpen¹⁰⁹, M.C. van Woerden¹⁰⁹, M. Vanadia^{135a,135b}, W. Vandelli³², A. Vaniachine¹⁶⁰, P. Vankov¹⁰⁹, G. Vardanyan¹⁸⁰, R. Vari^{134a}, E.W. Varnes⁷, C. Varni^{53a,53b}, T. Varol⁴³, D. Varouchas¹¹⁹, A. Vartapetian⁸, K.E. Varvell¹⁵², J.G. Vasquez¹⁷⁹, G.A. Vasquez^{34b}, F. Vazeille³⁷, D. Vazquez Furelos¹³, T. Vazquez Schroeder⁹⁰, J. Veatch⁵⁷, V. Veeraraghavan⁷, L.M. Veloce¹⁶¹, F. Veloso^{128a,128c}, S. Veneziano^{134a}, A. Ventura^{76a,76b}, M. Venturi¹⁷², N. Venturi³², A. Venturini²⁵, V. Vercesi^{123a}, M. Verducci^{136a,136b}, W. Verkerke¹⁰⁹, A.T. Vermeulen¹⁰⁹, J.C. Vermeulen¹⁰⁹, M.C. Vetterli^{144,d}, N. Viaux Maira^{34b}, O. Viazlo⁸⁴, I. Vichou^{169,*}, T. Vickey¹⁴¹, O.E. Vickey Boeriu¹⁴¹, G.H.A. Viehhauser¹²², S. Viel¹⁶, L. Vigani¹²², M. Villa^{22a,22b}, M. Villaplana Perez^{94a,94b}, E. Vilucchi⁵⁰, M.G. Vincet³¹, V.B. Vinogradov⁶⁸, A. Vishwakarma⁴⁵, C. Vittori^{22a,22b}, I. Vivarelli¹⁵¹, S. Vlachos¹⁰, M. Vogel¹⁷⁸, P. Vokac¹³⁰, G. Volpi¹³, H. von der Schmitt¹⁰³, E. von Toerne²³, V. Vorobel¹³¹, K. Vorobev¹⁰⁰, M. Vos¹⁷⁰, R. Voss³², J.H. Vosseveld⁷⁷, N. Vranjes¹⁴, M. Vranjes Milosavljevic¹⁴, V. Vrba¹³⁰, M. Vreeswijk¹⁰⁹, R. Vuillermet³², I. Vukotic³³, P. Wagner²³, W. Wagner¹⁷⁸, J. Wagner-Kuhr¹⁰², H. Wahlberg⁷⁴, S. Wahrmund⁴⁷, K. Wakamiya⁷⁰, J. Walder⁷⁵, R. Walker¹⁰², W. Walkowiak¹⁴³, V. Wallangen^{148a,148b}, C. Wang^{35b}, C. Wang^{36b,at}, F. Wang¹⁷⁶, H. Wang¹⁶, H. Wang³, J. Wang⁴⁵, J. Wang¹⁵², Q. Wang¹¹⁵, R.-J. Wang⁸³, R. Wang⁶, S.M. Wang¹⁵³, T. Wang³⁸, W. Wang^{153,au}, W. Wang^{36a,av}, Z. Wang^{36c}, C. Wanotayaroj⁴⁵, A. Warburton⁹⁰, C.P. Ward³⁰, D.R. Wardrope⁸¹, A. Washbrook⁴⁹, P.M. Watkins¹⁹, A.T. Watson¹⁹, M.F. Watson¹⁹, G. Watts¹⁴⁰, S. Watts⁸⁷, B.M. Waugh⁸¹, A.F. Webb¹¹, S. Webb⁸⁶, M.S. Weber¹⁸, S.M. Weber^{60a}, S.W. Weber¹⁷⁷, S.A. Weber³¹, J.S. Webster⁶, A.R. Weidberg¹²², B. Weinert⁶⁴, J. Weingarten⁵⁷, M. Weirich⁸⁶, C. Weiser⁵¹, H. Weits¹⁰⁹, P.S. Wells³², T. Wenaus²⁷, T. Wengler³², S. Wenig³², N. Wermes²³, M.D. Werner⁶⁷, P. Werner³², M. Wessels^{60a}, T.D. Weston¹⁸, K. Whalen¹¹⁸, N.L. Whallon¹⁴⁰, A.M. Wharton⁷⁵, A.S. White⁹², A. White⁸, M.J. White¹, R. White^{34b}, D. Whiteson¹⁶⁶, B.W. Whitmore⁷⁵, F.J. Wickens¹³³, W. Wiedenmann¹⁷⁶, M. Wielers¹³³, C. Wiglesworth³⁹, L.A.M. Wiik-Fuchs⁵¹, A. Wildauer¹⁰³, F. Wilk⁸⁷, H.G. Wilkens³², H.H. Williams¹²⁴, S. Williams¹⁰⁹, C. Willis⁹³, S. Willocq⁸⁹, J.A. Wilson¹⁹, I. Wingerter-Seez⁵, E. Winkels¹⁵¹, F. Winklmeier¹¹⁸, O.J. Winston¹⁵¹, B.T. Winter²³, M. Wittgen¹⁴⁵, M. Wobisch^{82,u}, A. Wolf⁸⁶, T.M.H. Wolf¹⁰⁹, R. Wolff⁸⁸, M.W. Wolter⁴², H. Wolters^{128a,128c}, V.W.S. Wong¹⁷¹, N.L. Woods¹³⁹, S.D. Worm¹⁹, B.K. Wosiek⁴², J. Wotschack³², K.W. Wozniak⁴², M. Wu³³, S.L. Wu¹⁷⁶, X. Wu⁵², Y. Wu⁹², T.R. Wyatt⁸⁷, B.M. Wynne⁴⁹, S. Xella³⁹, Z. Xi⁹², L. Xia^{35c}, D. Xu^{35a}, L. Xu²⁷, T. Xu¹³⁸, W. Xu⁹², B. Yabsley¹⁵², S. Yacoob^{147a}, D. Yamaguchi¹⁵⁹, Y. Yamaguchi¹⁵⁹, A. Yamamoto⁶⁹, S. Yamamoto¹⁵⁷, T. Yamanaka¹⁵⁷, F. Yamane⁷⁰, M. Yamatani¹⁵⁷, T. Yamazaki¹⁵⁷, Y. Yamazaki⁷⁰, Z. Yan²⁴, H. Yang^{36c}, H. Yang¹⁶, Y. Yang¹⁵³, Z. Yang¹⁵, W.-M. Yao¹⁶, Y.C. Yap⁴⁵, Y. Yasu⁶⁹, E. Yatsenko⁵, K.H. Yau Wong²³, J. Ye⁴³, S. Ye²⁷, I. Yeletsikh⁶⁸, E. Yigitbasi²⁴, E. Yildirim⁸⁶, K. Yorita¹⁷⁴, K. Yoshihara¹²⁴, C. Young¹⁴⁵, C.J.S. Young³², J. Yu⁸, J. Yu⁶⁷, S.P.Y. Yuen²³, I. Yusuff^{30,aw}, B. Zabinski⁴², G. Zacharis¹⁰, R. Zaidan¹³, A.M. Zaitsev^{132,aj}, N. Zakharchuk⁴⁵, J. Zalieckas¹⁵, A. Zaman¹⁵⁰, S. Zambito⁵⁹, D. Zanzi⁹¹, C. Zeitnitz¹⁷⁸, G. Zemaityte¹²², A. Zemla^{41a}, J.C. Zeng¹⁶⁹, Q. Zeng¹⁴⁵, O. Zenin¹³², T. Ženiš^{146a}, D. Zerwas¹¹⁹, D. Zhang^{36b}, D. Zhang⁹², F. Zhang¹⁷⁶, G. Zhang^{36a,av}, H. Zhang¹¹⁹, J. Zhang⁶, L. Zhang⁵¹, L. Zhang^{36a}, M. Zhang¹⁶⁹, P. Zhang^{35b}, R. Zhang²³, R. Zhang^{36a,at}, X. Zhang^{36b}, Y. Zhang^{35a,35d}, Z. Zhang¹¹⁹, X. Zhao⁴³, Y. Zhao^{36b,ax}, Z. Zhao^{36a},

A. Zhemchugov⁶⁸, B. Zhou⁹², C. Zhou¹⁷⁶, L. Zhou⁴³, M. Zhou^{35a,35d}, M. Zhou¹⁵⁰, N. Zhou^{36c}, Y. Zhou⁷, C.G. Zhu^{36b}, H. Zhu^{35a}, J. Zhu⁹², Y. Zhu^{36a}, X. Zhuang^{35a}, K. Zhukov⁹⁸, A. Zibell¹⁷⁷, D. Zieminska⁶⁴, N.I. Zimine⁶⁸, C. Zimmermann⁸⁶, S. Zimmermann⁵¹, Z. Zinonos¹⁰³, M. Zinser⁸⁶, M. Ziolkowski¹⁴³, L. Živković¹⁴, G. Zobernig¹⁷⁶, A. Zoccoli^{22a,22b}, R. Zou³³, M. zur Nedden¹⁷, L. Zwalinski³²

¹ Department of Physics, University of Adelaide, Adelaide, Australia

² Physics Department, SUNY Albany, Albany, NY, United States

³ Department of Physics, University of Alberta, Edmonton, AB, Canada

⁴ (a) Department of Physics, Ankara University, Ankara; (b) Istanbul Aydin University, Istanbul; (c) Division of Physics, TOBB University of Economics and Technology, Ankara, Turkey

⁵ LAPP, CNRS/IN2P3 and Université Savoie Mont Blanc, Annecy-le-Vieux, France

⁶ High Energy Physics Division, Argonne National Laboratory, Argonne, IL, United States

⁷ Department of Physics, University of Arizona, Tucson, AZ, United States

⁸ Department of Physics, The University of Texas at Arlington, Arlington, TX, United States

⁹ Physics Department, National and Kapodistrian University of Athens, Athens, Greece

¹⁰ Physics Department, National Technical University of Athens, Zografou, Greece

¹¹ Department of Physics, The University of Texas at Austin, Austin, TX, United States

¹² Institute of Physics, Azerbaijan Academy of Sciences, Baku, Azerbaijan

¹³ Institut de Física d'Altes Energies (IFAE), The Barcelona Institute of Science and Technology, Barcelona, Spain

¹⁴ Institute of Physics, University of Belgrade, Belgrade, Serbia

¹⁵ Department for Physics and Technology, University of Bergen, Bergen, Norway

¹⁶ Physics Division, Lawrence Berkeley National Laboratory and University of California, Berkeley, CA, United States

¹⁷ Department of Physics, Humboldt University, Berlin, Germany

¹⁸ Albert Einstein Center for Fundamental Physics and Laboratory for High Energy Physics, University of Bern, Bern, Switzerland

¹⁹ School of Physics and Astronomy, University of Birmingham, Birmingham, United Kingdom

²⁰ (a) Department of Physics, Bogazici University, Istanbul; (b) Department of Physics Engineering, Gaziantep University, Gaziantep; (d) Istanbul Bilgi University, Faculty of Engineering and Natural Sciences, Istanbul; (e) Bahcesehir University, Faculty of Engineering and Natural Sciences, Istanbul, Turkey

²¹ Centro de Investigaciones, Universidad Antonio Narino, Bogota, Colombia

²² (a) INFN Sezione di Bologna; (b) Dipartimento di Fisica e Astronomia, Università di Bologna, Bologna, Italy

²³ Physikalisches Institut, University of Bonn, Bonn, Germany

²⁴ Department of Physics, Boston University, Boston, MA, United States

²⁵ Department of Physics, Brandeis University, Waltham, MA, United States

²⁶ (a) Universidade Federal do Rio De Janeiro COPPE/EE/IF, Rio de Janeiro; (b) Electrical Circuits Department, Federal University of Juiz de Fora (UFJF), Juiz de Fora; (c) Federal University of Sao Joao del Rei (UFSJ), Sao Joao del Rei; (d) Instituto de Fisica, Universidade de Sao Paulo, Sao Paulo, Brazil

²⁷ Physics Department, Brookhaven National Laboratory, Upton, NY, United States

²⁸ (a) Transilvania University of Brasov, Brasov; (b) Horia Hulubei National Institute of Physics and Nuclear Engineering, Bucharest; (c) Department of Physics, Alexandru Ioan Cuza University of Iasi, Iasi; (d) National Institute for Research and Development of Isotopic and Molecular Technologies, Physics Department, Cluj Napoca; (e) University Politehnica Bucharest, Bucharest; (f) West University in Timisoara, Timisoara, Romania

²⁹ Departamento de Fisica, Universidad de Buenos Aires, Buenos Aires, Argentina

³⁰ Cavendish Laboratory, University of Cambridge, Cambridge, United Kingdom

³¹ Department of Physics, Carleton University, Ottawa, ON, Canada

³² CERN, Geneva, Switzerland

³³ Enrico Fermi Institute, University of Chicago, Chicago, IL, United States

³⁴ (a) Departamento de Fisica, Pontificia Universidad Católica de Chile, Santiago; (b) Departamento de Fisica, Universidad Técnica Federico Santa María, Valparaíso, Chile

³⁵ (a) Institute of High Energy Physics, Chinese Academy of Sciences, Beijing; (b) Department of Physics, Nanjing University, Jiangsu; (c) Physics Department, Tsinghua University, Beijing 100084; (d) University of Chinese Academy of Science (UCAS), Beijing, China

³⁶ (a) School of Physics, Shandong University, Shandong; (b) School of Physics and Astronomy, Key Laboratory for Particle Physics, Astrophysics and Cosmology, Ministry of Education; Shanghai Key Laboratory for Particle Physics and Cosmology, Tsung-Dao Lee Institute, Shanghai Jiao Tong University; (c) Department of Modern Physics and State Key Laboratory of Particle Detection and Electronics, University of Science and Technology of China, Anhui, China

³⁷ Université Clermont Auvergne, CNRS/IN2P3, LPC, Clermont-Ferrand, France

³⁸ Nevis Laboratory, Columbia University, Irvington, NY, United States

³⁹ Niels Bohr Institute, University of Copenhagen, Copenhagen, Denmark

⁴⁰ (a) INFN Gruppo Collegato di Cosenza, Laboratori Nazionali di Frascati; (b) Dipartimento di Fisica, Università della Calabria, Rende, Italy

⁴¹ (a) AGH University of Science and Technology, Faculty of Physics and Applied Computer Science, Krakow; (b) Marian Smoluchowski Institute of Physics, Jagiellonian University, Krakow, Poland

⁴² Institute of Nuclear Physics Polish Academy of Sciences, Krakow, Poland

⁴³ Physics Department, Southern Methodist University, Dallas, TX, United States

⁴⁴ Physics Department, University of Texas at Dallas, Richardson, TX, United States

⁴⁵ DESY, Hamburg and Zeuthen, Germany

⁴⁶ Lehrstuhl für Experimentelle Physik IV, Technische Universität Dortmund, Dortmund, Germany

⁴⁷ Institut für Kern- und Teilchenphysik, Technische Universität Dresden, Dresden, Germany

⁴⁸ Department of Physics, Duke University, Durham, NC, United States

⁴⁹ SUPA – School of Physics and Astronomy, University of Edinburgh, Edinburgh, United Kingdom

⁵⁰ INFN e Laboratori Nazionali di Frascati, Frascati, Italy

⁵¹ Fakultät für Mathematik und Physik, Albert-Ludwigs-Universität, Freiburg, Germany

⁵² Departement de Physique Nucleaire et Corpusculaire, Université de Genève, Geneva, Switzerland

⁵³ (a) INFN Sezione di Genova; (b) Dipartimento di Fisica, Università di Genova, Genova, Italy

⁵⁴ (a) E. Andronikashvili Institute of Physics, Iv. Javakishvili Tbilisi State University, Tbilisi; (b) High Energy Physics Institute, Tbilisi State University, Tbilisi, Georgia

⁵⁵ II Physikalisches Institut, Justus-Liebig-Universität Giessen, Giessen, Germany

⁵⁶ SUPA – School of Physics and Astronomy, University of Glasgow, Glasgow, United Kingdom

⁵⁷ II Physikalisches Institut, Georg-August-Universität, Göttingen, Germany

⁵⁸ Laboratoire de Physique Subatomique et de Cosmologie, Université Grenoble-Alpes, CNRS/IN2P3, Grenoble, France

⁵⁹ Laboratory for Particle Physics and Cosmology, Harvard University, Cambridge, MA, United States

⁶⁰ (a) Kirchhoff-Institut für Physik, Ruprecht-Karls-Universität Heidelberg, Heidelberg; (b) Physikalisches Institut, Ruprecht-Karls-Universität Heidelberg, Heidelberg, Germany

⁶¹ Faculty of Applied Information Science, Hiroshima Institute of Technology, Hiroshima, Japan

⁶² (a) Department of Physics, The Chinese University of Hong Kong, Shatin, N.T., Hong Kong; (b) Department of Physics, The University of Hong Kong, Hong Kong; (c) Department of Physics and Institute for Advanced Study, The Hong Kong University of Science and Technology, Clear Water Bay, Kowloon, Hong Kong, China

⁶³ Department of Physics, National Tsing Hua University, Hsinchu, Taiwan

- ⁶⁴ Department of Physics, Indiana University, Bloomington, IN, United States
- ⁶⁵ Institut für Astro- und Teilchenphysik, Leopold-Franzens-Universität, Innsbruck, Austria
- ⁶⁶ University of Iowa, Iowa City, IA, United States
- ⁶⁷ Department of Physics and Astronomy, Iowa State University, Ames, IA, United States
- ⁶⁸ Joint Institute for Nuclear Research, JINR Dubna, Dubna, Russia
- ⁶⁹ KEK, High Energy Accelerator Research Organization, Tsukuba, Japan
- ⁷⁰ Graduate School of Science, Kobe University, Kobe, Japan
- ⁷¹ Faculty of Science, Kyoto University, Kyoto, Japan
- ⁷² Kyoto University of Education, Kyoto, Japan
- ⁷³ Research Center for Advanced Particle Physics and Department of Physics, Kyushu University, Fukuoka, Japan
- ⁷⁴ Instituto de Física La Plata, Universidad Nacional de La Plata and CONICET, La Plata, Argentina
- ⁷⁵ Physics Department, Lancaster University, Lancaster, United Kingdom
- ⁷⁶ ^(a) INFN Sezione di Lecce; ^(b) Dipartimento di Matematica e Fisica, Università del Salento, Lecce, Italy
- ⁷⁷ Oliver Lodge Laboratory, University of Liverpool, Liverpool, United Kingdom
- ⁷⁸ Department of Experimental Particle Physics, Jožef Stefan Institute and Department of Physics, University of Ljubljana, Ljubljana, Slovenia
- ⁷⁹ School of Physics and Astronomy, Queen Mary University of London, London, United Kingdom
- ⁸⁰ Department of Physics, Royal Holloway University of London, Surrey, United Kingdom
- ⁸¹ Department of Physics and Astronomy, University College London, London, United Kingdom
- ⁸² Louisiana Tech University, Ruston, LA, United States
- ⁸³ Laboratoire de Physique Nucléaire et de Hautes Energies, UPMC and Université Paris-Diderot and CNRS/IN2P3, Paris, France
- ⁸⁴ Fysiska institutionen, Lunds universitet, Lund, Sweden
- ⁸⁵ Departamento de Física Teórica C-15, Universidad Autónoma de Madrid, Madrid, Spain
- ⁸⁶ Institut für Physik, Universität Mainz, Mainz, Germany
- ⁸⁷ School of Physics and Astronomy, University of Manchester, Manchester, United Kingdom
- ⁸⁸ CPPM, Aix-Marseille Université and CNRS/IN2P3, Marseille, France
- ⁸⁹ Department of Physics, University of Massachusetts, Amherst, MA, United States
- ⁹⁰ Department of Physics, McGill University, Montreal, QC, Canada
- ⁹¹ School of Physics, University of Melbourne, Victoria, Australia
- ⁹² Department of Physics, The University of Michigan, Ann Arbor, MI, United States
- ⁹³ Department of Physics and Astronomy, Michigan State University, East Lansing, MI, United States
- ⁹⁴ ^(a) INFN Sezione di Milano; ^(b) Dipartimento di Fisica, Università di Milano, Milano, Italy
- ⁹⁵ B.I. Stepanov Institute of Physics, National Academy of Sciences of Belarus, Minsk, Belarus
- ⁹⁶ Research Institute for Nuclear Problems of Byelorussian State University, Minsk, Belarus
- ⁹⁷ Group of Particle Physics, University of Montreal, Montreal, QC, Canada
- ⁹⁸ P.N. Lebedev Physical Institute of the Russian Academy of Sciences, Moscow, Russia
- ⁹⁹ Institute for Theoretical and Experimental Physics (ITEP), Moscow, Russia
- ¹⁰⁰ National Research Nuclear University MEPhI, Moscow, Russia
- ¹⁰¹ D.V. Skobeltsyn Institute of Nuclear Physics, M.V. Lomonosov Moscow State University, Moscow, Russia
- ¹⁰² Fakultät für Physik, Ludwig-Maximilians-Universität München, München, Germany
- ¹⁰³ Max-Planck-Institut für Physik (Werner-Heisenberg-Institut), München, Germany
- ¹⁰⁴ Nagasaki Institute of Applied Science, Nagasaki, Japan
- ¹⁰⁵ Graduate School of Science and Kobayashi-Maskawa Institute, Nagoya University, Nagoya, Japan
- ¹⁰⁶ ^(a) INFN Sezione di Napoli; ^(b) Dipartimento di Fisica, Università di Napoli, Napoli, Italy
- ¹⁰⁷ Department of Physics and Astronomy, University of New Mexico, Albuquerque, NM, United States
- ¹⁰⁸ Institute for Mathematics, Astrophysics and Particle Physics, Radboud University Nijmegen/Nikhef, Nijmegen, Netherlands
- ¹⁰⁹ Nikhef National Institute for Subatomic Physics and University of Amsterdam, Amsterdam, Netherlands
- ¹¹⁰ Department of Physics, Northern Illinois University, DeKalb, IL, United States
- ¹¹¹ Budker Institute of Nuclear Physics, SB RAS, Novosibirsk, Russia
- ¹¹² Department of Physics, New York University, New York, NY, United States
- ¹¹³ Ohio State University, Columbus, OH, United States
- ¹¹⁴ Faculty of Science, Okayama University, Okayama, Japan
- ¹¹⁵ Homer L. Dodge Department of Physics and Astronomy, University of Oklahoma, Norman, OK, United States
- ¹¹⁶ Department of Physics, Oklahoma State University, Stillwater, OK, United States
- ¹¹⁷ Palacký University, RCPM, Olomouc, Czech Republic
- ¹¹⁸ Center for High Energy Physics, University of Oregon, Eugene, OR, United States
- ¹¹⁹ LAL, Univ. Paris-Sud, CNRS/IN2P3, Université Paris-Saclay, Orsay, France
- ¹²⁰ Graduate School of Science, Osaka University, Osaka, Japan
- ¹²¹ Department of Physics, University of Oslo, Oslo, Norway
- ¹²² Department of Physics, Oxford University, Oxford, United Kingdom
- ¹²³ ^(a) INFN Sezione di Pavia; ^(b) Dipartimento di Fisica, Università di Pavia, Pavia, Italy
- ¹²⁴ Department of Physics, University of Pennsylvania, Philadelphia, PA, United States
- ¹²⁵ National Research Centre "Kurchatov Institute" B.P. Konstantinov Petersburg Nuclear Physics Institute, St. Petersburg, Russia
- ¹²⁶ ^(a) INFN Sezione di Pisa; ^(b) Dipartimento di Fisica E. Fermi, Università di Pisa, Pisa, Italy
- ¹²⁷ Department of Physics and Astronomy, University of Pittsburgh, Pittsburgh, PA, United States
- ¹²⁸ ^(a) Laboratório de Instrumentação e Física Experimental de Partículas - LIP, Lisboa; ^(b) Faculdade de Ciências, Universidade de Lisboa, Lisboa; ^(c) Department of Physics, University of Coimbra, Coimbra; ^(d) Centro de Física Nuclear da Universidade de Lisboa, Lisboa; ^(e) Departamento de Física, Universidade do Minho, Braga; ^(f) Departamento de Física Teórica y del Cosmos, Universidad de Granada, Granada, Spain; ^(g) Dep Física and CEFITEC de Faculdade de Ciências e Tecnologia, Universidade Nova de Lisboa, Caparica, Portugal
- ¹²⁹ Institute of Physics, Academy of Sciences of the Czech Republic, Praha, Czech Republic
- ¹³⁰ Czech Technical University in Prague, Praha, Czech Republic
- ¹³¹ Charles University, Faculty of Mathematics and Physics, Prague, Czech Republic
- ¹³² State Research Center Institute for High Energy Physics (Protvino), NRC KI, Russia
- ¹³³ Particle Physics Department, Rutherford Appleton Laboratory, Didcot, United Kingdom
- ¹³⁴ ^(a) INFN Sezione di Roma; ^(b) Dipartimento di Fisica, Sapienza Università di Roma, Roma, Italy
- ¹³⁵ ^(a) INFN Sezione di Roma Tor Vergata; ^(b) Dipartimento di Fisica, Università di Roma Tor Vergata, Roma, Italy
- ¹³⁶ ^(a) INFN Sezione di Roma Tre; ^(b) Dipartimento di Matematica e Fisica, Università Roma Tre, Roma, Italy
- ¹³⁷ ^(a) Faculté des Sciences Ain Chock, Réseau Universitaire de Physique des Hautes Energies - Université Hassan II, Casablanca; ^(b) Centre National de l'Energie des Sciences Techniques Nucleaires, Rabat; ^(c) Faculté des Sciences Semlalia, Université Cadi Ayyad, LPHEA-Marrakech; ^(d) Faculté des Sciences, Université Mohamed Premier and LPTPM, Oujda; ^(e) Faculté des sciences, Université Mohammed V, Rabat, Morocco
- ¹³⁸ DSM/IRFU (Institut de Recherches sur les Lois Fondamentales de l'Univers), CEA Saclay (Commissariat à l'Energie Atomique et aux Energies Alternatives), Gif-sur-Yvette, France

- ¹³⁹ Santa Cruz Institute for Particle Physics, University of California Santa Cruz, Santa Cruz, CA, United States
¹⁴⁰ Department of Physics, University of Washington, Seattle, WA, United States
¹⁴¹ Department of Physics and Astronomy, University of Sheffield, Sheffield, United Kingdom
¹⁴² Department of Physics, Shinshu University, Nagano, Japan
¹⁴³ Department Physik, Universität Siegen, Siegen, Germany
¹⁴⁴ Department of Physics, Simon Fraser University, Burnaby, BC, Canada
¹⁴⁵ SLAC National Accelerator Laboratory, Stanford, CA, United States
¹⁴⁶ (a) Faculty of Mathematics, Physics & Informatics, Comenius University, Bratislava; (b) Department of Subnuclear Physics, Institute of Experimental Physics of the Slovak Academy of Sciences, Kosice, Slovak Republic
¹⁴⁷ (a) Department of Physics, University of Cape Town, Cape Town; (b) Department of Physics, University of Johannesburg, Johannesburg; (c) School of Physics, University of the Witwatersrand, Johannesburg, South Africa
¹⁴⁸ (a) Department of Physics, Stockholm University; (b) The Oskar Klein Centre, Stockholm, Sweden
¹⁴⁹ Physics Department, Royal Institute of Technology, Stockholm, Sweden
¹⁵⁰ Departments of Physics & Astronomy and Chemistry, Stony Brook University, Stony Brook, NY, United States
¹⁵¹ Department of Physics and Astronomy, University of Sussex, Brighton, United Kingdom
¹⁵² School of Physics, University of Sydney, Sydney, Australia
¹⁵³ Institute of Physics, Academia Sinica, Taipei, Taiwan
¹⁵⁴ Department of Physics, Technion: Israel Institute of Technology, Haifa, Israel
¹⁵⁵ Raymond and Beverly Sackler School of Physics and Astronomy, Tel Aviv University, Tel Aviv, Israel
¹⁵⁶ Department of Physics, Aristotle University of Thessaloniki, Thessaloniki, Greece
¹⁵⁷ International Center for Elementary Particle Physics and Department of Physics, The University of Tokyo, Tokyo, Japan
¹⁵⁸ Graduate School of Science and Technology, Tokyo Metropolitan University, Tokyo, Japan
¹⁵⁹ Department of Physics, Tokyo Institute of Technology, Tokyo, Japan
¹⁶⁰ Tomsk State University, Tomsk, Russia
¹⁶¹ Department of Physics, University of Toronto, Toronto, ON, Canada
¹⁶² (a) INFN-TIFPA; (b) University of Trento, Trento, Italy
¹⁶³ (a) TRIUMF, Vancouver, BC; (b) Department of Physics and Astronomy, York University, Toronto, ON, Canada
¹⁶⁴ Faculty of Pure and Applied Sciences, and Center for Integrated Research in Fundamental Science and Engineering, University of Tsukuba, Tsukuba, Japan
¹⁶⁵ Department of Physics and Astronomy, Tufts University, Medford, MA, United States
¹⁶⁶ Department of Physics and Astronomy, University of California Irvine, Irvine, CA, United States
¹⁶⁷ (a) INFN Gruppo Collegato di Udine, Sezione di Trieste, Udine; (b) ICTP, Trieste; (c) Dipartimento di Chimica, Fisica e Ambiente, Università di Udine, Udine, Italy
¹⁶⁸ Department of Physics and Astronomy, University of Uppsala, Uppsala, Sweden
¹⁶⁹ Department of Physics, University of Illinois, Urbana, IL, United States
¹⁷⁰ Instituto de Física Corpuscular (IFIC), Centro Mixto Universidad de Valencia – CSIC, Spain
¹⁷¹ Department of Physics, University of British Columbia, Vancouver, BC, Canada
¹⁷² Department of Physics and Astronomy, University of Victoria, Victoria, BC, Canada
¹⁷³ Department of Physics, University of Warwick, Coventry, United Kingdom
¹⁷⁴ Waseda University, Tokyo, Japan
¹⁷⁵ Department of Particle Physics, The Weizmann Institute of Science, Rehovot, Israel
¹⁷⁶ Department of Physics, University of Wisconsin, Madison, WI, United States
¹⁷⁷ Fakultät für Physik und Astronomie, Julius-Maximilians-Universität, Würzburg, Germany
¹⁷⁸ Fakultät für Mathematik und Naturwissenschaften, Fachgruppe Physik, Bergische Universität Wuppertal, Wuppertal, Germany
¹⁷⁹ Department of Physics, Yale University, New Haven, CT, United States
¹⁸⁰ Yerevan Physics Institute, Yerevan, Armenia
¹⁸¹ Centre de Calcul de l'Institut National de Physique Nucléaire et de Physique des Particules (IN2P3), Villeurbanne, France
¹⁸² Academia Sinica Grid Computing, Institute of Physics, Academia Sinica, Taipei, Taiwan

^a Also at Department of Physics, King's College London, London, United Kingdom.

^b Also at Institute of Physics, Azerbaijan Academy of Sciences, Baku, Azerbaijan.

^c Also at Novosibirsk State University, Novosibirsk, Russia.

^d Also at TRIUMF, Vancouver BC, Canada.

^e Also at Department of Physics & Astronomy, University of Louisville, Louisville, KY, United States of America.

^f Also at Physics Department, An-Najah National University, Nablus, Palestine.

^g Also at Department of Physics, California State University, Fresno, CA, United States of America.

^h Also at Department of Physics, University of Fribourg, Fribourg, Switzerland.

ⁱ Also at II Physikalisches Institut, Georg-August-Universität, Göttingen, Germany.

^j Also at Departament de Física de la Universitat Autònoma de Barcelona, Barcelona, Spain.

^k Also at Departamento de Física e Astronomia, Faculdade de Ciências, Universidade do Porto, Portugal.

^l Also at Tomsk State University, Tomsk, and Moscow Institute of Physics and Technology State University, Dolgoprudny, Russia.

^m Also at The Collaborative Innovation Center of Quantum Matter (CICQM), Beijing, China.

ⁿ Also at Università di Napoli Parthenope, Napoli, Italy.

^o Also at Institute of Particle Physics (IPP), Canada.

^p Also at Horia Hulubei National Institute of Physics and Nuclear Engineering, Bucharest, Romania.

^q Also at Department of Physics, St. Petersburg State Polytechnical University, St. Petersburg, Russia.

^r Also at Borough of Manhattan Community College, City University of New York, New York City, United States of America.

^s Also at Department of Financial and Management Engineering, University of the Aegean, Chios, Greece.

^t Also at Centre for High Performance Computing, CSIR Campus, Rosebank, Cape Town, South Africa.

^u Also at Louisiana Tech University, Ruston, LA, United States of America.

^v Also at Institutio Catalana de Recerca i Estudis Avancats, ICREA, Barcelona, Spain.

^w Also at Department of Physics, The University of Michigan, Ann Arbor, MI, United States of America.

^x Also at Graduate School of Science, Osaka University, Osaka, Japan.

^y Also at Fakultät für Mathematik und Physik, Albert-Ludwigs-Universität, Freiburg, Germany.

^z Also at Institute for Mathematics, Astrophysics and Particle Physics, Radboud University Nijmegen/Nikhef, Nijmegen, Netherlands.

^{aa} Also at Department of Physics, The University of Texas at Austin, Austin, TX, United States of America.

^{ab} Also at Institute of Theoretical Physics, Ilia State University, Tbilisi, Georgia.

^{ac} Also at CERN, Geneva, Switzerland.

^{ad} Also at Georgian Technical University (GTU), Tbilisi, Georgia.

- ^{ae} Also at Ochadai Academic Production, Ochanomizu University, Tokyo, Japan.
- ^{af} Also at Manhattan College, New York, NY, United States of America.
- ^{ag} Also at The City College of New York, New York, NY, United States of America.
- ^{ah} Also at Departamento de Fisica Teorica y del Cosmos, Universidad de Granada, Granada, Spain.
- ^{ai} Also at Department of Physics, California State University, Sacramento, CA, United States of America.
- ^{aj} Also at Moscow Institute of Physics and Technology State University, Dolgoprudny, Russia.
- ^{ak} Also at Departement de Physique Nucleaire et Corpusculaire, Université de Genève, Geneva, Switzerland.
- ^{al} Also at Institut de Física d'Altes Energies (IFAE), The Barcelona Institute of Science and Technology, Barcelona, Spain.
- ^{am} Also at School of Physics, Sun Yat-sen University, Guangzhou, China.
- ^{an} Also at Institute for Nuclear Research and Nuclear Energy (INRNE) of the Bulgarian Academy of Sciences, Sofia, Bulgaria.
- ^{ao} Also at Faculty of Physics, M.V.Lomonosov Moscow State University, Moscow, Russia.
- ^{ap} Also at National Research Nuclear University MEPhI, Moscow, Russia.
- ^{aq} Also at Department of Physics, Stanford University, Stanford, CA, United States of America.
- ^{ar} Also at Institute for Particle and Nuclear Physics, Wigner Research Centre for Physics, Budapest, Hungary.
- ^{as} Also at Giresun University, Faculty of Engineering, Turkey.
- ^{at} Also at CPPM, Aix-Marseille Université and CNRS/IN2P3, Marseille, France.
- ^{au} Also at Department of Physics, Nanjing University, Jiangsu, China.
- ^{av} Also at Institute of Physics, Academia Sinica, Taipei, Taiwan.
- ^{aw} Also at University of Malaya, Department of Physics, Kuala Lumpur, Malaysia.
- ^{ax} Also at LAL, Univ. Paris-Sud, CNRS/IN2P3, Université Paris-Saclay, Orsay, France.
- * Deceased.